Analyses of small Rho-GTPases signaling molecules during vertebrate development and angiogenesis

INAUGURAL-DISSERTATION

zur

Erlangung der Doktorwürde

der Naturwissenschaftlich-Mathematischen Gesamtfakultät

der

Ruprecht-Karls-Universität

Heidelberg

2011

vorgelegt von

Diplom Biologe

Christian Tobias Dietz

aus Mannheim

Tag der mündlichen Prüfung:

Gutachter: Prof. Dr. Thomas Wieland

Institut für Experimentelle und Klinische Pharmakologie
und Toxikologie der Medizinischen Fakultät Mannheim,
Ruprecht-Karls-Universität Heidelberg

PD Dr. Jens Kroll

Forschungsbereich Vaskuläre Biologie der
Medizinischen Fakultät Mannheim,
Ruprecht-Karls-Universität Heidelberg,
und des Deutsches Krebsforschungszentrum, Heidelberg

Die vorliegende Arbeit wurde in der Abteilung für Vaskuläre Biologie und Tumorangiogenese am Centrum für Biomedizin und Medizintechnik Mannheim (CBTM)7zwischen März 2007 und Dezember 2010 durchgeführt.

Erklärung

1.) Ich erkläre hiermit, dass ich die vorgelegte Dissertation selbst verfasst und mich dabei keiner anderen als der von mir ausdrücklich bezeichneten Quellen und Hilfen bedient habe.

2) Ich erkläre hiermit, dass ich an keiner anderen Stelle ein Prüfungsverfahren beantragt bzw. die Dissertation in dieser oder anderer Form bereits anderweitig als Prüfungsarbeit verwendet oder einer anderen Fakultät als Dissertation vorgelegt habe.

Mannheim, den 17.02.2011

_____

Christian Dietz

List of publications

Parts of this thesis are comprised in the following publications:

Jens Kroll[*], Daniel Epting[*], Katrin Kern, **Christian T. Dietz**, Yuxi Feng, Hans-Peter Hammes, Thomas Wieland and Hellmut G. Augustin (2009)
Inhibition of Rho-dependent kinases ROCK I/II activates VEGF-driven retinal neovascularization and sprouting angiogenesis.
Am J Physiol Heart Circ Physiol 296:893-899, 2009.

Daniel Epting[*], Björn Wendik[*], Katrin Bennewitz, **Christian T. Dietz**, Wolfgang Driever and Jens Kroll (2010)
The Rac1 regulator ELMO1 controls vascular morphogenesis in zebrafish.
Circ Res. 107:45-55, 2010.

The following publications are in preparation:

Christian T. Dietz[*], Nicole Hahn[*], Kristina Jörgens, Daniel Epting, Sandra Kühl, Katrin Bennewitz, Hellmut G. Augustin and Jens Kroll (2011)
The BTB-kelch protein Kleip regulates vascular permeability *in vitro* and *in vivo*.

Christian T. Dietz, Sandra Kühl and Jens Kroll (2011)
The BTB-kelch protein Kleip is required for normal lung maturation.

[*] Authors contributed equally to this work

Für meine Familie

Danksagung

Ich möchte mich ganz herzlich bei allen bedanken, die zum Gelingen dieser Doktorarbeit beigetragen haben.

Herrn Prof. Dr. Thomas Wieland danke ich recht herzlich, dass er mir die Möglichkeit gegeben hat, meine Dissertation an der Naturwissenschaftlich-Mathematischen Gesamtfakultät der Ruprecht-Karls-Universität und dem DKFZ in Heidelberg durchzuführen. Vielen Dank für die wissenschaftliche Betreuung innerhalb meines Ph.D.-Programmes.

Herrn Prof. Dr. Hellmut Augustin danke ich, dass ich diese Arbeit in seiner Abteilung für Vaskuläre Biologie und Tumorangiogenese durchführen durfte. Außerdem danke ich ihm für die zurückhaltende, aber immer zielgerichtete Betreuung meiner Arbeit. Seine wertvollen Anregungen und Ratschläge habe ich immer geschätzt.

Mein ganz besonderer Dank gilt Herrn PD Dr. Jens Kroll, für die Bereitstellung des interessanten Promotionthemas. Insbesondere danke ich ihm für seine Unterstützung und Betreuung, sowie für den wissenschaftlichen Freiraum während der Bearbeitung verschiedenster Fragestellungen.

Ein ganz großes Dankeschön auch an all diejenigen, die täglich mit mir die Zeit an der „bench“ verbracht haben und zu einer tollen Laboratmosphäre beigetragen haben. Hervorzuheben ist dabei Frau Dr. Sandra Kühl, ohne deren aufopferungsvolles Engagement diese Arbeit nicht zustande gekommen wäre. Ganz herzlich möchte ich mich aber auch bei Dr. Daniel Epting, Katrin Bennewitz und der Fischer Gruppe für die unvergessliche Zeit und die daraus entstandenen Freundschaften bedanken.

Zudem möchte ich mich noch bei Kristina Jörgens, Melanie Grassl, Carleen Depperman und Anja Runge bedanken, die mir durch ihre Expertise eine große Stütze waren.

Aus dem Heidelberger Labor bedanke ich mich vor allem bei Arne Bartol, Elias Loos, Junhao Hu, Maria Riedel und Dorothee Terhardt. Ohne euch wäre die Zeit am Mikrotom nur halb so schön gewesen. Außerdem danke ich euch für die vielen ausgeliehenen Antikörper.

Für das Korrekturlesen, sowie der Formatierung dieser Arbeit möchte ich mich bei Dr. Daniel Epting, Kathrin Schäker und meiner Schwester Daniela bedanken.

Der größte Dank gilt jedoch meiner Freundin Tina Siebholz, meinen Eltern und meiner Familie, die mir zeitlebens und in allen Lebenslagen mit Rat und Tat zur Seite standen und mir die Möglichkeit gegeben haben diesen Weg zu gehen.
Vielen Dank für die fortwährende Unterstützung.

„Das Ende eines Dinges ist der Anfang eines anderen.“
(Leonardo da Vinci)

Table of Contents

List of FIGURES and TABLES

I. Zusammenfassung

Die Mitglieder der Rho-Familie der kleinen GTPasen wurden ursprünglich durch ihre Beteiligung an einer Vielzahl von zellulären Prozessen identifiziert. Sie sind unter anderem an der Regulation des F-Aktin-Zytoskelettes und der Mikrotubuli-Dynamik, Zellpolarität, Vesikeltransport und Genexpression beteiligt. Zudem wurde in neueren Studien den G-Proteinen eine Funktion als Schlüsselregulator innerhalb der Angiogenese zugewiesen. So konnte gezeigt werden, dass der G-Protein-Signaltransduktionsweg dabei stark mit angiogenen Prozessen wie der Regulation der vaskulären Permeabilität, dem Umbau der extrazellulären Matrix, der endothelialen Migration, Proliferation, Morphogenese und dem Überleben assoziiert ist. Vieles von unserem derzeitigen Kenntnisstand bezüglich der G-Protein-Signalweiterleitung wurde überwiegend durch *In-vitro*-Experimente oder durch *In-vivo*-Studien mit wirbellosen Tieren gewonnen. Jedoch ist wenig über ihre Regulation und Funktion bei Wirbeltieren bekannt. Aus diesem Grund lag das Ziel dieser Arbeit darin, die Funktion von ausgewählten G-Proteinen während der Wirbeltierentwicklung und insbesondere in der Angiogenese zu charakterisieren. Erst kürzlich wurde das mit dem Guanin-Nukleotid-Austausch-Faktor (GEF) Ect-2 interagierende BTB-kelch-Protein KLEIP (KLHL20) mit der Angiogenese als neuer und wichtiger Regulator der endothelialen Funktion, welcher die VEGF-induzierte Aktivierung der kleinen GTPase RhoA kontrolliert, assoziiert. Um die Funktion von Kleip während der Angiogenese *in vivo*, sowie in der Entwicklung, zu studieren, wurde das *Kleip*-Gen in Mäusen ausgeschaltet. Die konstitutive Inaktivierung von *Kleip* mittels der Gene-Trap-Methode führte zu einem teilweisen letalen Phänotyp. Ein geringer Anteil von Kleip-defizienten Embryonen starb während der Embryonalentwicklung infolge von kranialen Blutungen. Diese Fehlfunktion innerhalb der Aufrechterhaltung der vaskulären Integrität wurde weiterhin durch Studien mit Spleiß-blocking Morpholino-induzierter *klhl20* Herunterregulation in Zebrafischembryonen, sowie durch einen *In-vitro*-Permeabilitäts-Transwell-Assay unterstützt. Die embryonalen Gefäße in *Kleip*-Mutanten wiesen nach *whole-mount* Immunfärbungen im Vergleich zu ihren Wildtyp-Geschwistern deutlich erweiterte kraniale Gefäße auf. Dieses deutet neben den beobachteten Blutungen ebenfalls auf einen Fehler in der Rekrutierung von muralen Zellen zu den sich bildenden Gefäßen hin. Interessanterweise zeigten spezifische NG2 Immunfärbungen keine Veränderungen in der durch Perizyten vermittelten Gefäßstabilisierung. Diese Beobachtungen lassen in ihrer Gesamtheit daher eher einen Fehler innerhalb der adhesiven Eigenschaften von Endothelzellen vermuten. Desweiteren wurde Kleip als unverzichtbares Molekül für die neonatale Entwicklung identifiziert. Homozygote Nachkommen zeigten eine durch Atemnot verursachte hohe Säuglingssterblichkeit von ungefähr 50 Prozent. Histologische Untersuch-ungen der Lungen von neugeborenen Mutanten zeigten einen reduzierten Alveolarraum und eine deutliche

Verdickung der alveolaren Septen. Diese beiden morphologischen Veränderungen sind charakteristische Merkmale für Mängel in der Lungenreifung. Demnach zeigen unsere Studien den hohen Stellenwert von Kleip für die Lungen-Morphogenese und lassen eine mögliche Beteiligung in der Pathogenese des respiratorischen Distress-Syndromes (RDS) erkennen.
In zusätzlichen Teilprojekten wurden weitere ausgewählte Proteine der G-Protein-Signalkaskade im Hinblick auf die Angiogenese untersucht. Einerseits konnte zum ersten Mal gezeigt werden, dass der von dock180 und elmo1 gebildete GEF für die kleine GTPase Rac1 im Zebrafischendothel exprimiert wird. Außerdem resultierte die räumlich und zeitlich begrenzte Expressionsminderung von *elmo1* im ventralen Mesoderm mittels einem photoaktivierbaren Morpholino in einer starken Beeinträchtigung in der Entwicklung der Fischvaskulatur, wodurch elmo1 eine zellautonome Funktion im Endothel zugwiesen wird.

Neben der Analyse von GEFs und deren Rolle in der Angiogenese wurden auch die nachgelagerten Mediatoren des RhoA Signalweges untersucht. In früher durchgeführten Angiogenese relevanten Studien führte die pharmakologische Hemmung der beiden Serin/Threonin-Kinasen ROCK I/II mit dem relativ unspezifischen Inhibitor Y-27632 zu gegensätzlichen Ergebnissen. In dieser Arbeit konnte gezeigt werden, dass die Inhibition der ROCK I/II-Aktivität durch den Einsatz des Inhibitors H-1152 zu einer verstärkten Signalweiterleitung im Endothel führt. Folglich wird beiden Kinasen eine Rolle als negative Regulatoren der Angiogenese nachgesagt. Zusammenfassend konnten alle untersuchten G-Protein-Signalmoleküle als essentielle Regulatoren in der Bildung eines funktionellen Gefäßsystems identifiziert werden.

II. Summary

The members of the Rho family of small GTPases were originally identified to be involved in a variety of cellular processes, including regulation of F-actin cytoskeleton and microtubule dynamics, cell polarity, vesicle transport and gene expression. In recent studies G-proteins have been implicated to function as key modulators of angiogenesis. G-protein signaling is thereby strongly associated with angiogenic processes, such as the regulation of vascular permeability, remodeling of the extracellular matrix, endothelial migration, proliferation, morphogenesis, and survival. Much of our knowledge regarding G-protein signaling was hitherto predominantly obtained by *in vitro* experiments or by *in vivo* studies performed in invertebrates. However, little is known about their regulation and function in vertebrates. Thus, this thesis was aimed at uncovering the role of selected G-proteins during vertebrate development with the focus on angiogenesis. Recently, the guanine nucleotide exchange factor (GEF) Ect-2 interacting BTB-kelch protein KLEIP (KLHL20) was implicated in angiogenesis as a novel and essential regulator of endothelial function that controls the VEGF-induced activation of the small GTPase RhoA. In order to unravel Kleip's function during angiogenesis *in vivo*, as well as during development, the *Kleip* gene was disrupted in mice. Constitutive inactivation of *Kleip* accomplished by gene-trapping led to a partially lethal phenotype. Some *Kleip*-deficient embryos died between midgestation and birth due to cranial hemorrhages. This dysfunction in maintaining vascular integrity was furthermore supported by studies with splice-blocking morpholino-induced downregulation of *klhl20* in zebrafish embryos as well as by an *in vitro* transwell permeability assay. *Whole-mount* immunostainings of the embryonic vasculature in *Kleip*-mutants exhibited in comparison to their wild-type littermates significantly extended cranial vessels suggesting as well as for the bleedings a failure in the recruitment of mural cells to the nascent vessels. Interestingly, specific NG2 immunostainings displayed no alterations in pericyte coverage-mediated vessel stabilization thereby rather indicating defects in endothelial adhesion. Moreover, Kleip was identified to be indispensable for neonatal development. Homozygous offspring exhibited a high neonatal mortality from around 50% due to respiratory failure. Histological analysis of newborn mutant lungs exhibited reduced airspace, and marked thickening of alveolar septae, which represent the characteristic features of maturation defects. Thus, our studies demonstrate the importance of Kleip for lung morphogenesis and suggest that it could possibly be involved in the pathogenesis of respiratory distress syndroms (RDS).

In additional subprojects selected proteins of the G-protein signaling cascade were characterized with regard to angiogenesis. On the one hand it could be shown for the first time that the dock180 and elmo1 formed GEF for the small GTPase Rac1 is expressed in the zebrafish endothelium. Furthermore, the spatially and temporarily restricted photoactivatable morpholino-based expression-silencing of *elmo1* in the ventral mesoderm severely impaired

the formation of the fish vasculature, suggesting an endothelial cell autonomous function of elmo1.

Next to the analysis of GEFs during angiogenesis the downstream mediators of RhoA signaling were analyzed. In previous studies the pharmacological inhibition of both serine/threonine kinases ROCK I/II with the relative unspecific inhibitor Y-27632 revealed contrary results. Here it could be demonstrated that inhibition of ROCK I/II activity with the inhibitor H-1152 enhanced endothelial signaling implicating that both kinases function as negative regulators of sprouting angiogenesis. In conclusion, all analyzed G-protein signaling molecules were identified as essential regulators involved in the formation of a functional vasculature.

1. Introduction

1.1 Blood vessel development

The development of a functional vasculature is a crucial and complex process during development in the vertebrate embryo. The embryo receives its nutrition and oxygen through diffusion across short distances in the earliest stages of embryonic development (100-150µm). However, with the growth of the embryo it becomes harder to maintain a sufficient supply for the developing tissues and organs over longer distances, as well as in the elimination of all by-products. These requirements are evolutionary compensated through the formation of the cardiovascular system, the first functional organic unit in vertebrates.
Beyond this, the vasculature serves as a communication system between several tissues and organs in the adult, which is accomplished by messenger molecules such as hormones. The development of a functional vascular network is thereby subdivided into two distinct temporarily distinguishable events, called vasculogenesis and angiogenesis (Semenza, 2007).

1.1.1 Vasculogenesis

In general, the process of vasculogenesis is characterized by the *de novo* formation of a primitive vascular network (Adams and Alitalo, 2007; Risau, 1997). During the initial steps of vasculogenesis (Figure 1), which start in the mouse around embryonic day (E) 7.5, a common progenitor of endothelial and hematopoietic cells, called hemangioblast, is derived from the mesoderm (Herbert et al., 2009; Park et al., 2005; Vogeli et al., 2006). An assembly of these cells results in the formation of the blood islands, which consist of a peripheral layer of angioblasts, the intermediates of the endothelial lineage, and the inner cells of hematopoietic precursor cells. In a subsequent step the honeycomb-shaped primary capillary plexus is established by an alignment of angioblasts which are connected with each other through cellular protrusions. Afterwards, the cytoplasm of angioblasts degenerates and becomes contained in vacuoles that fuse with the vacuoles of neighboring angioblasts consequently forming lumenized vessels (Downs, 2003). This step is accompanied with the differentiation of endothelial cells from the angioblasts. In contrast, a direct aggregation of angioblasts gives rise to the major embryonic blood vessels, like the dorsal aorta and cardinal vein (Adams and Alitalo, 2007). Additionally, vasculogenesis is not restricted to embryonic development, because endothelial progenitor cells that are contributed to vessel formation can still be detected in the adult (Rafii et al., 2002). However, the importance and the extent of this mechanism remain controversial.

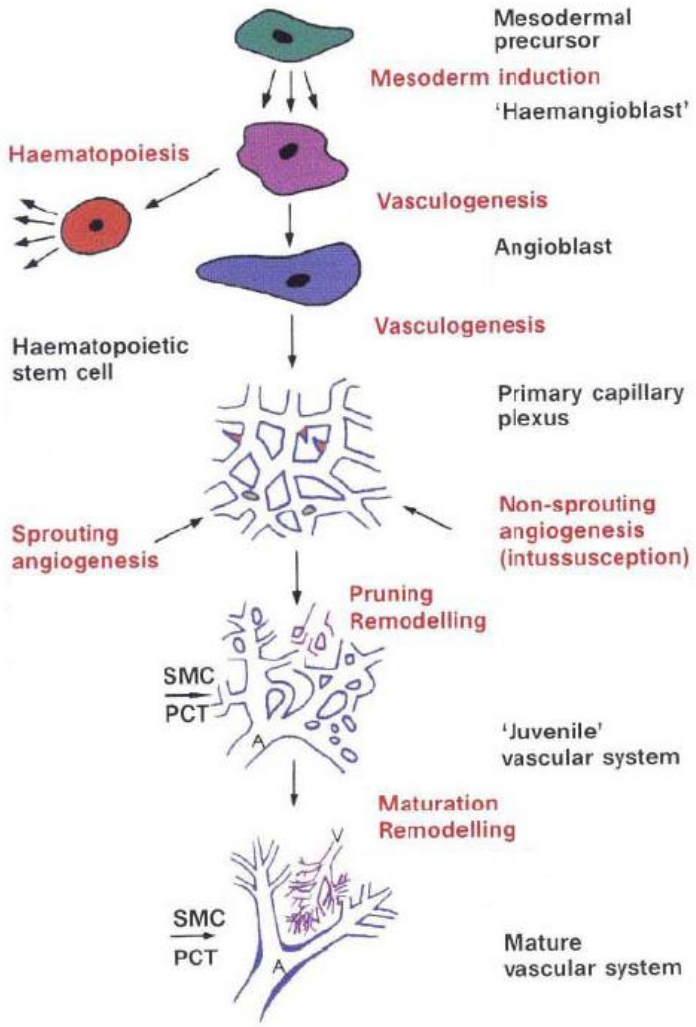

Figure 1: Schematic overview of vascular development.
Mesodermal cells differentiate into the bipotential progenitor cell, called hemangioblasts, of the endothelial and hematopoietic cell lineage. During vasculogenesis the angioblasts of the endothelial lineage form the honeycomb-shaped primary capillary plexus, which gets remodeled and extended by non-sprouting and sprouting angiogenesis. In the following maturation step the vessels get stabilized by the recruitment of mural cells, like pericytes (PCT) and smooth muscle cells (SMCs).(Adapted by permission from Macmillan Publishers Ltd: Nature (Risau, 1997), copyright 1997)

1.1.2 Angiogenesis

In the following step, the immature and poorly functional vasculature undergoes a remodeling and expansion process, which is termed angiogenesis. The process of angiogenesis (Figure 1) normally occurs embryonically and is completed in the adult. Angiogenesis starts around E8.5-E9.5 in the developing mouse embryo. However, under some physiological conditions angiogenesis can be induced, like during ovarian cycle and wound healing. Thereby angiogenesis can be subdivided into two distinct processes, namely sprouting angiogenesis and non-sprouting angiogenesis. Sprouting angiogenesis is defined in sprouting of capillaries from pre-existing vessels, whereas non-sprouting angiogenesis is characterized by the

splitting of already existing vessels along their longitudinal axis (Burri et al., 2004; Djonov and Makanya, 2005; Makanya et al., 2009; Risau, 1997).

In this intussuspective process of non-sprouting angiogenesis the new developing vessels are formed by insertion of interstitial tissue into the lumen of a pre-existing vessel or by bridging the vessel lumen with interstitial tissue columns. Intussuseception, first discovered in lungs, also includes the establishment of new vessels by formation of loops in large veins.

Finally, the developing circulatory system needs to be specified into different calibers and types of vessels (Figure 2). This differentiation process in which the arterial and venous systems emanate is known as arteriovenous differentiation. During arterial differentiation, termed arteriogenesis, the maturating arteries have to resist a growing shear stress and pulsatile flow. The ensuring of vessel stability is effected by the modification of the basal lamina and the recruitment of mural cells, including vascular smooth muscle cells (SMCs) and pericytes (von Tell et al., 2006).

Arteries with an extended luminal vessel diameter are surrounded by a thick layer of SMCs, providing viscoelastic and vasomotor properties that enable the regulation of arterial perfusion. In contrast the venous low-pressure system is enveloped by fewer SMCs.

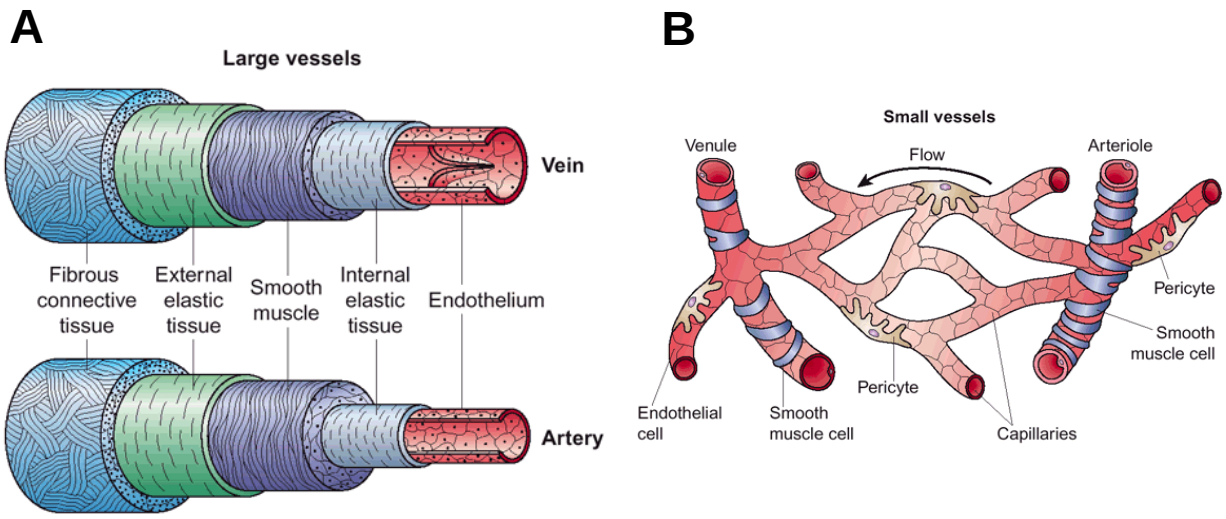

Figure 2: Morphology of small and large blood vessels stabilized by mural cells.
Vessel wall assembly is heterogeneous between vessels that differ in size, as well as between their arteriovenous differentiation state. Larger vessels are surrounded by multiple layers of cellular and extracellular materials (A). In general the vascular wall of larger vessel is composed of an inner endothelium (tunica intima) surrounded by a layer of SMCs (tunica media), external elastic tissue and fibrous connective tissue (tunica adventitia). In contrast to veins large arteries are enveloped in a thicker layer of SMCs to resist high shear stress and pulsatile flow, while the system of fine capillaries is covered by pericytes (B). Additionally, veins are the only vessels that have valves for preventing backflow of blood. (Adapted by permission from Macmillan Publishers Ltd: Nature Medicine (Cleaver and Melton, 2003), copyright 2003)

1.1.3 Arteriovenous differentiation

The differentiation of the arteriovenous system during development is a further critical step for proper formation of a functional vascular network during angiogenesis. In recent years it was believed that arteriovenous differentiation is mediated by physiological factors like the onset of blood flow and blood pressure, but several studies in mice and zebrafish models rather indicate the involvement of genetic regulation mechanisms (Swift and Weinstein, 2009; Torres-Vaazquez et al., 2003). Increasing evidence pointed out that the multifunctional angiogenic growth factor vascular endothelial growth factor (VEGF) is also involved in the promotion of arterial identity. Transgenic Vegf overexpressing mice display a numerical increase (Visconti et al., 2002), whereas in contrast a reduction of Vegf in zebrafish causes a numerical decrease of arteries (Lawson et al., 2002). A further arterial differentiation mechanism that is partially linked to VEGF signaling represents the DELTA/NOTCH signaling pathway. Several members of this family, including the ligands Delta4 (Dll4), Jagged (Jag)-1, Jag-2 and their transmembrane receptors Notch1, Notch3, and Notch4 are predominantly expressed by the arterial endothelium (Villa et al., 2001).

It has been shown in *in vitro* experiments that cultured endothelial cells exposed to VEGF-A upregulate surface markers, such as DLL4, the NOTCH receptors and ephrinB2 (Hainaud et al., 2006; Williams et al., 2006). The NOTCH ligand/receptor interaction mediates a direct activation of NOTCH, which in turn results in its proteolytical cleavage accompanied with the release of the NOTCH intracellular domain (ICD). The ICD is translocated to the nucleus, where it forms a complex with transcriptional regulators and induces the expression of transcription factors like e.g. HEY and HES. Mouse mutants that lack components of the Delta/Notch signaling pathway display severe vascular defects and die *in utero* (Fischer et al., 2004; Gale et al., 2004; Krebs et al., 2004). Other mediators involved in transcriptional regulation of arterial specification are the forkhead box transcription factors FOXC1 and FOXC2 (Seo et al., 2006). The chicken ovalbumin upstream promoter-transcription factor II (COUP-TFII) is among all known molecules that are restricted to the mediation of arterial identity the only molecule which is specifically contributed in the defining of the venous cell fate (You et al., 2005).

Another mechanism required for maintenance of both arterial and venous differentiation after vascular network formation comprises the interaction of ephrinB2/EphB4 (Heroult et al., 2006). Because of the fact that the transmembrane protein ephrinB2 is expressed on arterial endothelium and its receptor EphB4 on venous endothelium both proteins are frequently used as molecular markers for the identification of arteries and veins. Mutant mice either deficient for ephrinB2 or EphB4 die between E10.5-E11.5 days after gestation due to vascular maturation and arteriovenous differentiation defects (Gerety et al., 1999; Wang et al., 1998). This local distribution of ephrinB2 and EphB4 suggests an important role for the

controlling of vascular morphogenesis (Adams et al., 1999). Other molecules involved in arteriovenous differentiation include the neuropilins, which also display a distinct expression pattern. Neuropilin (Nrp) 1 is exclusively expressed in arteries, whereas Nrp2 is restricted to venous and lymphatic endothelial cells (Gu et al., 2003; Yuan et al., 2002).

1.2 Molecular regulation of angiogenesis

The formation of a functional vascular network is a tightly controlled sequence of events that include the angiogenic activation phase and a resolution phase (Carmeliet, 2003; Folkman and DAmore, 1996). Both phases are well orchestrated by the interplay of several growth factors, chemokines, transcription factors, and adhesion molecules. The existing vessels dilate during the activation phase, followed by the degradation of the extracellular matrix through the activation of matrix metalloproteinases (MMPs) as well as by an increase in vascular permeability. Afterwards, migration and proliferation of endothelial and mural cells occur to assemble new vessel sprouts. In the subsequent resolution phase, the mural cells, consisting of SMCs and pericytes, are recruited to the nascent vasculature to ensure vessel stability and perfusion, also known as arteriogenesis. This phase is finally completed by the assembly of a basement membrane between the endothelial cells and the SMCs (Pepper, 1997). Taken together, only a well coordinated combination of genetic programming and extrinsic influences result in a functional network of blood vessels.

1.2.1 Sprouting angiogenesis and vessel maturation

Sprouting angiogenesis is initiated by various signaling pathways and genetic programs that follow a series of sequential activation steps. First, the expression of angiogenic regulators such as vascular endothelial growth factor (VEGF) or endothelial nitric oxide synthase (eNOS) gets activated (Ku et al., 1993; Ziche et al., 1997; Ziche et al., 1994). During this activation phase VEGF stimulates the expression of nitric oxide (NO) with the help of eNOS, which catalyzes this production. In response to the VEGF signaling the NO release mediates vasodilatation coincidental with the VEGF-induced permeability. Vascular permeability is accompanied with the rearrangement of intercellular adhesion molecules, such as vascular endothelial (VE)-cadherin and the platelet endothelial cell adhesion molecule (PECAM)-1 (Dvorak et al., 1999).

The extracellular matrix (ECM) and basal lamina requires a remodeling/breakdown to facilitate angiogenic sprouting formation, which is mediated by several proteinases, such as metalloproteases, plasminogen activators, heparinases and cathepsins (Carmeliet, 2003). Moreover, the degradation of ECM liberates matrix-bound growth factors like VEGF and basic fibroblast growth factor (bFGF) (Lee et al., 2005; Turner et al., 2005).

Subsequently, the liberation enables the guided migration of the developing vessel sprout (Figure 3) towards a VEGF gradient. The branching vessel can be subdivided into several types of specialized endothelial cells with distinct cellular fate specifications (De Smet et al., 2009; Horowitz and Simons, 2008). During this navigation process the front situated cell, termed “tip-cell”, utilizes its numerous filopodial extensions for sensing and responding to guidance cues, like VEGF, in their microenviroment (Gerhardt et al., 2003; Ruhrberg, 2003). Endothelial cells that are located behind the tip cell are called stalk. Stalk cells are essential for the elongation of the vessel branch, which is accomplished by proliferation. This type of endothelial cells features further characteristics, like the formation of junctions and lumen. Additionally, stalk cells are trailed by the recently discovered phalanx cells that ensure cell quiescence elicited to their coverage of mural cells and their tight junctions (Gerhardt, 2008).

During the resolution phase of angiogenesis, the newly formed blood vessels are stabilized by the vascular basement membrane and by the recruitment of mural cells, like SMCs and pericytes. At least four signaling pathways contribute to this blood vessel maturation process. Upon VEGF stimulation platelet derived growth factor (Pdgf) B is primarily secreted by endothelial cells thereby mediating the recruitment of pericytes, which express its receptor Pdgfr-β (Hellstrom et al., 2001; von Tell et al., 2006). Mice lacking either Pdgf-B or Pdgfr-β display diminished pericyte coverage in many, but not all organs (Hellstrom et al., 1999; Lindahl et al., 1997). Finally, deficient animals die around birth because of leaky microvessels and multiple microaneurysms (Leveen et al., 1994; Soriano, 1994) induced to endothelial cell overproliferation and failure in forming inter-endothelial junctions (von Tell et al., 2006).

Another signaling system involved in vessel growth and stabilization is the angiopoietin/Tie-system, which consists of the angiopoetins (Ang-1 and Ang-2) and their tyrosine kinase receptors (Tie1 and Tie2). Ang-1 is constitutively expressed by numerous cell types, whereas its apparent counterpart Ang-2 is almost exclusively endothelial specific. While the binding of the growth factor Ang-1 to the receptor Tie-2 implicates cell quiescence and vessel stability, the binding of Ang-2 to Tie-2 controls vascular homeostasis through an autocrine loop mechanism (Scharpfenecker et al., 2005). In the absence of angiogenic growth factors the Ang-2/Tie2 interaction mediates vessel regression caused by detachment of the endothelium from SMCs (Maisonpierre et al., 1997; Visconti et al., 2002). In contrast, their presence enhances pro-angiogencic function (Visconti et al., 2002). However, the complete role of angiopoietin signaling during vessel maturation is not fully understood. Further signaling pathways that are associated with vessel maturation and stabilization include the transforming growth factor (TGF)-β superfamily (Goumans et al., 2009) and the interaction of the G-protein-coupled receptor Edg1 with its ligand sphingosine-1-phosphate (Kluk and Hla, 2002).

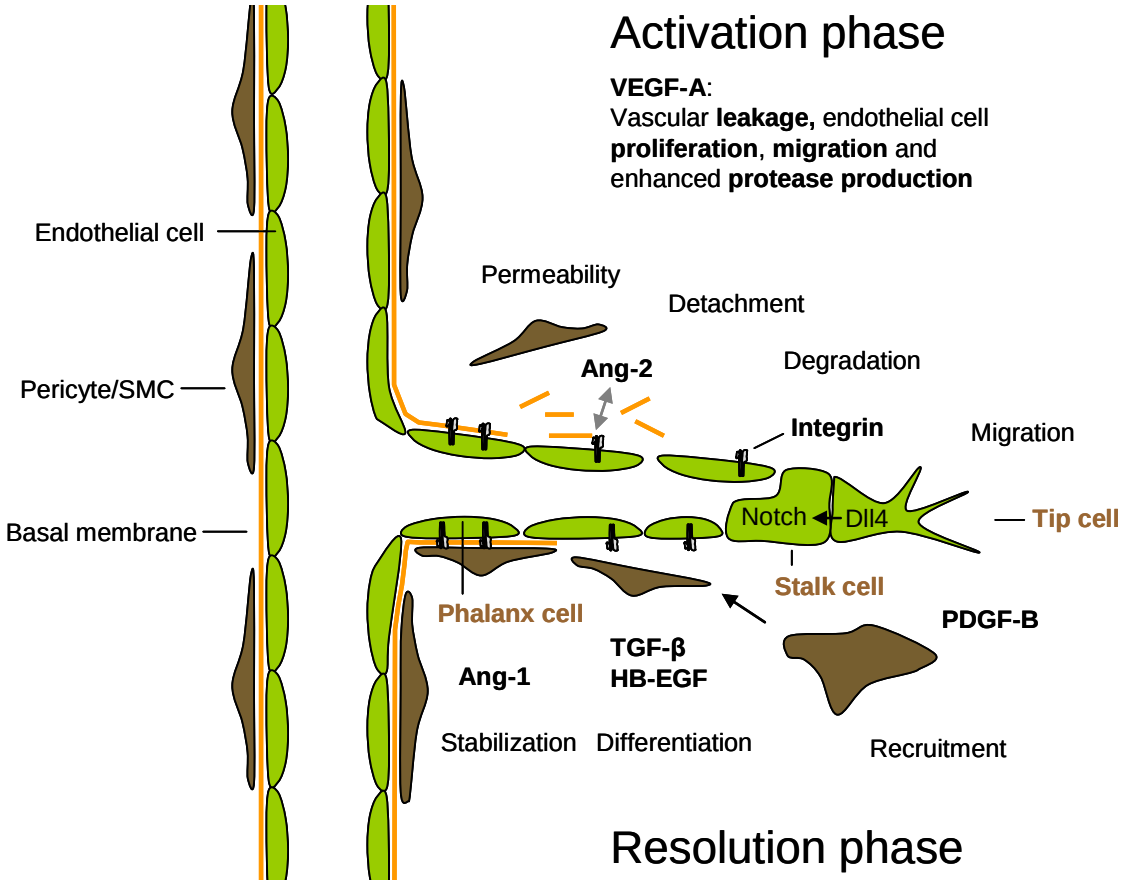

Figure 3: Regulation of angiogenesis.
The activation phase of angiogenesis is induced by VEGF signaling that causes an increase in vascular permeability, followed by proteases mediated degradation of basal lamina and extracellular matrix, endothelial cell migration and proliferation. Vessel destabilization is supported by Ang-2 which enhances the detachment of endothelial cells from SMCs. During the vessel guidance process towards the growth factor gradient the developing sprout can be subdivided in tip, stalk and phalanx cells. The tip cell stalk cell identity is thereby regulated by the Dll4/Notch signaling pathway. During resolution phase, vessels are stabilized by PDGF-B-mediated recruitment of pericytes. Ang-1 and TGF-β signaling further support vessel maturation by pericyte differentiation and stabilization, respectively. (Adapted by permission from PhD thesis of Markus Thomas)

1.2.2 Hypoxia

Hypoxia was identified as the potent key regulator to induce angiogenesis during embryonic development as well as through tumor progression. Hypoxia serves in this regulation process as an important homeostatic mechanism that links vascular oxgen supply to metabolic demand via a tightly controlled interplay of hypoxia inducible factors (HIFs) and HIF hydroxylases. The induction of angiogenesis is mediated by transcritption factors of the HIF family, which consists of three family members (HIF-1 to -3). The transcription factors form heterodimers existing of either one of three HIF-α subunits together with the HIF-1β subunit. HIF-α subunits are inducible by hypoxia, whereas HIF-1β subunits are constitutively located

in the nucleus. Under normal oxygen conditions the two independent hydroxylation sites on the HIF-α subunits provide a dual mechanism of inactivation. On the one hand HIF-α subunits get modificated through the prolyl-hydroxylases and degraded by the proteasomal degradation pathway, whereas the catalytic hydroxylation of the second site results in inhibition of transcriptional activity (Ivan et al., 2001; Mahon et al., 2001; Masson et al., 2001). In contrast, under low oxygen conditions hydroxylases are inactive and mediate the translocalization of the HIF-α subunits into the nucleus. After accumulation of the subunits the transcription factors initiate the expression as well as the segregation of angiogenic growth factors, such as VEGF, bFGF, angiopoietins, and their receptors (Pugh and Ratcliffe, 2003).

1.2.3 Guidance molecules

The vascular system of vertebrates, as well as their nervous system, reveals anatomic and structural similarities. Recent studies have highlighted that both blood vessels and nerves often follow parallel routes and require a precise control over their guidance and growth to establish a functional network. Normally the assembly of an artery, a vein, and a nerve form the neurovascular bundle which implicate, based on the close proximity, an advantage for both systems. On the one hand the supply of large nerves with oxygen and nutrients is ensured by the surrounding vessels, whereas on the other hand especially arteries require innervations to control vasoconstriction or dilation (Larrivee et al., 2009). In the past, several molecules, also known as guidance cues, were identified to play an important role in the guidance of nerves. Guidance molecules, mostly consisting of secreted ligands and membrane receptors, were first characterized in the nervous system, before their possible role was identified in the vascular system. The outgrowing axons carry specialized terminal cells, termed the axonal growth cones that mediate the navigation through the tissue by sensing attractive or repulsive signaling cues. Moreover, an equivalent of the growth cones was assigned to the tip cells of the growing vascular sprouts (le Noble et al., 2008).

1.2.4 Vascular guidance

Among the numerous growth factors involved in vascular development, members of the VEGF family were identified as the key regulators. In humans and mice the VEGF family includes five members (Figure 4), namely VEGF-A to VEGF-D, and placenta growth factor (PLGF). In recent years the two related proteins VEGF-E, identified in parapoxvirus (Ogawa et al., 1998), and VEGF-F in snake venom could be added (Suto et al., 2005) to the VEGF family. All VEGF family members mediate their signaling through binding to tyrosine-kinase receptors, like VEGFR-1 (Flt-1), VEGFR-2 (KDR, Flk1) and VEGFR-3 (Flt-4). The approximately 230kDa VEGF receptors belong to the transmembrane proteins and are

composed of an extra- and intracellular domain. The extracellular domain consists of seven (VEGFR-1 and -2) or six (VEGF-3) immunoglobulin (Ig) like domains and the intracellular domain is organized by a split tyrosine-kinase. Upon binding of VEGF, the VEGFRs form homo- and heterodimers which mediate its activation via an autophosphorylation of several tyrosine residues located in the intracellular domain. Activated receptors recruit intracellular mediators which activate different downstream signaling pathways. VEGFR-1 and VEGFR-2 are almost exclusively expressed on endothelial cells, whereas VEGFR-3 is primarily expressed by lymphatic endothelial cells in the healthy adult. Although VEGFR-3 signaling is mainly restricted to lymphangiogenesis it could be shown that VEGFR-3 is also expressed on endothelial cells and involved in cardiovascular development (Dumont et al., 1998).

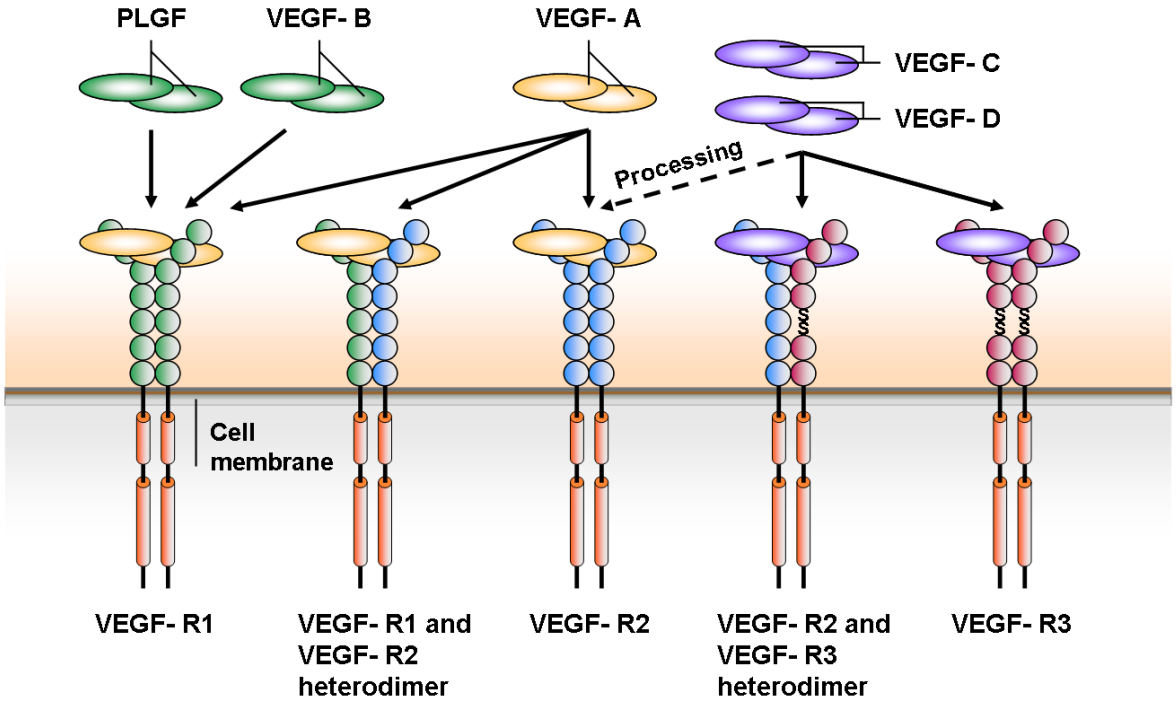

Figure 4: Schematic overview of VEGF-receptors and ligands.
The mammalian vascular endothelial growth factors (VEGF) A-D and Placental growth factor (PLGF) bind to three VEGF receptor tyrosine kinases (VEGFR), which are able to form homo- or heterodimers. For instance, VEGF-A binds to VEGFR-1 and-2, while VEGF-B and PLGF preferentially bind VEGFR1. Proteolytic processing of VEGF-C and -D features VEGFR2-binding. (Adapted and modified by permission from Macmillan Publishers Ltd: Nature Reviews Molecular Cell Biology (Olsson et al., 2006), copyright 2006)

The most predominant form of the approximately 40kDa secreted ligands which preferentially form homodimers is VEGF-A (Muller et al., 1997; Neufeld et al., 1999). Due to alternative splicing of the *VEGF-A* mRNA various number of isoforms with different biological functions are generated (Neufeld et al., 1999). In general, the binding of VEGF-A to VEGFR-2 induces

endothelial cell proliferation, migration and survival (Ferrara et al., 2003). Furthermore, its signaling is linked to cellular processes, such as the regulation of protease production and vascular permeability (Senger, 1983). The targeted inactivation of a single *Vegf-a* allele results in embryonic lethality between E11.5 to E12.5 due to vascular abnormalities (Carmeliet et al., 1996; Ferrara et al., 1996), whereas a complete disruption of *Vegf-a* leads even to an earlier lethal phenotype (E9.5-E10.5) with severe vascular malformations. Similar observations were made in transgenic mice that lack receptor Vegfr-2 (Shalaby et al., 1995). Additionally, mice deficient for Vegfr-1 display a disorganized vascular endothelium caused by endothelial cell overgrowth resulting in embryonic death around E8.5 (Fong et al., 1995). In context to the tip-cell/stalk-cell communication it could be shown that Vegfr-2 is prominent expressed in the tips of the sprouts. Tip cells sense and initiate the direct migration towards the Vegf-a gradient via its actin-rich protrusions, also known as filopodia. However, the tip cells are not capable to elongate the vessel sprout because they do not proliferate. In contrast, the sprout extension is accompanied by the subsequently following stalk cells that still possess this efficiency. An additional system involved in vessel guidance includes the DELTA/NOTCH system. Although its signaling is less associated to chemotactic guidance of the forming sprouts, it may be rather important in the regulation of the tip-cell/stalk-cell identity (Gerhardt, 2008). In several studies mainly performed in mouse retinae and zebrafish it has been recently shown, that Dll4 is upregulated in the tip cells in response to VEGF stimulation and hypoxia (Diez et al., 2007; Lobov et al., 2007). The binding of Dll4 to its Notch-1 receptor on the neighboring cell activates a signaling cascade, which mediates the transformation of these cell into a stalk cell with its typical quiescent and non-sprouting identity. Furthermore, it has been hypothesized that NOTCH-1 signaling coincidentally leads to a downregulation of VEGFR-2 levels (Williams et al., 2006). This model is supported by *in vivo* findings in which mice and zebrafish deficient for Dll4 exhibit a numeric increase of endothelial tip cells (Gerhardt, 2008).

1.3 Role of Rho-GTPases during angiogenesis

Small guanosine triphosphatases (GTPases) from the Ras superfamily of monomeric 20-30 kDa GTP-binding proteins are known to be key regulators of many diverse developmental and cellular events (Wennerberg et al., 2005). Especially the subfamily of Ras homologous (Rho) proteins, with its extensively characterized members RhoA, Rac1, and Cdc42, are involved in processes including the regulation of cytoskeletal dynamics, cell division, gene expression, cell proliferation, apoptosis, vesicle transport, and transcription factor activity during normal as well as during pathological conditions (Bryan and D'Amore, 2007). To this day 23 members of Rho GTPases have been identified in mammals where all of them display an ubiquitous distribution pattern during development (Bustelo et al., 2007). In recent years a growing number of studies have implicated the RhoA-GTPases to be involved in the regulation of several angiogenic processes, such as vascular permeability, ECM remodeling, proliferation, morphogenesis, migration, and survival. RhoA-GTPases were identified to function as essential downstream effectors of VEGF signaling. They act as molecular switches cycling between an active guanosine triphosphate (GTP)-bound and an inactive guanosine diphosphate (GDP)-loaded state. Thus, only the activated state of small GTPases binds effectors and allows transmission of upstream signals. This cyclic activation and inactivation process is spatiotemporally controlled and tightly coordinated by three known classes of regulatory proteins. Guanine nucleotide exchange factors (GEFs) promote the activation by the displacement of GDP to GTP, while the GTPase-activating proteins stimulate the intrinsic GTP-hydrolytic activity of Rho GTPases, leading to a return to the GDP-bound conformation (Beckers et al., 2010; Rossman et al., 2005; Tcherkezian and Lamarche-Vane, 2007). In addition, the third class of regulatory proteins consists of the Rho guanine nucleotide dissociation inhibitors (GDIs), which are believed to block the GTPase cycling by sequestration of the GTPase within the cytosol and the stabilization of the GDP-bound form (DerMardirossian and Bokoch, 2005). Among the array of Rho-GTPases the serine/threonine Rho-associated coiled-coil protein kinases (ROCKs) are the best studied RhoA effectors. ROCKs regulate the contractility of the actomyosin cytoskeleton via phosphorylation of myosin light chain (MLC) and the myosin-subunit of myosin phosphatase. In addition, they are also involved in the activation of LIM-kinase, which in turn contributes to Rho-induced reorganization of the actin cytoskeleton via its mediator protein cofilin (Zhao and Manser, 2005). However its function during the angiogenic process of vascular branching is discussed controversially (van Nieuw Amerongen and van Hinsbergh, 2009). Some reports assume that ROCKs mediate pro-angiogenic properties (Hata et al., 2008; Yin et al., 2007), whereas others implicate ROCK to function anti-angiogenically. For instance, the transient inhibition of RhoA/ROCK-signaling caused an augmentation of blood vessel sprouting and length (Mavria et al., 2006; Su et al., 2004).

The first phases of sprouting angiogenesis are associated with enhanced vascular permeability, which is initiated by alterations in adherens and tight junctions-mediated integrity (Mehta and Malik, 2006). Today it is well known that RhoA-signaling promotes vascular permeability whereas the small GTPases Rac1 and Cdc42 appear to regulate barrier function in an antagonistic manner via stabilization of the integrity of junctional complexes. Further, the features and functions of small GTPases in endothelial permeability will be explained in detail in chapter 1.4.2.2. Beside the importance of small GTPases in the regulation of vascular permeability they have been implicated in degradation of the basement membrane and the remodeling of the ECM. Several studies primarily performed in non-endothelial cells have demonstrated that Rho-signaling induces the expression and secretion of MMPs, which in turn results in the modulation of the ECM (Turchi et al., 2003; Turner et al., 2005). In contrast to these findings Rac1-signaling mediates opposing effects due to the inhibition of MMP activity which is caused by enhanced expression of tissue inhibitors of MMPs (TIMPs) (Engers et al., 2001). A similar role of RhoA- and Rac1-signaling in ECM reorganization has been reported for endothelial cells. While ectopic expression of constitutive active RhoA leads to an increase in MMP-9 secretion and lamelliopodia formation (Abecassis et al., 2003), an overexpression of its antagonist TIMP-2 inhibits the migratory activity consistent with the subsequent inactivation of Rac1 due to the disassembly of the Paxilin-Crk-DOCK180 complex (Oh et al., 2006). Noteworthy is here the dedicator of cytokinesis 180 (DOCK180) protein, which acts as a nucleotide exchange factor for the Rho-protein Rac1 through its Docker GEF domain. Several reports could show that DOCK180 reveal essential functions during phagocytosis, cell migration, dorsal closure and in the organization of the cytoskeleton (Lu and Ravichandran, 2006). Based on the fact that small GTPases are key mediators in the regulation of cytoskeletal rearrangements they are furthermore important for the angiogenic process of endothelial cell migration. In general, the forward movement of a cell is accomplished by the activation of Cdc42 and Rac1 which in turn regulate the reorganization of the cytoskeleton and mediate the formation of filopodia (Cdc42) and lamellipodia (Rac1) at its leading edge. On the other hand simultaneous RhoA-signaling promotes cytoskeletal contraction at the rear site of the cell, resulting in the cellular detachment and retraction of the cell (Raftopoulou and Hall, 2004). Moreover, the migratory process of endothelial cell during angiogenesis is tightly connected to proliferation, which is important for the elongation of the developing vessel sprout. In the past several signaling pathways such as the Ras/MAPK pathway have been identified to be important for the regulation of endothelial cell cycle progression. Another pivotal process involved in proliferation represents the Rho-protein-mediated mechanism of cytoskeleton modulation. Its importance for proliferation has been demonstrated by the pharmacological disruption of the cytoskeleton, which in turn results in a cell cycle arrest in the G1 phase (Huang and Ingber,

2002). This suggests that the actin cytoskeleton reorganization is necessary for the transition from the G1 to the S phase. Several reports indicate that Rho/ROCK signaling alters cell cycle regulatory proteins via multiple mechanisms. For instance, the levels of Cyclin D1 and p21(Cip) are upregulated via Ras/MAPK signaling, Cyclin A via LIM-kinase signaling and p27(Kip1) via a yet unknown mechanism (Croft and Olson, 2006). Furthermore, activated Rac1 and Cdc42 were also identified to increase the expression levels of Cyclin A and Cyclin D1 and to participate in the proteasomal degradation of p21 (Cip) (Bao et al., 2002; Page et al., 1999; Philips et al., 2000).

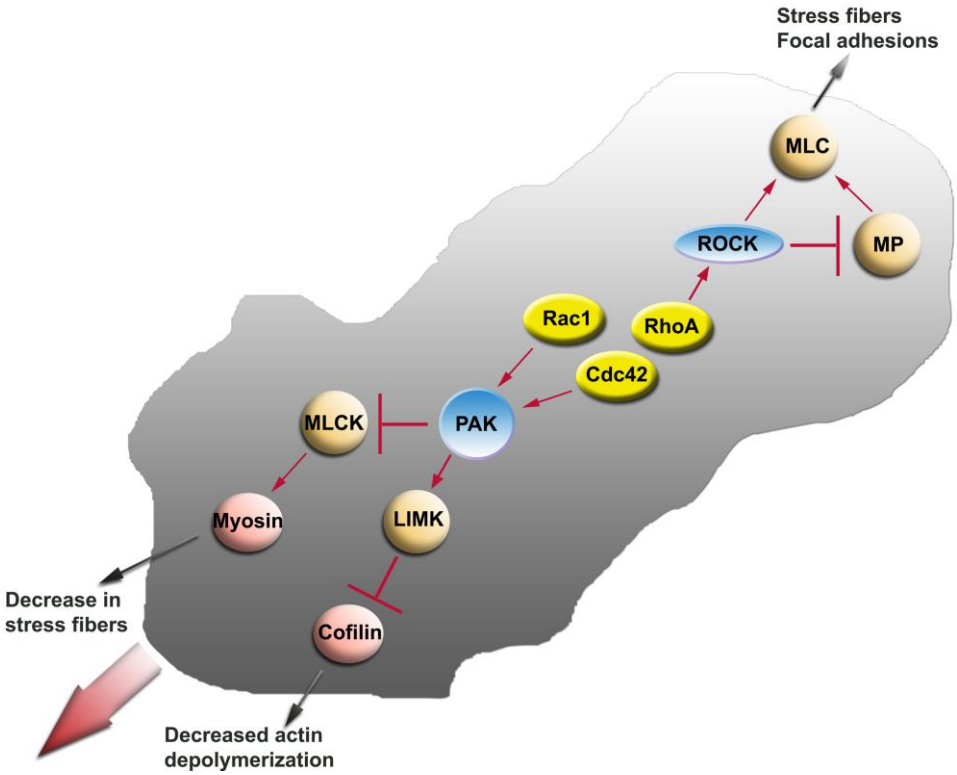

Figure 5: Endothelial migration is coordinated by Rho-proteins.
At the leading edge of the cell, the spatial activated small GTPases Cdc42 and Rac1 stimulate several distinct downstream targets (e.g. PAK) which mediate the rearrangement of the actin cytoskeleton. While Cdc42 signaling promotes the formation of migratory and actin-rich filopodia, activated Rac1 mediates lamellipodia formation. At the rear site RhoA signaling elicits the simultaneous detachment of the cell due to the actomyosin-based cytoskeletal contraction. Only a well coordinated interplay of both events leads to endothelial cell migration. (Adapted and modified by permission from Springer Science & Business: Cellular and Molecular Life Sciences (Bryan and D'Amore, 2007), copyright 2007)

In addition to that only seven of twenty three Rho GTPase family members have been so far deleted in mice. Although global RhoA knockout mice do not exist, it has been suggested that they display a lethal phenotype, like it was described for Rac1 and Cdc42 knockouts (Heasman and Ridley, 2008). In contrast, the characterized phenotypes of conditional Rac1- and global RhoB-knockouts indicate the importance for small GTPases in angiogenesis.

While specific deletion of Rac1 in Tie-2 expressing endothelial cells results in embryonic lethality around E9.5 due to defects in vascular development (Tan et al., 2008), others did not observe angiogenic deficiencies by the usage of a Pdgfb-iCreER-inducible system (D'Amico et al., 2010). In addition, RhoB-null mice are viable and display beside their growth retardation no major developmental defects (Liu et al., 2001). However, it has been shown that RhoB-mice exhibit a delay and altered vessel sprouting within the retina (Adini et al., 2003).

1.4 Endothelial barrier function and vascular permeability

In the vasculature endothelial cells mediate the separation of blood from the surrounding tissue. However, the endothelium is not a rigid structure it is moreover a semi-permeable barrier which regulates the exchange of plasma fluids and proteins as well as the cellular transmigration between the blood and interstitial space (Mehta and Malik, 2006).

Under normal healthy conditions the endothelial cells of the adult vasculature are adhered tightly to each other and their proliferation is contact-inhibited (Lampugnani et al., 1997; Vinals and Pouyssegur, 1999). Only one in every 10.000 endothelial cells is in the cell division cycle (Engerman et al., 1967; Hobson and Denekamp, 1984). In this state of so called “endothelial cell quiescence” the cells are less sensitive to growth factors (Lampugnani et al., 2003) and protected from apoptosis. This characteristic is maintained by cell-cell and cell-matrix protein interactions. The cell-cell interactions are mediated by adhesive properties of specific proteins that comprise the two classes of adherens junctions (AJs) and tight junctions (TJs), whereas the cell-matrix protein interactions are achieved by focal adhesions, primarily composed of integrins. AJ organization is important for vascular development and remodeling, whereas tight junctions are more essential for the regulation of endothelial barrier function. Though, the crucial regulation of endothelial permeability is indispensable for maintaining vascular homeostasis and physiological function. In contrast, an uncontrolled and lasting increase in permeability due to microvascular barrier dysfunction and endothelial hyperpermeability is closely linked to pathophysiological conditions and diseases, including inflammation, sepsis, ischemia, diabetes and tumor metastasis (Kumar et al., 2009).

1.4.1 Vascular integrity mediated by endothelial cell junctions

In general, the endothelial-cell junctions, TJs as well as AJs, represent a complex network of homophilic transmembrane proteins that form a pericellular zipper-like structure along the cell border. In comparison to the epithelium where TJs are usually located at the apical side of the intercellular cleft, endothelial cells reveal intermingled tight and adherens junctions all the way along the cleft (Dejana, 2004). Furthermore, in contrast to epithelial cells, endothelial

cells lack typical desmosomes (Dejana et al., 2009). Although, TJs and AJs display similar features both are formed by different molecules. In the endothelium AJs represent the majority of interendothelial junctions. AJs are mainly composed of VE-cadherin, a transmembrane receptor whose extracellular domain homophilically binds to extracellular domain of a further VE-cadherin molecule expressed on the surface of an adjacent cell. However, in its absence neuronal (N)-cadherin expression is increased and supports barrier stabilization (Navarro et al., 1998). Mice with an inactivation of VE-cadherin gene die at E9.5 of gestation because of impaired vascular remodeling and maturation accomplished by an increase in the number of apoptotic cells (Carmeliet et al., 1999; Gory-Faure et al., 1999). VE-cadherin depleted endothelial cells were successive disconnected from each other and detached from the basement membrane, implicating vessel regression, collapse and hemorrhages. A similar vascular phenotype displays the mice with an endothelial-specific deletion of N-cadherin (Luo and Radice, 2005). Moreover, N-cadherin is recommended to be important for mediating pericytic-endothelial interaction (Gerhardt et al., 2000; Tillet et al., 2005). In contrast, the core components of endothelial TJs are mainly formed by the adhesive properties of the claudin family (Furuse and Tsukita, 2006; Van Itallie and Anderson, 2006), which includes the vascular specific and predominant expressed member Claudin-5 (Nitta et al., 2003). Additional transmembrane adhesion proteins that are involved in the assembly of TJs includes the members of the occludin family, junctional adhesion molecules (JAMs) and endothelial cell selective adhesion molecule (ESAM) (Dejana et al., 2009). Both AJs and TJs are connected to cytoskeletal and signaling proteins through their cytoplasmatic tail, which allows on the one hand the anchoring of the adhesion proteins to the actin cytoskeleton as well as the transfer of intracellular signals (Dejana, 2004). The AJ component cadherin is associated directly to several intracellular partners including the catenins, like β-catenin, plakoglobin and p-120 (Nyqvist et al., 2008), whereas the interaction of the TJs with the cytoskeleton is mediated through the proteins Zonula occludens (ZO)1, ZO2 and Cingulin (Matter and Balda, 2003). Beside the specialized junctional complexes of AJs and TJs EC express further molecules with adhesive properties including the immunglobulins PECAM-1 (CD31), S-endo-1 (also known as MUC18 or CD146) and Nectin (Dejana, 2004). In addition the cell-matrix interaction is achieved by focal adhesions that are primarily formed by the integrin family. Integrins are type I transmembrane glycoproteins and comprises in mammals over nineteen α- and eight β-subunits, which combine differentially and give rise to an array of 25 heterodimeric adhesive molecules (Humphries, 2000). Next to the mediation of cellular connections to ECM proteins like collagen, fibronectin, laminin or proteoglycans, integrins are also contributed to cellular migration and activation of intracellular pathways (Gumbiner, 1996). Among all integrins ten are reported to be expressed on endothelial cells. The most prominent form is thereby $\alpha_v\beta_3$ integrin, which is

strongly upregulated on EC during angiogenesis is $\alpha_v\beta_3$ integrin. Its targeted inhibiton via specific antagonists leads to an increase in venular permeability (Wu et al., 2001). Moreover mice lacking the α_v subunit exhibit extensive vasculogenesis and angiogenesis consisting with intracerebral hemorrhages (Bader et al., 1998).

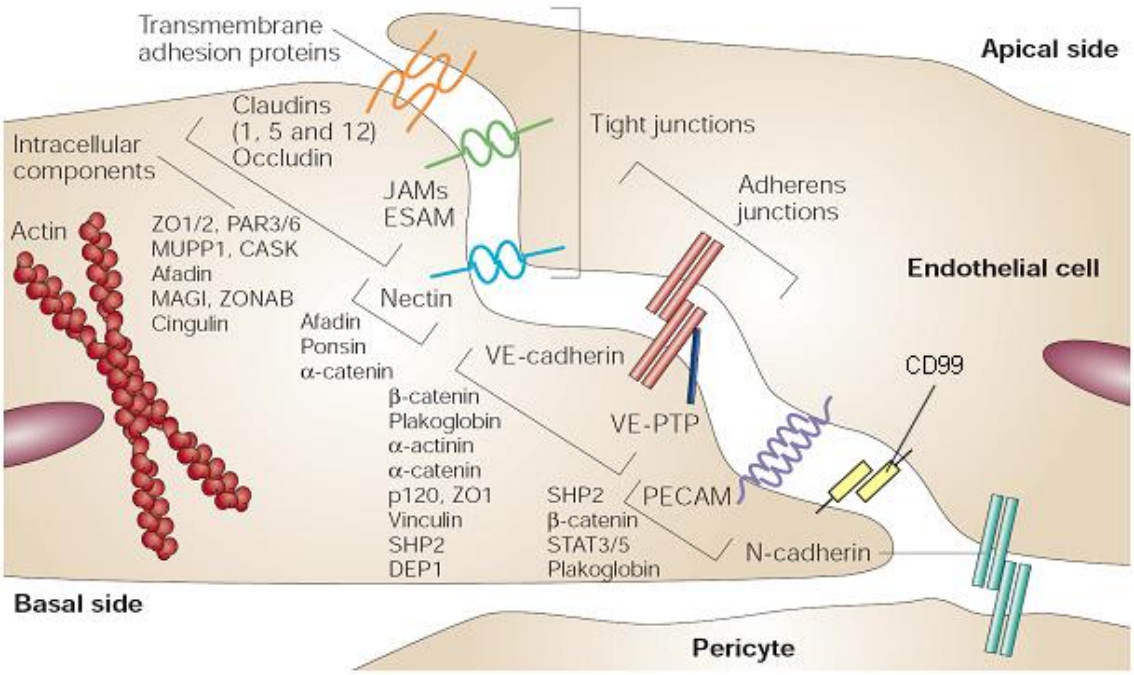

Figure 6: Schematic overview of the molecular organization of endothelial cell-junctions. Vascular barrier function is mediated through tight (TJs) and adherens (AJs) junctions which are composed of transmembrane adhesion proteins. At TJs adhesion is promoted by members of the claudin and occludin family as well as by the junctional adhesion molecule (JAM) family, whereas at endothelial AJs, adhesion is exclusively mediated through vascular endothelial (VE)-cadherin. Transmembrane adhesion proteins thereby bind to different intracellular partners that are associated to intracellular signaling and reorganization of the actin cytoskeleton. Platelet endothelial cell adhesion molecule (PECAM-1) represents a further molecule contributed to cell-cell adhesion. In contrast endothelial expressed neuronal (N)-cadherin probably mediates binding to pericytes or other mesenchymal cells. (Adapted by permission from Macmillan Publishers Ltd: Nature Reviews Molecular Cell Biology (Dejana, 2004) , copyright 2004)

1.4.2 Regulation of junctional permeability

1.4.2.1 Intracellular signal transduction

Vascular permeability is mediated by a least two major pathways that allow solutes to traverse the endothelium, namely the paracellular and transcellular pathway. The first is controlled by a coordinated opening and closure of interendothelial junctions that allows free passaging of macromolecules in the range of 3 nm in diameter and beneath (Vandenbroucke et al., 2008). In contrast, the transcellular pathway promotes the transport via vesicular transport systems, fenestrae and biochemical transporters (Dvorak et al., 1996). However, in the following the focus will be set on the regulation of the paracellular pathway.

1.4.2.2 Role of small GTPases in control of vascular permeability

In the past much attention has been given to the regulation of AJs, with their major component VE-cadherin. Although the binding of catenins to VE-cadherin is required for maintaining AJ integrity, the p120 binding to VE-cadherin is probably the most important component in mediating AJ stability (Xia et al., 2003). Unlike β-catenin and plakoglobin, p120 is not associated to the actin cytoskeleton (Reynolds and Roczniak-Ferguson, 2004). Moreover, p120 functions as a scaffold for regulatory proteins, such as cadherins, kinases, phosphatases and RhoGTPases, which in turn modulate AJs function by controlling the phosphorylation state of p120 and other AJ binding partners (Mehta and Malik, 2006; Reynolds and Roczniak-Ferguson, 2004). In addition to that further studies allocate p120 to play role in the regulation of VE-cadherin expression, because of its interaction properties with the molecular motor kinesin and transcription factor kaiso (Kondapalli et al., 2004; Yanagisawa et al., 2004). All of these described p120-functions are capable to control endothelial permeability by multiple mechanisms. In general the regulation of vascular permeability is accompanied with the dynamic interactions between the junctional proteins among each other and with the actin cytoskeleton. Both events are tightly controlled by small GTPases. In a quiescent endothelium AJs and TJs are stabilized by a cortical actin band (Spindler et al., 2010), whereas RhoA-mediated reorganization of actin into contractile stress fibers leads to disassociation of the adhesion-mediating components, which in turn leads to an increase of vascular permeability. Stress fibers are thereby composed of filamentous (F) actin and myosin II. In one of the first steps of stress fiber formation the MLC gets phosphorylated by a MLC kinase (MLCK) in a Ca^{2+}/calmodulin-dependent manner (Goeckeler and Wysolmerski, 1995). Though, the phosphorylation state of MLC is additionally enhanced through the coincidental inhibition of the MLC phosphatase activity. Both steps are mediated through the Rho kinases (ROCKs), downstream effectors of the small GTPase RhoA (Amano et al., 2000). Consisting with the induced actin-myosin contraction, centripetal forces are generated that actively pulls membranes of adjacent cells apart. This event in turn results in disassociation of AJs, thereby producing interendothelial gaps (Millan et al., 2010; Moy et al., 1996).

A further mechanism that is responsible for AJ disassociation and interendothelial gap formation involves microtubule disassembly (Mehta and Malik, 2006). Vasoactive agents, including TNF-α, thrombin and TGF-β, have been reported to cause microtubule disassembly and induce barrier breakdown through increased endothelial contraction (Birukova et al., 2005). Microtubule destabilization is induced by a RhoA/Rock-dependent, but MLCK-independent, signaling pathway (Petrache et al., 2003). Instead it has been recently demonstrated that thrombin-stimulated endothelial cells mediate their signaling through the Lim domain containing kinase 1 (LIMK1), another downstream target of ROCK, and thereby

regulating microtubule disassembly and stress fiber formation/linking microtubule dynamics to actin-myosin contraction (Gorovoy et al., 2005).

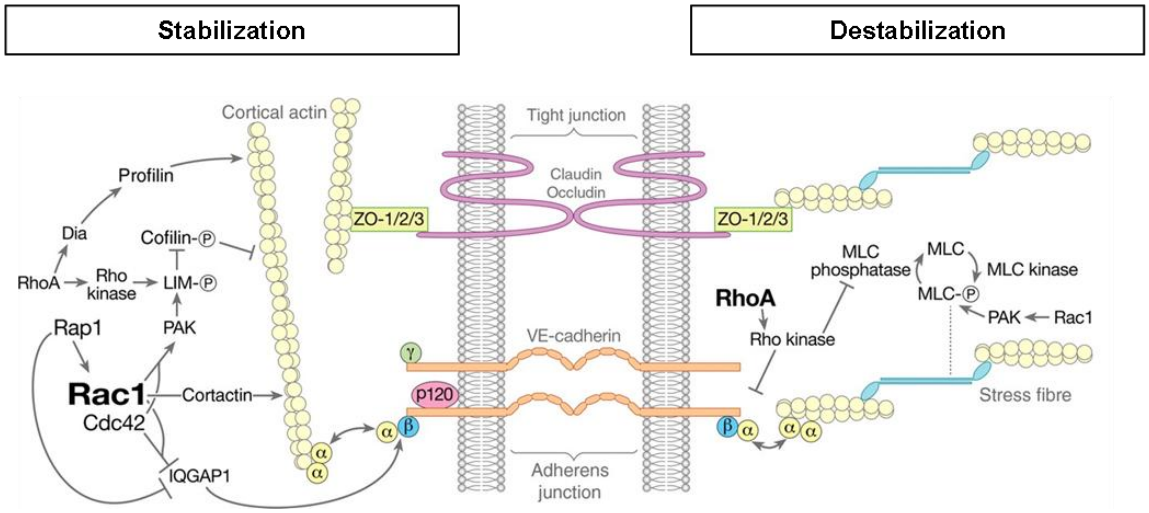

Figure 7: Vascular barrier integrity is regulated by small GTPases.
The assembly and disassembly of tight junctions and adherens junctions and thus endothelial permeability is primarily mediated through small GTPases. While RhoA-signaling primarily destabilizes cell-cell-interaction Rac1 and Cdc42 are involved in maintaining and strengthening of the integrity. For further details see text. (Adapted by permission from Oxford University Press: Cardiovascular Research (Spindler et al., 2010), copyright 2010)

Beside the involvement of small GTPases in cytoskeleton dynamics, they are also involved in the regulation of vascular integrity on the level of cell junctions. Several permeability-increasing agonists which mediate their signaling via small GTPases such as thrombin and VEGF induces tyrosine-phosphorylation of AJ components like VE-cadherin, β-catenin or p120-catenin (Dejana et al., 2008). For instance, the Ser665 residue phoshorylation of VE-cadherin due to VEGF-signaling leads to its internalization in a clathrin-dependent manner (Gavard and Gutkind, 2006). However, binding of p120 to VE-cadherin prevents endocytosis, introducing the concept that p120 may acts as a plasma membrane retention signal (Dejana et al., 2008). In addition, the level of cytoplasmatic p120 increases after cadherin internalization, which in turn results in decrease of active RhoA and enhances the levels of barrier stabilizing GTPases, Rac1 and Cdc42 (Lampugnani et al., 1997). Moreover Rac1 improves barrier conditions by inducing the tranlocalization of the cortical actin-modulating protein cortactin from the cytoplasm to the cell borders, where it accumulates (Jacobson et al., 2006; Weed et al., 1998; Zhao et al., 2009). Another mechanism involved in the cortical actin strengthening of endothelial barrier includes the LIM kinase/cofilin pathway. With the help of epithelial cells it has been shown that the small GTPases Rac1 and Cdc42 are capable to activate LIM kinase via their specific effectors of the PAK family, which in turn leads to cofilin phosphorylation (Bernard, 2007). Thus, the inactivation of cofilin prevents its

binding to actin and filament disassociation, which leads to the stabilization of the cortical actin cytoskeleton (Bamburg and Wiggan, 2002).

In addition, RhoA and ROCK were primarily associated to the negative regulation of barrier-mediating properties it has been recently shown that they are also partially involved in stabilization of the actin cytoskeleton. On the one hand ROCKs were identified to inhibit cofilin-mediated actin disassembly by LIM-kinase phosphorylation (Bernard, 2007; Sahai and Marshall, 2002), while on the other hand RhoA promotes the strengthening of cortical actin via its effector Dia in a profilin-dependent manner (Sahai and Marshall, 2002; Watanabe et al., 1997). In order to strengthen the endothelial barrier the modulation of cortical actin is not the only mechanism. Several other mediators, such as prostaglandins and atrial natriuretic peptide, were identified in the past to increase cyclic adenosine monophosphate (cAMP), which in turn activates Rac1 and Cdc42 via the Epac/Rap1 signaling cascade (Birukova et al., 2008; Birukova et al., 2007). Taken together, vascular permeability is primarily mediated through RhoA-signaling which is induced by binding of permeability-increasing agonists to their respective receptors on the EC surface. In contrast the small GTPases Rac1, Cdc42 and Rap1 act antagonistically by maintaining and stabilizing micorvascular endothelial barrier function.

1.5 Lung development

During evolution of vertebrates several organs with hierarchical tubular networks were formed with its prominent representative, the vascular system (Horowitz and Simons, 2008). Another organ with highly branched structures is represented by the lungs which are developed relatively late in evolution according to terrestrial live. In general, lung morphogenesis can be subdivided into five morphologically and biochemically defined stages. In the initial phase of murine lung development, the embryonic phase (E9-11.5), lung buds and major bronchi are getting formed. This stage is continued by the pseudoglandular stage (E11.5-E16.5), which is characterized by the formation of the respiratory tree due to branching morphogenesis. The following canalicular stage (E16.5-E17.5) is mainly marked by the expansion of the terminal bronchioles, which in turn form the respiratory ducts and sacs. During the saccular stage (E17.5-P5) the respiratory endothelium undergoes a differentiation process. Furthermore, the lung mesenchyme gets thinner coincidentally with an increase in vascularity of saccules. In the final alveolar stage (>P5) the developing lungs mature, whereby growth and septation of the alveoli occur (Maeda et al., 2007). In correlation to the vascular network which is continuously formed by a monolayer of endothelial cells the respiratory system only consists of epithelial cells. However both systems reveal similarities in the formation of such tubular structures. Branching morphogenesis occurs in both systems

based on a migratory process of specified cells towards a hypoxia induced guidance cue (Centanin et al., 2008; Jarecki et al., 1999; Pugh and Ratcliffe, 2003). While epithelial cells of the developing tracheal system of *Drosophila melanogaster* or the respiratory tract of vertebrates react on the interaction of branchless and its tyrosine kinase receptor breathless or its mammalian orthologs such as fibroblast growth factor and the FGF-receptor respectively, migration in the vascular system is induced by the binding of VEGF-A to VEGFR2 (De Smet et al., 2009; Samakovlis et al., 1996; Sekine et al., 1999). Another similarity that is shared by both systems comprises the concept of tip and stalk cell formation. During *Drosophila* airway development, as well as in the vasculature of vertebrates, the determination of tip cell and stalk cell identity is controlled through Delta-Notch signaling. In contrast, this process is triggered by TGF-β signaling in the developing mammalian lung (Horowitz and Simons, 2008).

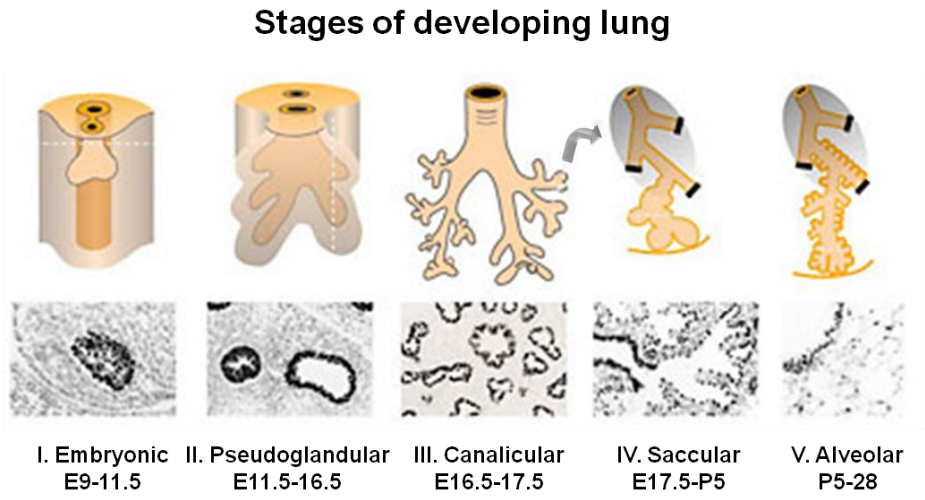

Figure 8: Schematic overview over the five stages of murine lung development.
In the initial phase of lung development, the embryonic phase (E9-11.5), lung buds and major bronchi are getting formed. This phase is followed by the pseudoglandular phase (E11.5-16.5) that is characterized by growth and dichotomous branching of the respiratory tube. In the following canalicular phase (E16.5-17.5) the terminal bronchioles expand to form the respiratory sacs and ducts. During the saccular phase (E17.5-P5) dilation of peripheral airspaces, as well as the differentiation of the respiratory endothelium occurs. Furthermore, this phase is characterized by an increasing vascularity of the saccules while the alveolar septae are attenuated. From stage P5 onwards, the alveolar phase growth and septation of the alveoli proceeds. (Adapted and modified from the webpage www.cincinnatichildrens.org; division pulmonary biology and (Maeda et al., 2007))

1.6 The family of kelch proteins

The first kelch protein was identified and characterized in *Drosophila melanogaster*, nearly two decades ago. The *Drosophila* kelch protein Orf1 is expressed in the actin-rich intracellular bridges, also known as the ring canals, which connect the 15 supporting nurse cells with the oocyte in the developing egg. This kelch protein is important for the regulation

and stabilization of the ring canals to maintain the cytoplasmic transport to the oocyte (Robinson et al., 1994; Xue and Cooley, 1993). The deletion of this protein leads to the defined and eponymous goblet-shaped chorion (Schupbach and Wieschaus, 1991) (Figure 9).

The family of kelch proteins includes to currently available information around 71 members within the human genome (Prag and Adams, 2003). However, little is known about their function. Nevertheless, those kelch proteins that were already characterized feature their importance for cellular processes, like for example the regulation of cellular morphology, migration and gene expression (Adams et al., 2000).

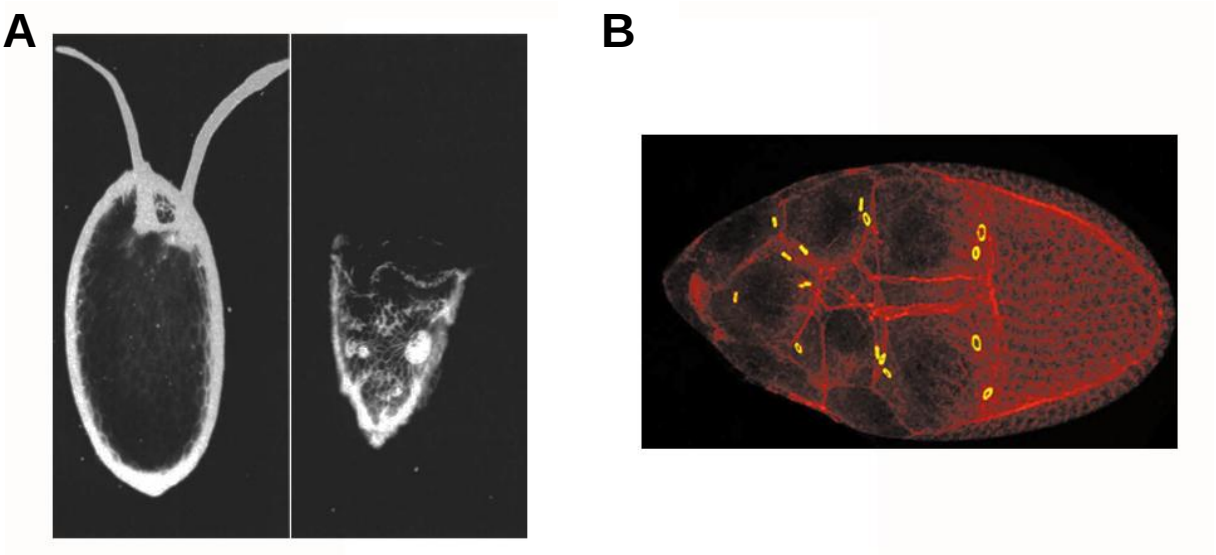

Figure 9: Identification of the kelch protein in *Drosophila melanogaster*.
The left side of (A) indicates the chorion of a wild-type egg, whereas on the right side the open ended chorion of the nomenclatured kelch mutant is represented. (B) Illustration of a *Drosophila* egg chamber after specific antibody staining for actin (red) and kelch (green). The colocalization of both proteins (yellow) display the expression pattern of kelch at ring canals of connecting nurse cells to each other and to the oocyte. (A: Adapted from (Schupbach and Wieschaus, 1991); B: Adapted by permission from Elsevier: Trends in Cell Biology (Adams et al., 2000), copyright 2000)

1.6.1 Organization and structure of the BTB-kelch-family members

The majority of the kelch family members belong to the group of BTB-domain containing kelch proteins, that consist in general of three motifs (Prag and Adams, 2003). In detail: BTB/POZ domain, the kelch domain and the BACK domain.

The BTB/POZ domain is located at the N-terminal site of several kelch proteins. BTB/POZ stands for *broad-complex, tramtrack and bric a brac/ poxvirus and zinc-finger*. The BTB/POZ domain is composed of around 120 aminoacids and mediates processes like protein-protein interaction (Stogios and Prive, 2004) and it controls Golgi complex localization (Nacak et al., 2006). Furthermore, it is involved in the regulation of the proteasomal protein degradation pathway (Geyer et al., 2003).

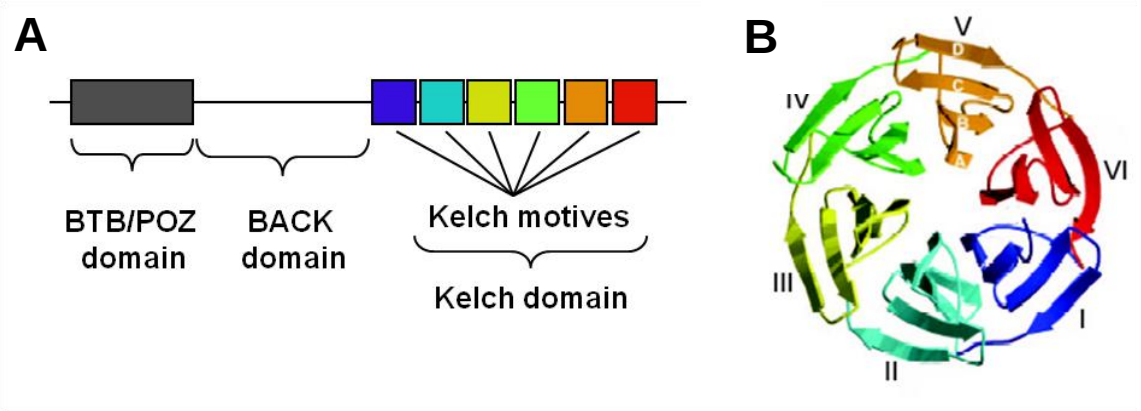

Figure 10: Representative illustration of BTB-kelch protein structure with the help of the KLEIP protein.
(A) Schematic of the BTB-kelch domain organization. The characteristic BTB/POZ domain is located at the N-terminal part, whereas the kelch domain, containing of the six-tandem kelch repeats (40-50 amino acid residues in length) is located at the C-terminal end. (B) Crystal structure analysis represents the β-propeller structure formed by the kelch domain mediating interaction with actin cytoskeleton. (Adapted from PhD thesis of Tanju Nacak)

The C-terminal site normally consists of the kelch repeats. Each kelch repeat is a sequence of 44-56 amino-acids in length. In addition, the clustering of four to seven kelch repeats establishes the functional unit, termed kelch domain. Crystal structure analyses have revealed that each kelch repeat forms a four-stranded antiparallel β-sheet (Prag and Adams, 2003). After assembling of all kelch repeats the kelch domain forms the characteristic β-propeller structure, which mediates the binding to cytoskeleton structures like actin-filaments or mikortubuli.
In between of the BTB/POZ and the kelch domain is the BACK domain located. The *BTB and C-terminal kelch repeat-domain* was mainly found in vertebrates (53 in humans), but its function is still speculative (Stogios and Prive, 2004).

1.6.2 Functional heterogeneity of the BTB-kelch-family members

In the last decade several novel BTB-kelch proteins were identified, but so far little is known about their physiological and biochemical function. However, those BTB-kelch-family members that were already identified and described in the past reveal heterogenous functionality. Nevertheless, the majority of the characterized kelch proteins display the common feature of being associated to the cytoskeleton, mediating its stabilization as well as playing an important role in membrane elongation and ruffling (Williams et al., 2005). Previous studies demonstrated that in the brain predominantly expressed BTB-kelch protein Mayven binds to actin filaments in stress fibers and cortical actin-rich regions, including the process tips in oligodendrocyte precursor cells. Moreover, Mayven has been reported to be involved in the dynamic organization of the actin-cytoskeleton and oligodendroccyte

elongation (Soltysik-Espanola et al., 1999; Williams et al., 2005). However, not all BTB-kelch family members interact with the actin cytoskeleton. The most considerable BTB-kelch family member which participates in the regulation of cellular microtubule stability is the neuronal expressed gigaxonin (Allen et al., 2005). Furthermore gigaxonin binds via its BTB/POZ domain to the ubiquitin-activating enzyme E1 and mediates the proteasomal degradation of its binding partner, the microtubule-associated protein 1B (MAP1B). Gigaxonin is not the only described BTB-kelch protein which is linked to the protein degradation pathway (Allen et al., 2005; Cleveland et al., 2009). Other BTB-kelch family members, such as KLHL9 (Sumara et al., 2007), KLHL12 (Rondou et al., 2008), KLHL13 (Sumara et al., 2007), KLHL21, KLHL22 (Maerki et al., 2009) and Keap1 (Kobayashi et al., 2004), were reported to function as substrate adaptors for the E3 ubiquitin ligase complexes. However little is known about their function *in vivo*. So far, only six BTB-kelch proteins have been deleted in mice. Mutations of each of these BTB-kelch molecules lead to severe and distinct developmental defects.

1.) The homozygous deletion of the BTB-kelch protein Keap1 results in postnatal lethality, because of a constitutive activation of the transcription factor Nrf2 (Wakabayashi et al., 2003).

2.) Deletion of KLHL10 results in infertility of heterozygous male mice (Yan et al., 2004),

3.) whereas the loss of the BTB-kelch protein giaxonin in mice and humans lead to a disease, called giant axonal neuropathy. This autosomal recessive neurodegeneration process is caused by an impaired axonal transport due to the accumulation of the microtubule-associated protein MAP8 (Ding et al., 2006).

4.) Further neurodegenerative changes were observed in the KLHL1 knockout mice, which displayed deficits in Purkinje cell function attended by abnormal gait and progressive loss of motor coordination (He et al., 2006b).

5.) In turn others could allocate the kelch family member ND1 a role in wound healing (Fujimura et al., 2004).

These distinct developmental defects suggest that the hitherto not widely recognized kelch family may harbor numerous other unknown molecules of major biological relevance.

1.6.3 The BTB-kelch protein KLEIP

The BTB-kelch protein kelch-like ECT2 interacting protein (KLEIP) was initially identified in a yeast two-hybrid screen as a actin-binding protein that is associated to epithelial-cell transforming gene 2 (ECT2) (Hara et al., 2004), a Rho nucleotide exchange factor involved in the regulation of cytokinesis (Miki et al., 1993; Tatsumoto et al., 1999). Like other BTB-kelch proteins KLEIP contains a BTB/POZ domain and a BACK domain, whereas in contrast the characteristic β-propeller is formed by six-tandem repeats of highly conserved 40-50-amino acid sequence. Phylogenetic analysis revealed amino acid identities of 43% between

Drosophila kelch and human KLEIP. However the *Drosophila* protein Diablo displays a higher homology and seems to be the orthologue of the human protein (Hara et al., 2004). Although the biological function of *Drosophila* Kelch is well characterized, the function of Diablo remains elusive. In the mammalian system KLEIP has several synonyms. It is also known as KLHL20 or Kelch X.

In recent years several studies were performed to identify KLEIPs role in cellular processes, with the outcome that KLEIP has a diverse function as it was already reported for other BTB-kelch proteins. At the beginning of this century KLEIP has been identified in *in vitro* studies to be involved in the actin assembly at the cell-cell adhesions sites of epithelial cells which are mediated through E-cadherin. Interestingly, KLEIP localization was only detected in areas of forming cell-cell-contacts, but not at maturated junctions (Hara et al., 2004). In addition to that it has been reported that the small RhoA-GTPase Rac1 promotes the E-cadherin mediated cell adhesion (Jou and Nelson, 1998; Takaishi et al., 1997). Experiments with constitutively activated Rac1 implicated the augmentation of KLEIP, as well as F-actin recruitment to the adhesion sites. From this findings it was proposed that KLEIP is necessary for Rac1-induced organization of the actin cytoskeleton (Hara et al., 2004). In contrast, others uncovered recently KLEIP to function as a substrate adaptor. Based on the capability of KLEIP to bind to the death-associated protein kinase (DAPK) via its kelch-repeat domain it is furthermore involved in the transportation of DAPK to Cullin3 (Cul3). Both proteins, KLEIP and Cul3, are components of the KLEIP-Cul3-ROC1 E3 ligase complex, which promotes the proteasomal degradation of DAPK due to its polyubiquitination (Lee et al., 2010). Nevertheless, little is known about the role of BTB-kelch proteins in context to angiogenic processes. In a previous study KLEIP was identified to be preferentially expressed in human umbilical vein endothelial cells (HUVECs), at which KLEIP-mRNA levels were strongly upregulated under hypoxic conditions. In addition to that hypoxia is known to be the strongest inducer of angiogenic signaling. Furthermore, functional analysis have demonstrated that KLEIP is important for the accumulation with ECT2 in a VEGF-dependent manner and functions as a bipartite nucleotide exchange factor for the small GTPase RhoA, thereby regulating several angiogenic processes, such as endothelial migration and sprouting angiogenesis (Nacak et al., 2007). In addition to KLEIP's interaction with the GEF ECT2 it has to be mentioned that Ect2-null mice die *in utero* (Hansen et al., 2003). However the reason for this lethal phenotype remains to be determined. Beside KLEIP, the protein KLHL6 represents another BTB-kelch protein which is contributed to angiogenesis. KLHL6 has been reported to be exclusively expressed in embryonic endothelial cells and B-lymphocytes. However, the KLHL6 knockout mice reveal no obvious vascular malformations, instead they display defects in B-cell proliferation and signaling (Kroll et al., 2005).

1.7 Aim of the study

In the field of understanding the guidance of vessel sprouts towards an angiogenic stimulus during angiogenesis *in vivo* much progress was achieved in the past. However, the downstream signaling pathways responsible for blood vessels formation are to this day poorly understood. In previously performed *in vitro* studies the cell-autonomous molecules of the RhoGTPase family, were mainly associated to cellular processes, such as morphogenesis, migration, cell division and adhesion (Heasman and Ridley, 2008). Moreover, it has been shown that the small GTPases RhoA, Rac1, Cdc42, as well as their downstream targets, regulate migration of endothelial cells during angiogenesis (Bryan and D'Amore, 2007; van Nieuw Amerongen and van Hinsbergh, 2009). However, the knowledge of small GTPases and their molecular mechanisms in controlling angiogenesis was predominantly acquired by *in vitro* experiments, so their functions *in vivo* remain to be determined. Thus, this present study was aimed at clarifying the role of selected G-protein signaling molecules during vertebrate development with the main focus on angiogenic processes.

The first and major part of this work deals with the characterization of the BTB-kelch protein Kleip. The nucleotide exchange factor for the small GTPase RhoA was recently identified in biochemical studies and in cellular functional assays as an essential regulator for endothelial migration and sprouting angiogenesis in a VEGF-dependent manner (Nacak et al., 2007). Based on the *in vitro* data our group allocated hypothetically a possible role for Kleip during *in vivo* angiogenic processes. In order to decipher its function during development Kleip-deficient mice were generated via the gene-trap technology and analyzed to distinct developmental stages.

The second part of this thesis gives a short insight into the signaling of the serine/threonine kinases ROCK I and ROCK II. In previous reports the inhibition of both downstream mediators of RhoA signaling with the relative unspecific inhibitor Y-27632 led to contrary findings in the field of angiogenesis that are still controversially discussed (Mavria et al., 2006; van Nieuw Amerongen et al., 2003). For the exploration of its endothelial function both kinases were pharmacological inhibited in this study with the specific inhibitor H-1152 and investigated.

Finally, the third part comprises the by ELMO1 and Dock180 formed complex, acting as an unusual bipartite GEF for Rac1. The small GTPase Rac1 was recently described as a pivotal factor for embryonic development as its endothelial specific deletion leads to an embryonic lethal phenotype (Tan et al., 2008). In order to analyze the function of the ELMO1/DOCK180 complex in vascular development its expression was silenced in transgenic zebrafish embryos.

2. Results

2.1 Role of Kleip during mouse development

The BTB-kelch protein KLEIP has been identified in several *in vitro* studies to be involved in the initialization of cell-cell adhesion and angiogenesis, as well as in proteasomal protein degradation, but so far nothing is known about its function during vertebrate development (Hara et al., 2004; Lee et al., 2010; Nacak et al., 2007). Previous protein alignment analysis revealed that human KLEIP displays a higher homology to *Drosophila* protein Diablo than to its eponymous kelch protein (Hara et al., 2004). In this present study it could be furthermore shown that KLEIP is an evolutionary highly conserved protein among vertebrates (Figure 1), which exhibits highly amino acids identities of 100% between human and mouse KLEIP. Beyond that, the zebrafish orthologue of mouse Kleip displays a sequence identity of 98%.

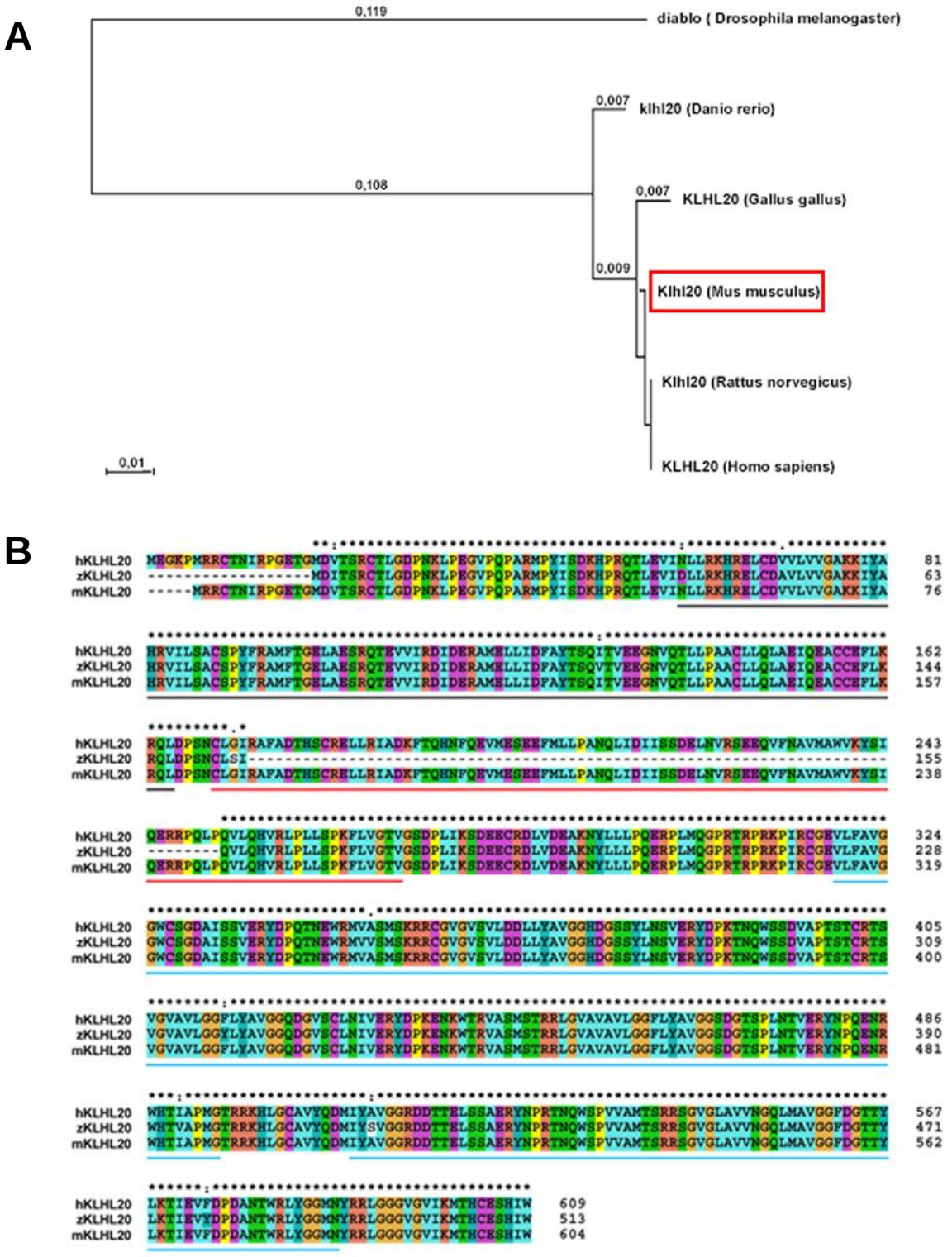

Figure 11: KLHL20 is highly conserved during vertebrate evolution.
(A) Phylogenetic analysis of KLHL20-related proteins (also known as KLEIP) from vertebrates and invertebrates. Among the vertebrates, especially the mammalia, KLHL20 is highly conserved throughout evolution. The bar indicates the relative evolutionary distance. (B) Multiple amino acid comparison of human (Homo sapiens), zebrafish (Danio rerio) and mouse (Mus musculus) KLHL20. Numbers represent amino acid positions. Conserved amino acids are labeled by asterisk. The bottom lines represent the protein specific domains: BTB/POZ domain (black line), BACK domain (red line) and the region of six-tandem kelch repeats forming Kelch domain (blue line). Accession codes: *Drosophila melanogaster* (Diablo: NP_524989.2), Danio rerio (Klhl20: NP_998166.1), Gallus gallus (KLHL20: NP_001026500.1), Mus musculus (Klhl20: NP_001034571.1), Rattus norwegicus (Klhl20: NP_001100662.1), Homo sapiens (KLHL20: NP_055273.2)

2.1.1 Kleip function during embryogenesis

2.1.1.1 Genetic approach for the deletion of murine Kleip

To dissect the function of the BTB-kelch protein Kleip during vertebrate development, the *Kleip* gene was disrupted in mice. For this reason the genetic modified embryonic stem cell line XF202 was purchased from the company baygenomics, which manipulated these cells via the gene trap technology. The feature of this method is the gene disruption mediated through an integration of a β-galactosidase (β-gal) encoding vector in sense orientation. However, the insertion of the vector into the mouse genome is a random process. Nevertheless due to a genetic screen the stem cell line XF202 was identified to display its vector integration somewhere within the intronic sequence between the first two encoding exons of the *Kleip* gene (Figure 12A). After implantation of modified ES cell containing blastocytes into pseudo-pregnant foster mothers and germline transmission in the resulting offspring bred heterozygous Kleip animals were used for the establishment of a specific genotyping protocol. In order to identify the exact integration site heterozygous Kleip mice were intercrossed and embryos were dissected at day 10.5 post coitum from pregnant mothers. Further DNA was isolated from the yolk sacs, while mRNA was isolated from the complete embryo. The DNA was than tested for β-gal integration via LacZ-polymerase chain reaction (PCR) to exclude the wild-type DNA for the following analysis. For the mapping of the β-gal integration site within this 20kb intronic sequence 20 sense-primers with a distance from approximately 1000bp from each other were designed. In the next step PCRs were performed with LacZ positive tested DNA, whereas these sense-primers were combined with the anti-sense primer Pr.21. Sense-primer Pr.20 was identified to be the closest to the β-gal integration site, because the combination of Pr.20 with Pr.21 generated a positive PCR signal (Figure. 12A and 12B). The β-gal integration into the *Kleip* gene was also confirmed by several other approaches, including genotyping with from yolk sacs isolated mRNA transcribed into cDNA, as well as by sequencing and restriction analyses (data not shown). In contrast, the wild-type signal is generated through the primers Pr.20 and the anti-sense primer Pr.22. Furthermore, expression studies with primers that bind behind the integration site revealed that homozygous Kleip embryos are not able to generate a functional *Kleip* mRNA (Figure 12C). Yet, it is currently not possible to verify those expression data by Western Blotting due to a lack of a functional antibody.

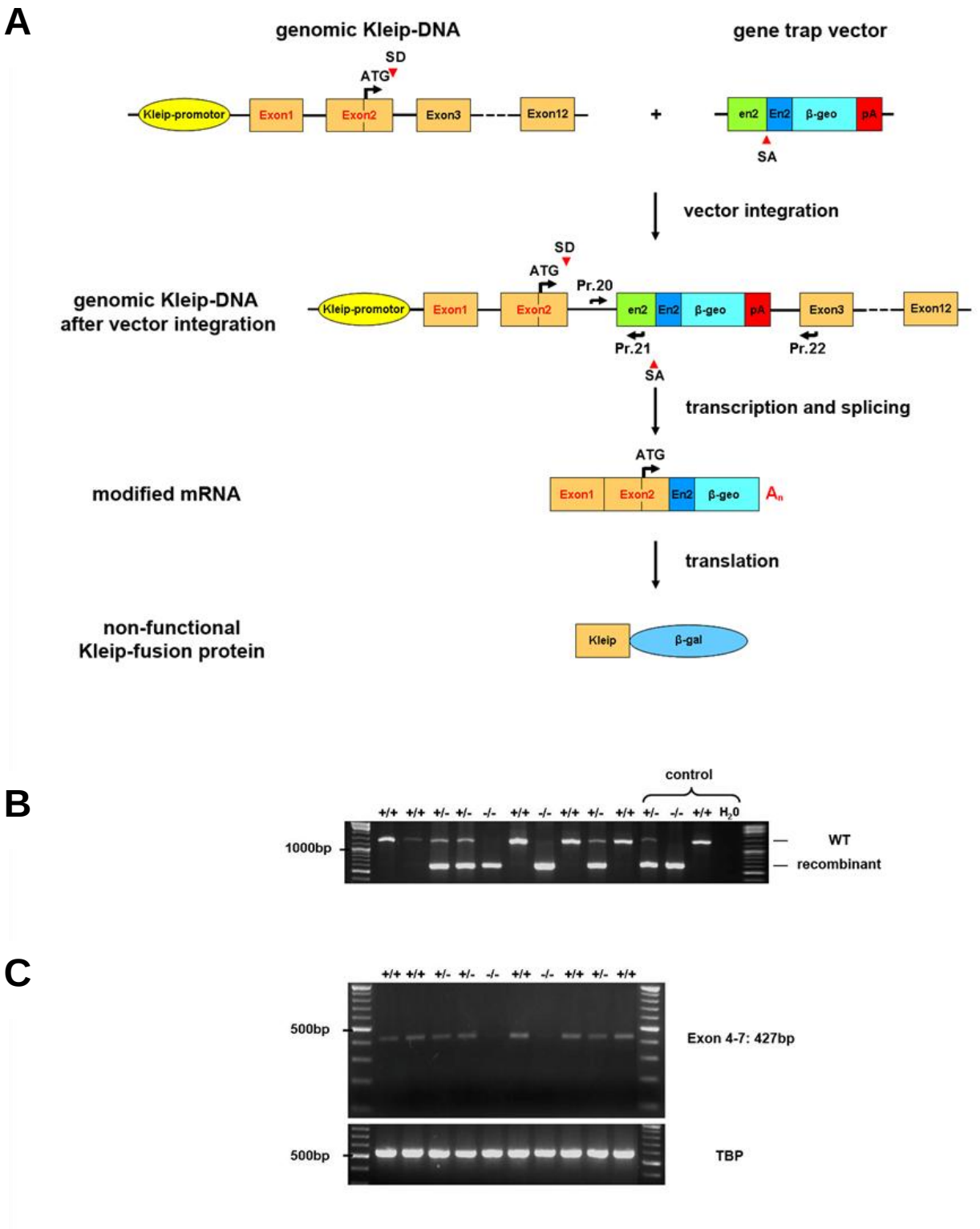

Figure 12: Generation of transgenic Kleip mice and its identification.
(A) Genomic *Kleip*-DNA and gene trap vector; genomic *Kleip*-DNA after random insertion of the gene trap vector in sense orientation; after transcription and splicing of the RNA transcript the trapped gene results in a truncated mRNA consisting of Exon1/Exon 2 together with ß-geo; translation leads to the Kleip-fusion protein. (**B**) Protocol establishment for the genotyping of Kleip$^{+/+}$-, Kleip$^{+/-}$- und Kleip$^{-/-}$-animals. Upper wild-type PCR signal is generated through the primer Pr.20 and Pr.22, lower PCR signal (recombinant band) is generated through the primer Pr.20 and Pr.21 after vector integration. (**C**) Kleip expression-analysis of different genotypes (samples from B) via RT-PCR shows a complete loss of Kleip mRNA in homozygous Kleip-embryos. Abbreviation: SD: Splice Donor; SA: Splice Acceptor; En2: engrailed; ß-geo: fusion gene of β-galactosidase (ß-gal) and neomycin resistance, pA: polyadenylation signal.

2.1.1.2 Loss of Kleip results in partial embryonic and neonatal lethality

After establishment of a specific genotyping protocol to distinguish between wild-type, heterozygous and homozygous animals, haplodeficient C57BL/6 mice were intercrossed and phenotopically characterized. To all analyzed time-points the genotypes of isolated embryos and born animals were recovered. As shown in figure 13 Kleip-deficiency was identified to result in partially both embryonic as well as postnatal mortality. At embryonic stage E11.5 27.9% of 158 analyzed mouse embryos lacked Kleip expression, whereas after delivery (P0) only 22.1% of 95 puppies were homozygous for Kleip (Figure 13B). These data represent that 20.8% of the Kleip deficient embryos die in utero.

A

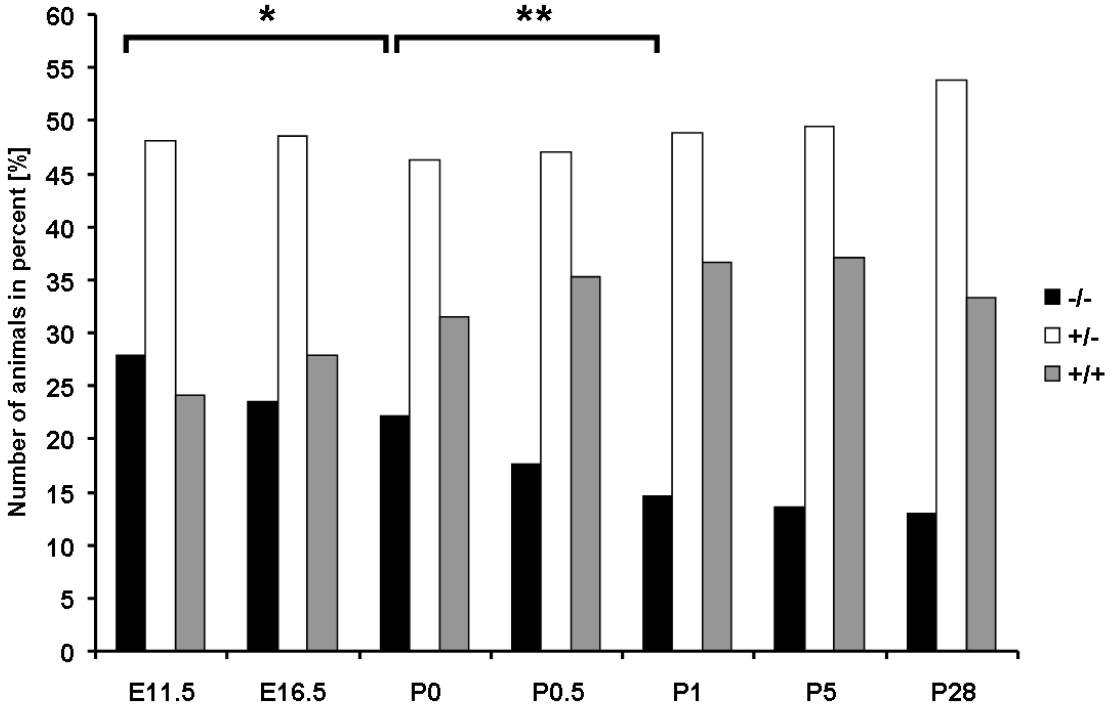

B

	E11.5	E16.5	P0	P0.5	P1	P5	P28
-/-	**44** (27.9%)	**16** (23.5%)	**21** (22.1%)	**15** (17.6%)	**12** (14.6%)	**11** (13.6%)	**29** (12.9%)
+/-	**76** (48.1%)	**33** (48.5%)	**44** (46.3%)	**40** (47.1%)	**40** (48.8%)	**40** (49.4%)	**121** (53.8%)
+/+	**38** (24.0%)	**19** (28.0%)	**30** (31.6%)	**30** (35.3%)	**30** (36.6%)	**30** (37.0%)	**75** (33.3%)
total	158	68	95	85	82	81	225

Figure 13: Global knockdown of Kleip in mice results in part to midgestional and neonatal lethality.
The diagram (A) represents the percentages of animals with indicated genotypes, recovered from heterozygous Kleip intercrosses (C57BL/6) at different embryonic stages or after birth. The group of neonates includes complete offspring sacrificed for experimental approaches as well as animals that were recovered dead between birth and postnatal stage P28. From embryonic stage 11.5 to birth around twenty-one percent of homozygous animals die in utero (*). Furthermore nearly fifty percent of Kleip deficient neonates do not survive the following 24 hours (**). Additionally, table (B) represents the total numbers of analyzed animals to distinct time-points.

The mild embryonic lethal phenotype can be further supported with the finding that in nine of thirty nine analyzed matings definitive no homozygous puppies were detected after birth. Moreover, nearly fifty percent of those homozygous embryos that reaches birth die shortly after, mainly within a few hours to one day (P1: 14.6%; n=82). However, an obvious cause of neonatal death was not clear from their appearance or behavior.

2.1.1.3 Kleip deficient embryos exhibit developmental defects and hemorrhages

In order to analyze the effects of Kleip-deficiency on embryonic development, embryos were analyzed to certain time-points. Till embryonic stage (E) 10.5 Kleip$^{-/-}$-embryos appeared developmentally normal (Figure 16). However, one day later at E11.5, Kleip-mutants displayed partially gross morphological changes (Figure 14A). Numeric determination of the embryonic somites, which was nearly similar between the analyzed Kleip$^{+/+}$ and Kleip$^{-/-}$ littermates, revealed that the observed gross morphological alterations were due to growth retardation. Further macroscopic analysis exposed that around 16% of the deficient Kleip embryos at E11.5 suffer from severe hemorrhages, which are predominantly located in the embryonic head. However, such bleedings sometimes also occurred in the passage of the head to torso.

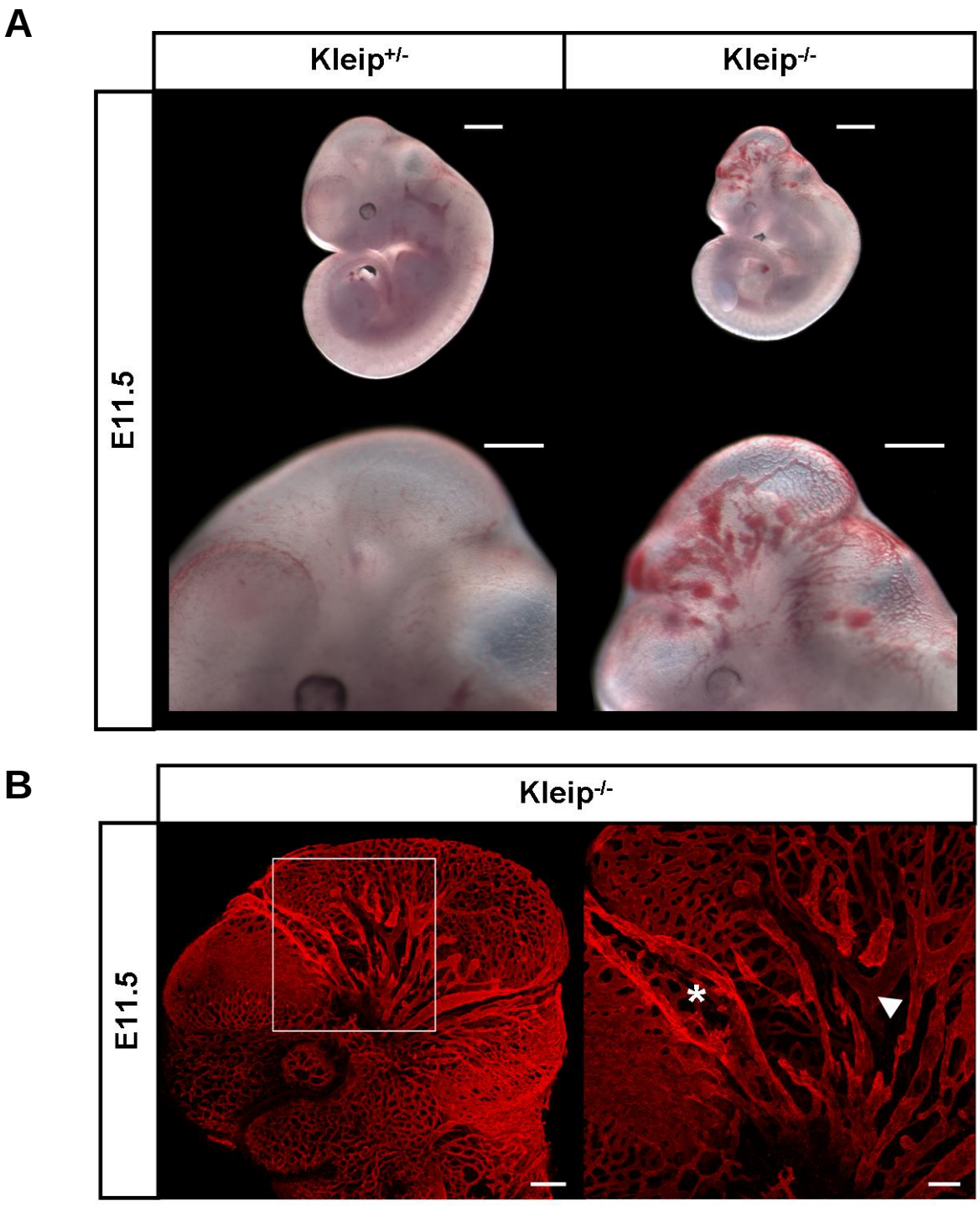

Figure 14: Kleip-deficiency causes growth retardation and hemorrhages.
In (A) one E11.5 heterozygous- and one homozygous- Kleip embryo are illustrated after dissection. Some Kleip$^{-/-}$-embryos revealed growth retardation and severe intracranial hemorrhages in comparison to their wild-type and heterozygous littermates. Scale bars, upper row 1mm, lower row 500µm. (B) Representative confocal image illustrates the Kleip$^{-/-}$-embryo from (A) after *whole-mount* endomucin immunofluorescence staining. The ruptured and dilated cranial vessel is indicated by asterisk. Blood vessel ablation is indicated by arrow. Scale bars, left image 250µm, right image 100µm.

2.1.1.4 Kleip-deficiency leads to cranial vessel dilatation

To study the function of Kleip during *in vivo* angiogenesis more in detail *whole-mount* endomucin stainings of E11.5 embryos were performed. Endomucin is a specific endothelial marker for the mucin like memebrane gylcoproteine, which is expressed in venous endothelium and in capillaries (Morgan et al., 1999). The performed analyses revealed no differences in vascular branching of the forming vessel network within the cranial mesenchyme of the developing brain. Instead the larger vessels in the mutant embryos appeared wider in vessel diameter and partially compressed than those observed in wild-type embryos (Figure 15). For quantification, the diameter of cranial vessels was measured in four different regions (I-V). The data indicate that the macrovessels in the region II of Kleip-null embryos (73.38 ± 2.84µm) are in comparison to wild-type embryos (52.61µm ± 2.52µm) up to 40 percent significantly extended. The measurements also revealed in region III a dilatation of microvessels in Kleip-deficient embryos from around 22%.

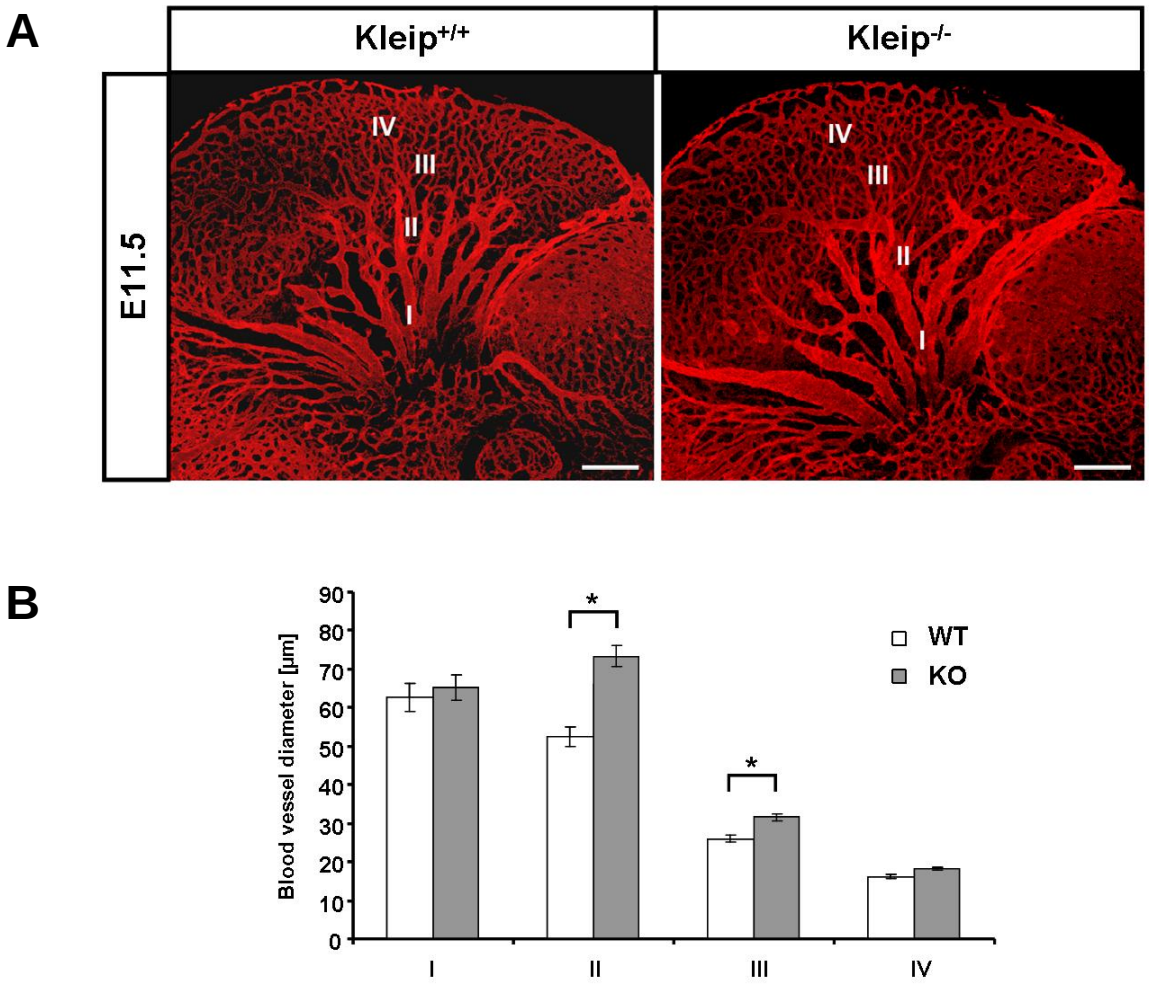

Figure 15: Loss of Kleip results in the dilatationof cranial vasculature.
(A) *Whole-mount* endomucin immunofluorescence staining of the cranial vasculature of E11.5 wild-type and Kleip-deficient embryos. Scale bars, 250µm. In (B) the diameter of macrovessels (I, II) and microvessels (III, IV) of E11.5 embryos were measured. For analysis 13 head halves of 7 homozygous and respectively 9 of 5 wild-type embryos were quantified. Values are mean ± s.e.m * p=0.0008 (II) and p=0.009 (III).

Such gross morphological changes of cranial vessels were also observed in E10.5 Kleip deficient embryos that were immunohistochemical stained for the endothelial specific marker CD31 and analyzed with a stereomicroscope (Figure 16). Consistent with the increased diameter of the macro- and microvessels of mutant embryos, those embryos suffering from massive hemorrhages revealed ruptured and ablated vessels, as shown in figure 14B. Beside the morphological differences in the cranial vasculature it is worth mentioning that Kleip-deficient embryos exhibited a moderate sprouting defect within the region of intersomitic vessels (Figure 16 H-I).

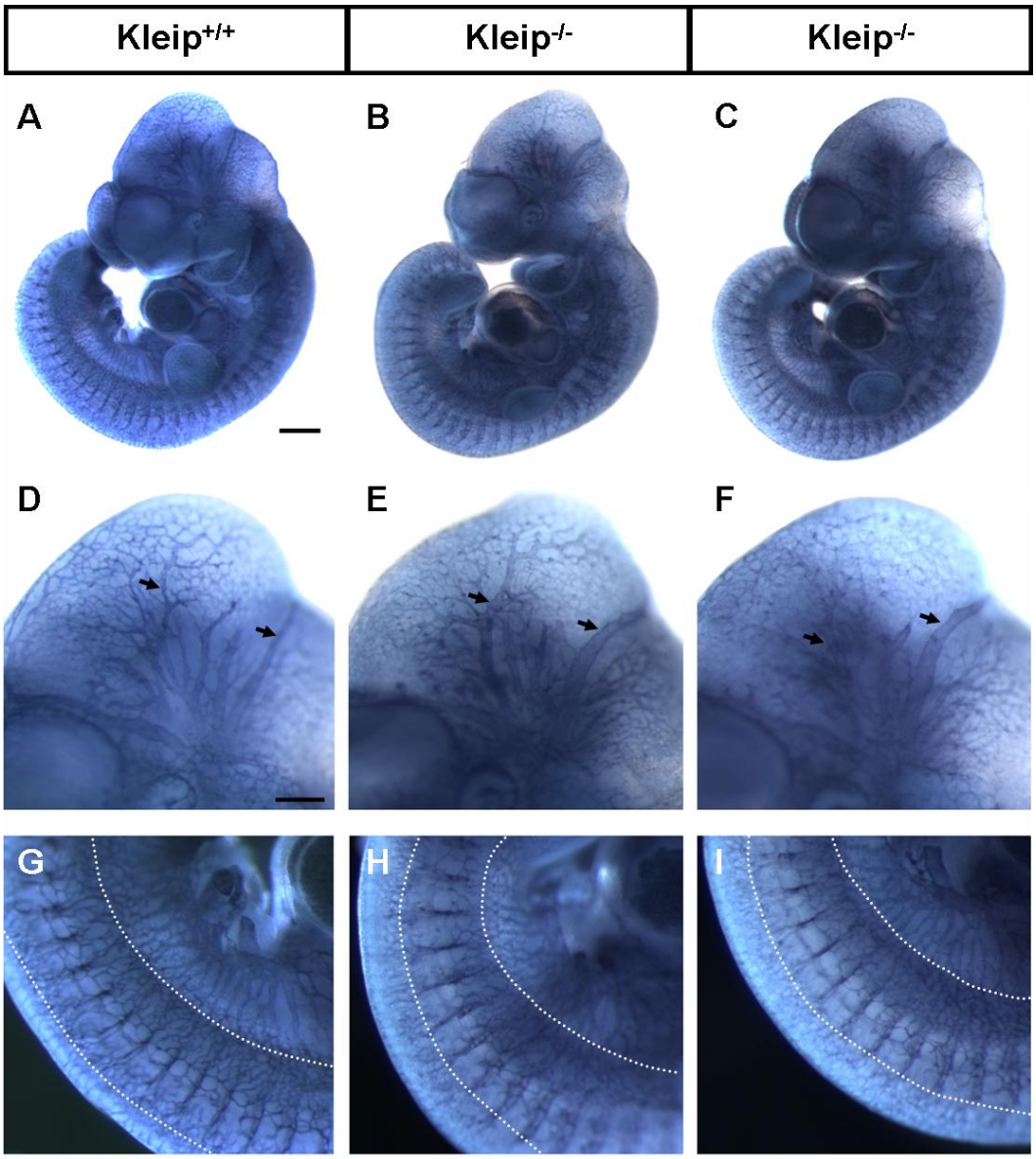

Figure 16: Kleip-deficient embryos exhibit a moderate angiogenic phenotype at E10.5.
CD31 *whole-mount* immunohistochemical stained homozygous Kleip-embryos (B, C) and wild-type littermates (A) displayed no gross morphological differences till embryonic stage (E) 11.5 when compared to each other. Instead Kleip-deficiency led to extended intracranial vessels (arrows; E&F). Furthermore, Kleip mutant displayed moderate sprouting defect within the region of intersomitic vessels (labeled by dotted lines, H &I). All images were captured on a stereomicroscope connected to a camera. Images A, D, G illustrates one Kleip wild-type embryo and B, C, E, F, H, I represent two homozygous littermates. Scale bars (A-C), 500µm, and (D-I) 250µm.

2.1.1.5 Kleip has no effect on endothelial network formation in a p-Sp-culture system

Previous results from *in vitro* experiments have demonstrated that KLEIP is necessary for endothelial migration and angiogenic sprouting (Nacak et al., 2007). Consisting with the findings observed in figures 15 and 16, in which Kleip-deficient animals display enlarged and partially compressed cranial vessel, the effect of Kleip during vascular network formation was analyzed in a further *ex vivo* approach, namely the paraaortic splanchnopleural (p-Sp-explant) assay. This assay was performed in cooperation with Anja Runge, a staff scientist of the Prof. Hellmut Augustin laboratory. For the generation of p-Sp –explants embryos were removed 9.5 days after fertilization and the p-Sp mesodermal tissue was isolated. This mesodermal tissue consists of the dorsal aorta, genital ridge/gonad, and pro/mesonephros-region (AGM-region). This AGM-region has been described as a possible origin of intraembryonic endothelial and hematopoiectic progenitors (de Bruijn et al., 2002; Dieterlen-Lievre et al., 2002; North et al., 2002). While explants were co-cultured for 14 days with OP9 stromal cells and stimulated with a cocktail of different chemokines, such as erythropoietin (EPO), interleukin-6 (IL-6) and murine stem cell factor (SCF) endothelial cells form in a first step a sheet-like structure. This initial step of the vascular bed formation represents vasculogenesis, whereas the following “vascular network formation” step, characterized by circular migration and sprouting of maturated endothelial cells into periphery, imitates the process of angiogenesis (Takakura et al., 1998). After specific immunostaining for the endothelial marker CD31 (Figure 17), no alterations regarding the migratory behavior or thickening of the agiogenic sprouts were observed in the explants of Kleip-deficient embryos when compared to the control.

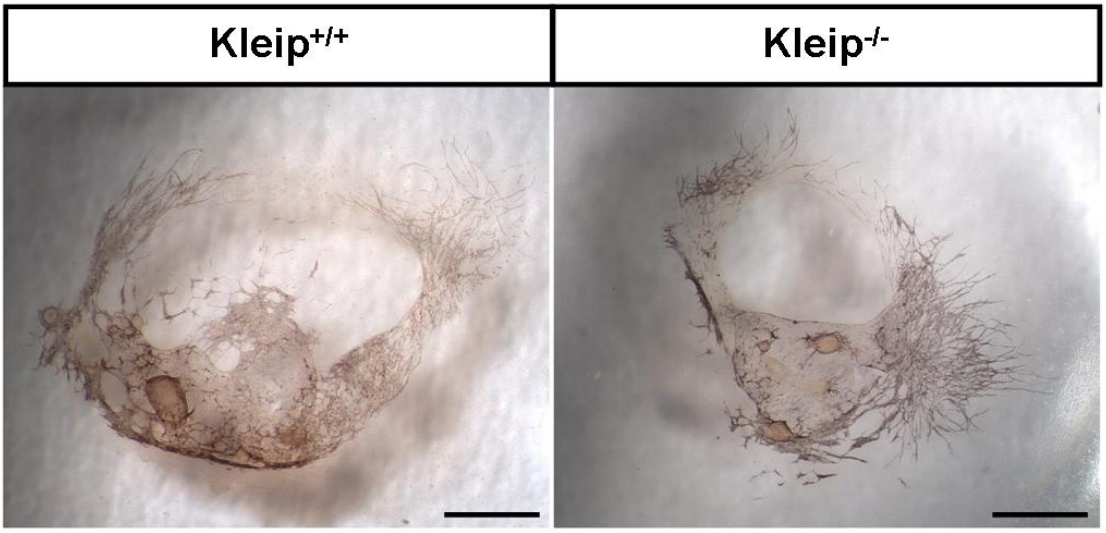

Figure 17: Vascular network formation in p-Sp explants of Kleip-deficient embryos is not affected.
Isolated P-Sp-explants of E9.5 Kleip-null or wild-type embryos were cultivated for 14 days on OP-9 feeder cells and stimulated with a cocktail of cytokines, consisting of interleukin-6 (IL-6), erythropoietin (Epo) and stem cell factor (SCF). After immunochemical staining for CD31 p-Sp-explants were analyzed. P-Sp-explants of homozygous Kleip embryos display a comparable vascular network formation as observed in wild-type embryos. Scale bars, 1mm.

2.1.1.6 Pericyte coverage is not affected in Kleip-deficient embryos

Several studies performed in mice lacking proteins that are involved in the recruitment of mural cells or mediate critical functions of endothelial cells display defects during angiogenesis and die frequently due to embryonic or perinatal hemorrhages (Carmeliet, 2003; Liu et al., 2000; McCarty et al., 2002; Zhu et al., 2002). To address the question, whether the observed hemorrhages in Kleip-null embryos are caused by defects in the association of mural cells to the endothelium, specific immunofluorescence *whole-mount* doublestainings for endomucin and NG2 were performed and subsequently analyzed and recorded with a confocal microscope. The proteoglycan NG2 is well known to be expressed in the macrosvasculature by smooth muscle cells and in nascent microvessels by pericytes (Ozerdem et al., 2001). Although the recorded images (Figure 18) convey the light impression that the amount of blood vessel surrounding pericytes is increased in Kleip-mutants as in comparison to their wild-type counterparts, comparable analysis revealed no obvious alterations in pericyte coverage. These results indicate that the observed hemorrhages in Kleip-null embryos are not caused by a failure in the recruitment of pericytes.

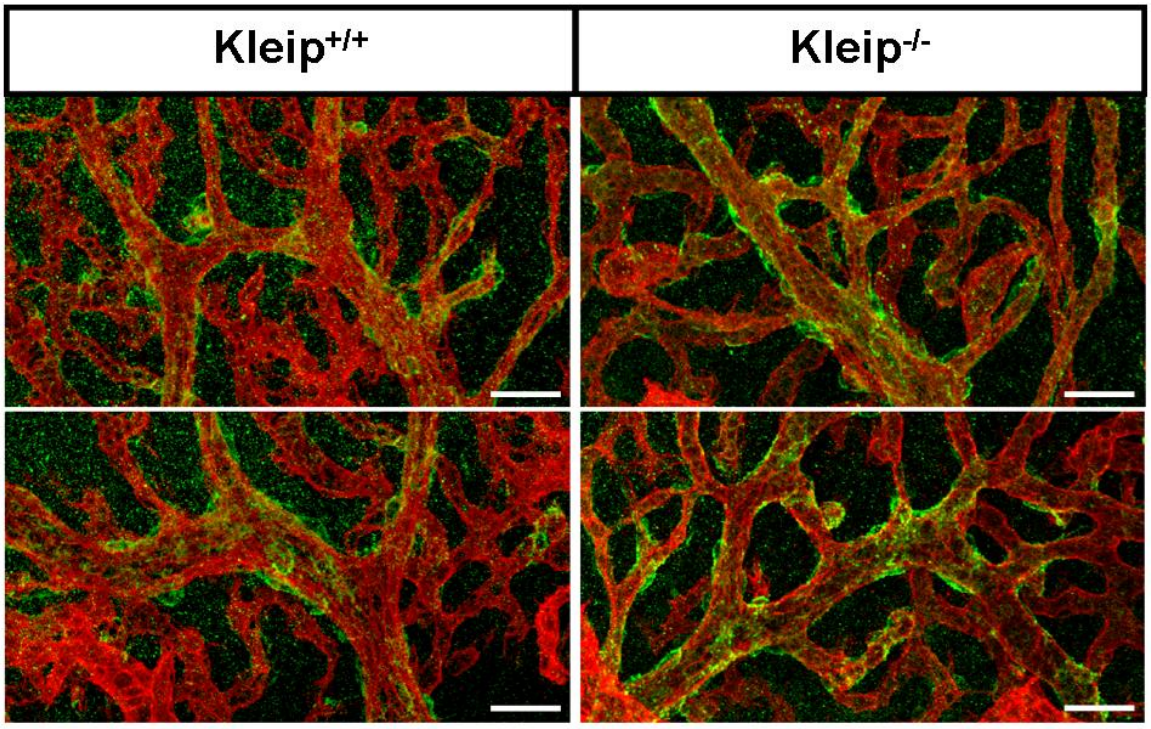

Figure 18: Pericytes cover properly the cranial vasculature of mutant Kleip embryos.
In order to identify possible alterations in the coverage of the embryonic vasculature by mural cells, E11.5 Kleip$^{+/+}$ and Kleip$^{-/-}$ embryos were *whole-mount* stained and confocal microscopic analyzed. Endomucin was used as a microvascular endothelial marker (red), whereas NG2 was utilized for the detection of pericytes (green). Comparable analyses exhibit no obvious changes in the pericyte-mediated stabilization. Scale bars, 50µm.

2.1.1.7 Partial embryonic lethality of Kleip-mutants is not caused by defects in extra-embryonic tissues

To date it is well known from several transgenic mouse lines that embryos can perish from any placental malformations and/or from vascular defects in the embryonic yolk sac (Adelman et al., 2000; Qian et al., 2000; Steingrimsson et al., 1998). To exclude such possible alterations the extraembryonic tissues were examined microscopically before and after immunohistochemical staining. As representative shown in figure 19A the freshly dissected yolk sac of a E11.5 staged homozygous embryo display a normal branched and with blood perfused vascular network similar to the yolk sac vasculature observed in wild-type embryos, indicating a proper blood circulation. These findings were furthermore confirmed by an immunohistochemical staining for the endothelial specific marker CD31 (Figure 19B).

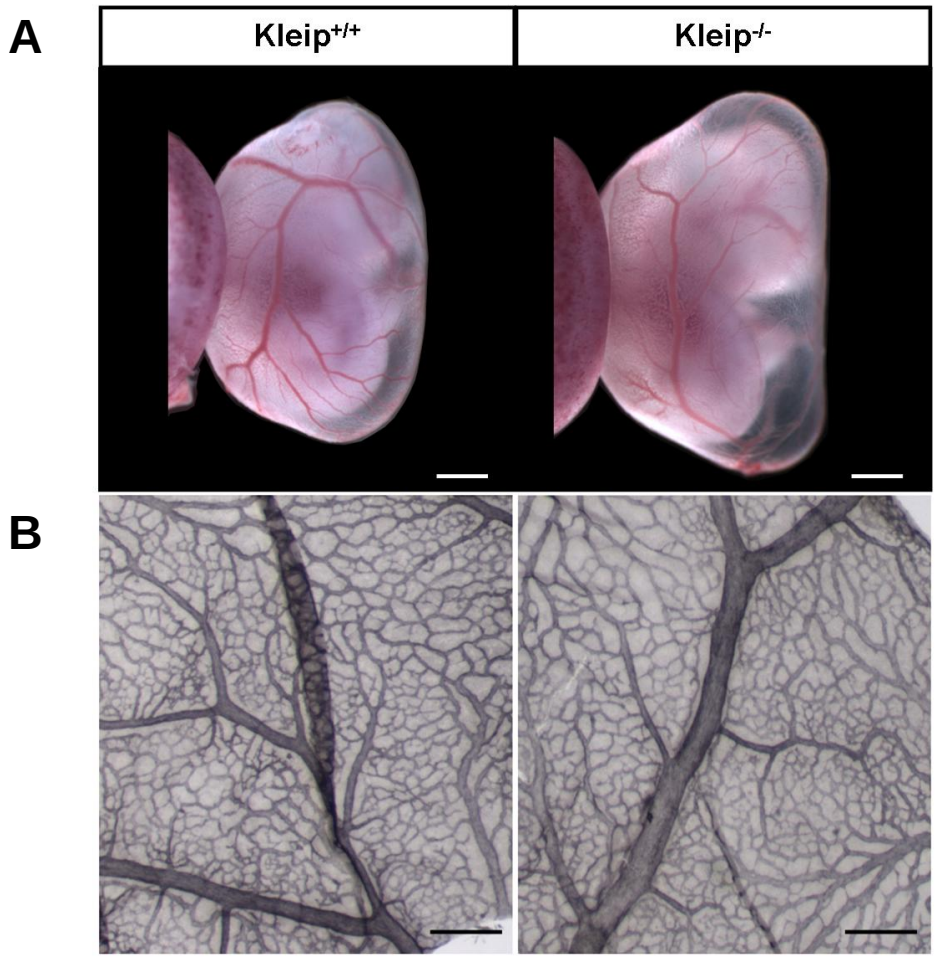

Figure 19: Normal vascular network morphogenesis in Kleip$^{-/-}$ yolk sacs.
In (A) one wild-type and one homozygous Kleip embryo, still surrounded by the yolk sac, are illustrated after dissection at E11.5. Even the yolk sacs of Kleip-deficient embryos exhibit a normal branched and with blood-perfused vasculature. Scale bars, 1mm. (B) Yolk sacs of both genotypes (+/+ and -/-) displayed a similar blood vessel pattern after specific CD31 immunohistochemical staining. Scale bars, 250µm.

Furthermore, it could be shown that to all analyzed time-points, from E11.5 to E13.5, the Kleip-mutation had no affect on the formation of the three distinct placental tissue layers, such as giant trophoblast cell layer, spongiotrophoblast layer, and labyrinthine layer. Especially the high vascularized labyrinth, characterized as the gateway of maternal and fetal exchange of oxygen, nutrients and waste, did not differ morphological from each other when CD31 stained placentas of wild-type embryos were compared with homozygous ones (Figure 20).

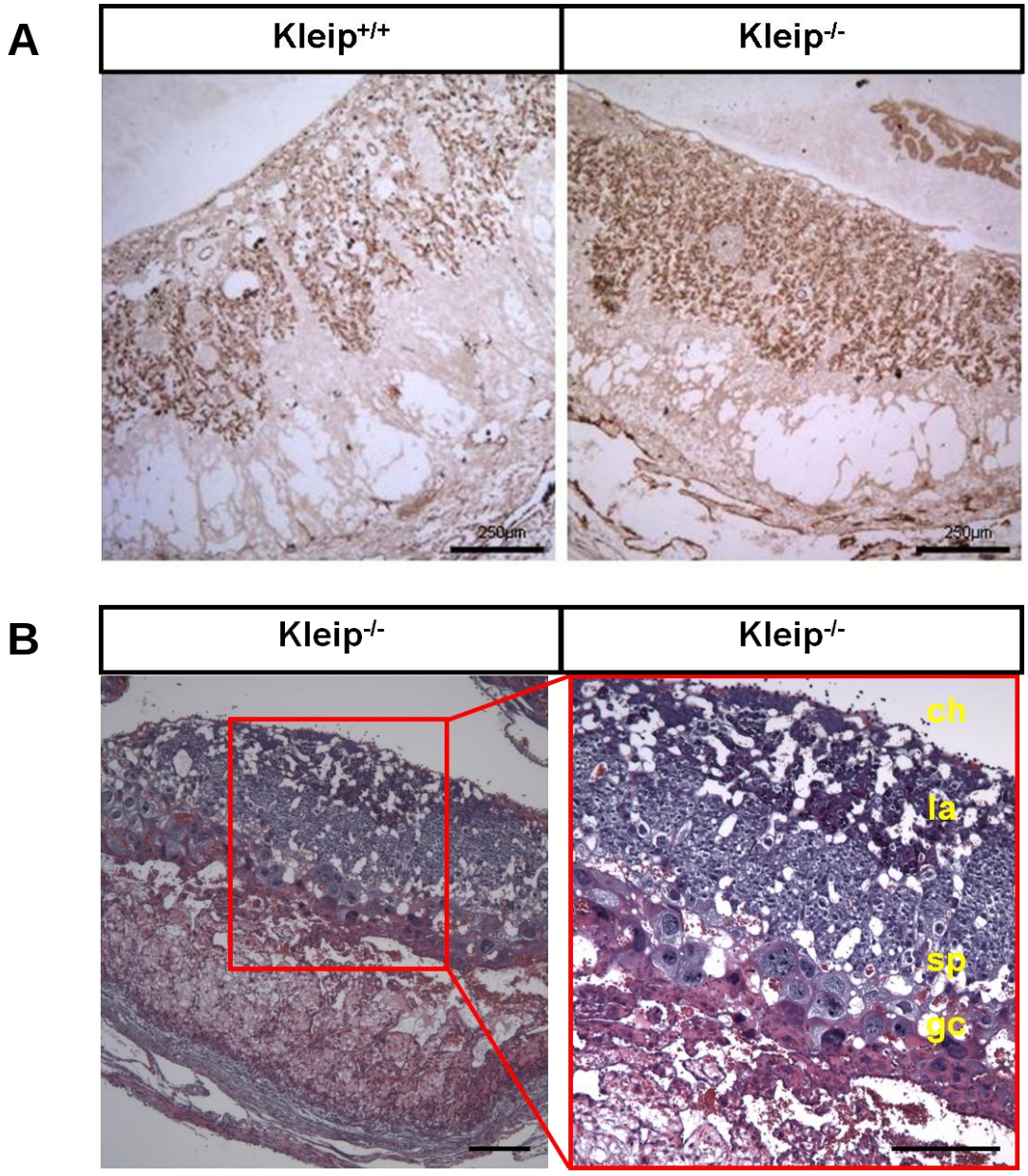

Figure 20: Placental tissue of Kleip-mutant embryos display no morphological changes.
(A) Paraffin sections (8µm) of Kleip$^{+/+}$ and Kleip$^{-/-}$ placentas (E13.5) after immunohistological staining of the vasculature with a CD31 antibody. Blood vessel network formation in the labyrinth of homozygous placentas resembled the extraembryonic tissue morphology of wild-type embryos. (B) Placentas of Kleip-deficient (E11.5) embryos display after H&E staining a proper distribution of the specific tissue layers. Abbreviation: ch: chorion; la: labyrinth; sp: spongiotrophoblasts; gc: giant cells. Scale bars, 250µm.

2.1.1.8 Silencing of klhl20 in zebrafish results in cranial hemorrhages

For the confirmation that loss of Kleip, a synonym for Klhl20, causes hemorrhages the zebrafish was used as an additional model organism. The practical advantages of the zebrafish model are beside the development of the embryo outside the mother's body the transparency of the zebrafish embryo itself. In this study the transgenic zebrafish line *tg(fli:EGFP)* was used, which express the fluorescent protein EGFP under the endothelial specific fli promoter. In order to test the functionality of the used splice blocking morpholino (SB-Mo), 8ng of this pre-mRNA splicing modifier was injected into the one cell stage of a fertilized egg. RT-PCR analysis after 72 hours post fertilization (hpf) revealed that the klhl20 knockdown is partially sufficient (Figure 21C). In comparison to control morpholino (co-Mo) injected embryos, two PCR products were detectable in those treated with the SB-Mo. The upper signal represents the wild-type transcript, whereas the lower signal is generated due to defective splicing. However, the stronger wild-type signal indicates that the SB-Mo is not capable to mediate a complete knockdown. Although high concentrations of the SB-Mo were used zebrafish embryos were to all analyzed time-points morphological indistinguishable from co-Mo injected counterparts (Figure 21A). However, 48 hours after *klhl2*0 morpholino injection the zebrafish embryos began to suffer from severe intracranial hemorrhages (Figure 21 A&B). At 48hpf and later stages the klhl20 morphants showed around 40% more bleedings, as in comparison to the control embryos (Figure 21D). These consistent appearing hemorrhages mostly concentrated in or near to the hindbrain ventricle indicate differences in endothelial barrier integrity.

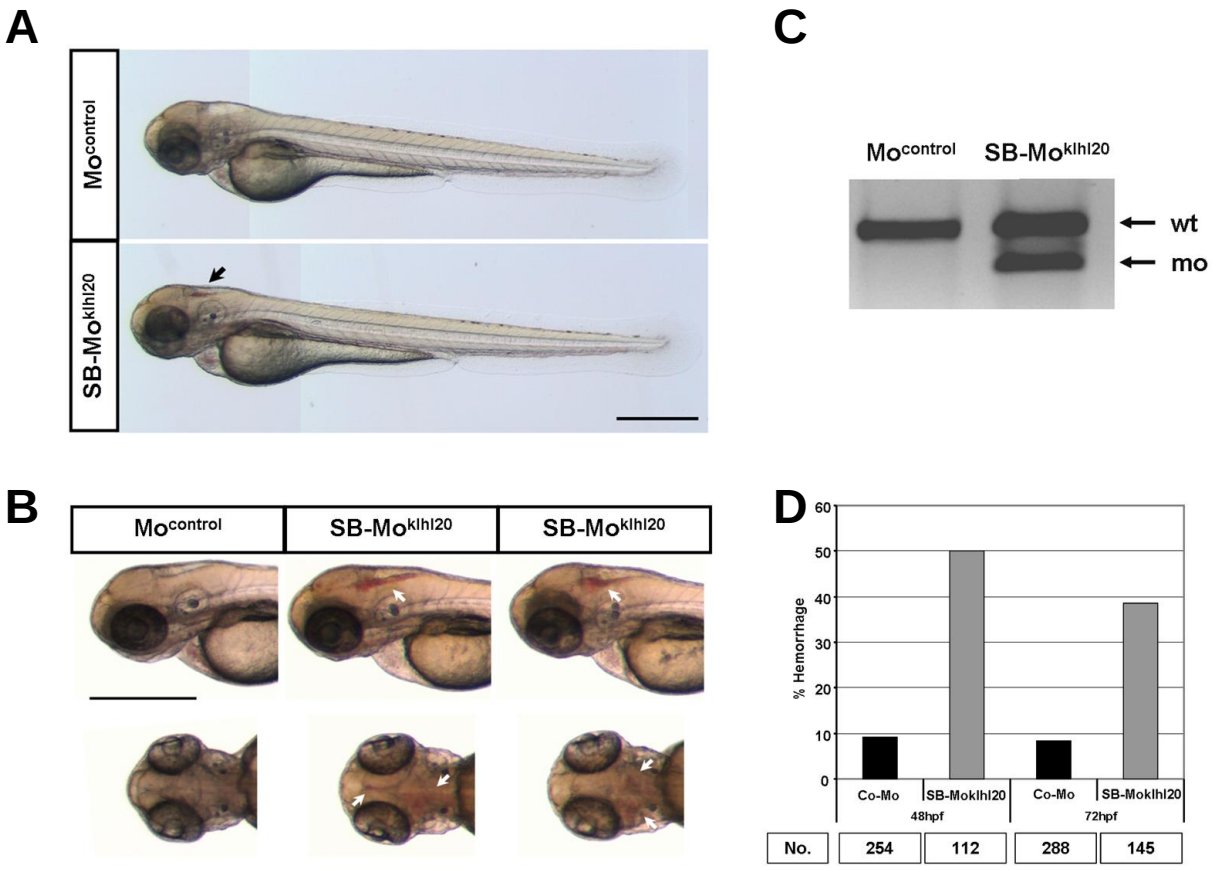

Figure 21: Klhl20 is essential to maintain vascular integrity *in vivo*.
Morpholino-based silencing of klhl20 does not affect zebrafish morphology (A). Representatively shown are one control morpholino (8ng) and one klhl20 splice blocking morpholino (8ng) injected embryo at 72hpf. Instead zebrafish embryos suffer from intracranial hemorrhages (A, B; arrows). Embryos were analyzed 48 and 72hpf under dissecting microscope. (B) Upper lane lateral view, lower lane dorsal view. (C) Expression silencing of klhl20 in zebrafish (72hpf) verified by RT-PCR. Upper signal represents wild-type transcript, lower signal the morphant transcript. (D) Quantification of observed intracranial hemorrhages after 48 and 72hpf in control morpholino versus splice blocking morpholino injected embryos. Scale bars, 500µm.

2.1.1.9 Loss of KLEIP increases *in vitro* permeability

In order to further examine directly the role of KLEIP in endothelial barrier function *in vitro*, immortalized human umbilical vein endothelial cells (HUE cells) were silenced for their KLEIP expression and were tested in a transwell permeability assay. In this experimental setting the control siRNA or with either one of two independent KLEIP siRNA treated HUE cells were plated 24 hours post transfection on collagen precoated transwell chambers. After 72h of cultivation FITC-dextran was added on top of the grown HUE monolayer in the upper chamber. To distinct time-points probes of the lower chambers were collected and photometrically with a wavelength of 492nm (excitation) and 520nm (emission) analyzed. Additionally, co siRNA transfected and with VEGF stimulated HUE cells were used as positive control. The collected data (Figure 22) revealed a rapid and significant increase in permeability within the first 240 minutes across KLEIP siRNA-treated endothelial

monolayers. Already after 30 minutes the detected fluorescence units were twice as high in those that were treated with KLEIP siRNA 1 as observed in the control. From this time-point on this specific KLEIP siRNA had an even more drastic and consistent effect on permeability than the VEGF stimulated control siRNA transfected HUE cells. To confirm the efficient silencing of KLEIP, control siRNA and KLEIP siRNA transfected HUE cells were lysed and KLEIP expression was analyzed by RT-PCR. Primers detecting the coding mRNA of the murine tata box-binding protein were used as loading control. Respectively a 75%-84% reduction of KLEIP mRNA expression was reached after KLEIP siRNA transfection (Figure 22B).

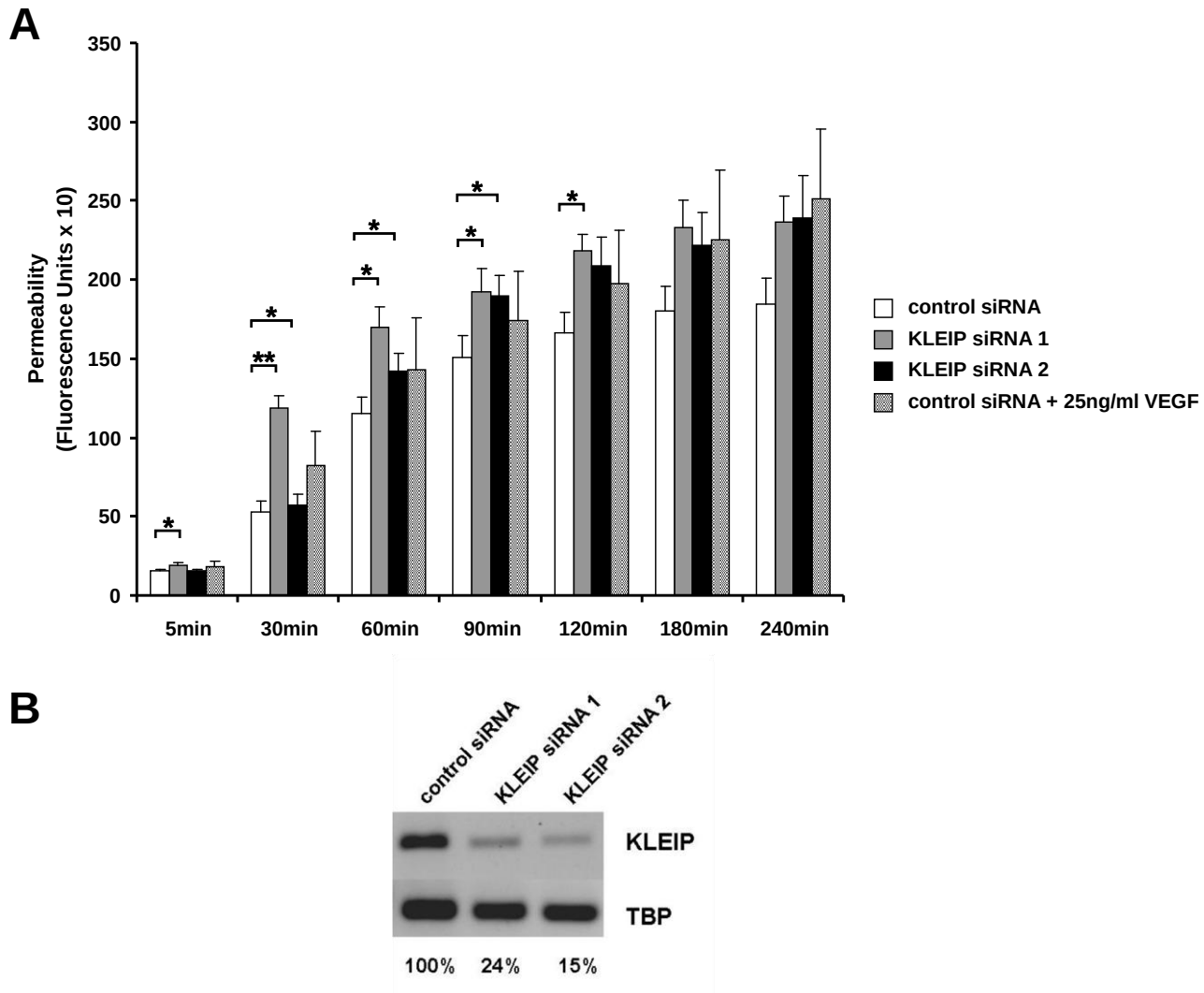

Figure 22: *In vitro* downregulation of KLEIP induces endothelial permeability.
(A) Immortalized HUE cells, either treated with control or specific KLEIP siRNA, were seeded on collagen precoated transwell chambers. After 72 hours of cultivation FITC-dextran was added to the upper chamber. To distinct time-points probes from the lower chamber were collected and photometrically analyzed. Experiments were performed in three independent trials. Results are expressed as mean ± s.e.m *p<0.05;** p<0.002 compared to control transfected cells. (B) RT-PCR analysis confirmed the specific down-regulation of KLEIP in HUE cells, after transfection with two independent siRNAs against KLEIP. Human TATA box-binding protein served as loading control.

2.1.1.10 Gene expression profiling of Kleip$^{-/-}$ isolated embryonic endothelial cells exhibit no significant change

After having demonstrated *in vivo*, as well as *in vitro*, that Kleip seems to be essential for the mediation of vascular integrity the effect of Kleip-deficiency on its downstream targets was furthermore investigated. For this reason microarray analysis were performed comparing mRNA of Kleip$^{+/+}$ and Kleip$^{-/-}$ endothelial cells isolated from E11.5 embryos via FACS sorting. Only the CD31^{+}CD34^{+} endothelial cells with purity over ≥ 98% after isolation were used. Prior to expression profiling the isolated endothelial cells were tested on their *Kleip* mRNA expression by semi quantitative RT- PCR (Figure 23). The obtained data indicate on the one hand that *Kleip* is expressed in endothelial cells of Kleip wild-type embryos, whereas it is missing in the vasculature of Kleip-mutants.

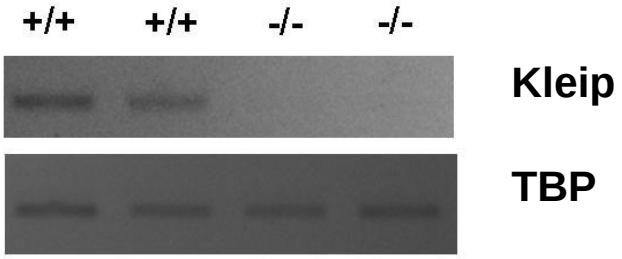

Figure 23: *Kleip* is expressed in murine endothelial cells.
Prior to expression profiling studies semi quantitative real-time PCR with transcribed endothelial mRNA isolated of E11.5 *Kleip*-mutant and wild-type embryos were performed. RT-PCR analysis indicates endothelial *Kleip* expression in wild-type embryos, whereas its expression is not detectable in Kleip-deficient embryos. Murine TATA box-binding protein was used as loading control.

For the performed illumina beadchip hybridization experiment the total number of three homozygous Kleip embryos and three wild-type littermates, from two independent dissections, were utilized. In table 1 some selected genes of the transcriptomic analysis are summarized that were at least 1.4-fold up- or downregulated. Among these genes six of them are known to be involved in angiogenic processes. In particular: SNF related kinase (Chun et al., 2009), BMX non-receptor tyrosine kinase (He et al., 2006a) and the RhoA guanine exchange factor Syx, also known as pleckstrin homology domain containing family G member 5 (Garnaas et al., 2008) are up-regulated. In contrast, genes like platelet-activating factor receptor (Hudry-Clergeon et al., 2005), Semaphorin 3F (Kessler et al., 2004) and CREB binding protein (Crebbp; (Tanaka et al., 2000) are down regulated. Because of the obvious marginal changes within the endothelial expressions pattern between Kleip wild-type and Kleip-deficient embryos further investigations for the identification of possible downstream target genes of Kleip were discontinued.

Table 1: Summary of selected genes down- or up-regulated in Kleip-deficient endothelial cells of E11.5 embryos.

Symbol	Regulation	Description	Function
Eif2c1	**-1,9**	Eukaryotic translation initiation factor 2C, 1	gene silencing
Ptafr	**-1,7**	Platelet-activating factor receptor	endothelial permeability
Uhrf2	**-1,6**	Ubiquitin-like, containing PHD and RING finger domains 2	cell cycle regulation
Sema3f	**-1,6**	Semaphorin 3F	chemorepulsive for endothelial cells
Nrg1	**-1,6**	Neuregulin 1	neurogenesis
L3mbtl3	**-1,6**	L(3)mbt-like 3 (Drosophila)	hematopoiesis
Ldb2	**-1,5**	LIM domain binding 2, transcript variant 2	Regulation of actin cytoskeleton
Clip1	**-1,5**	CAP-GLY domain containing linker protein 1	Microtubule dynamics
Crebbp	**-1,4**	CREB binding protein (Crebbp)	Hematopoiesis, angiogenesis, hemorrhages
Fzr1	**1,5**	Fizzy/cell division cycle 20 related 1 (Drosophila)	cell division
Bmx	**1,6**	BMX non-receptor tyrosine kinase	arteriogenesis, angiogensis, endothelial migration
Plekhg5	**1,7**	Pleckstrin homology domain containing family G member 5	endothelial migration, angiogenesis (mouse & zebrafish)
Hbb-y	**1,7**	Hemoglobin Y, beta-like embryonic chain	erythropoiesis
Ptbp1	**1,7**	Polypyrimidine tract binding protein 1, transcript variant 1	alternative splicing
Nsdhl	**1,7**	NAD(P) dependent steroid dehydrogenase-like	cholesterol biosynthesis
Snrk	**1,8**	SNF related kinase	endothelial migration, aterial-venous differentiation (zebrafish)
Klf3	**1,8**	Kruppel-like factor 3	adipogenesis, erythropoiesis

Note: The table represents genes that are at least 1.4-fold up- or downregulated. The bold typed genes are known to be relevant for angiogenic processes.

2.1.2 Kleip and its role during neonatal life

2.1.2.1 Homozygous Kleip puppies die neonatally due to respiratory distress

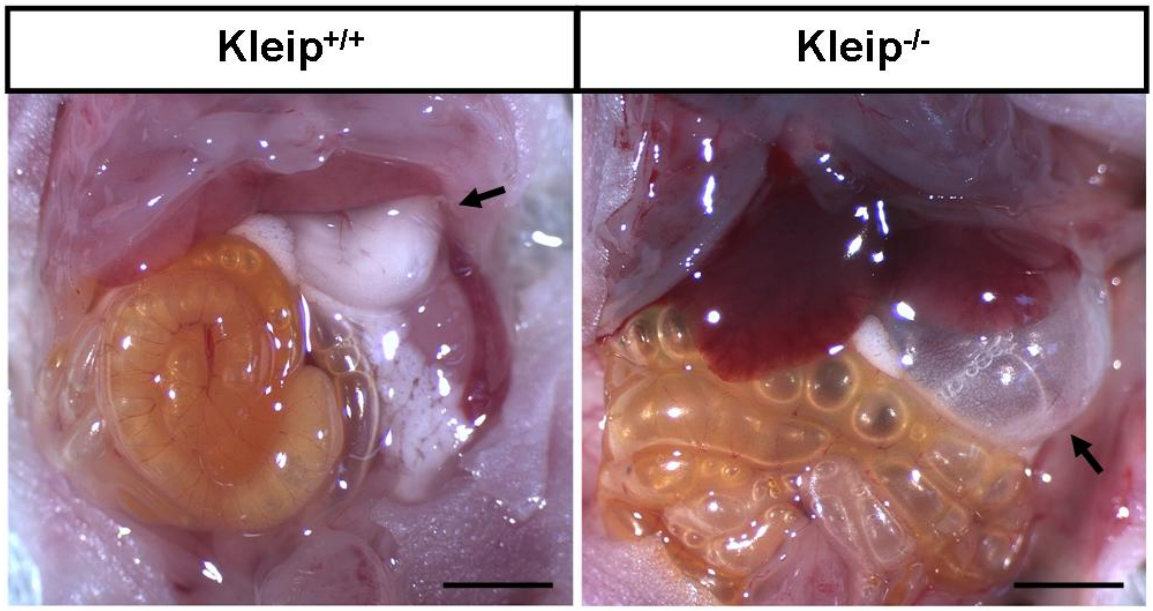

Figure 24: Kleip-mutant neonates suffer from aerophagia.
Immediately after sudden death Kleip-mutant puppies were macroscopically analyzed. As control, wild-type litters from the same heterozygous Kleip-intercross were sacrificed by decapitation. While perished Kleip$^{-/-}$-puppies (right image) suffered from with air-expanded stomachs (indicated by arrow) and intestinal-tract the control littermates (left image) showed a normal seized with milk filled stomach. Scale bars, 2mm.

In figure 13 it has been shown that disruption of *Kleip*-expression during mouse embryogenesis results in a marginal lethal phenotpye. Moreover, the majority of Kleip mutants die within 24 hours after birth presumably due to respiratory distress. Autopsies of dead newborns (P0.5) exhibit in some cases large amounts of air in their stomach and intestinal tract (Figure 24) as compared to wild-type puppies which showed instead a normal with milk filled stomach. The made observations suggest that these homozygous Kleip neonates failed to breathe properly. In previous studies the respiratory distress is sometimes attended by malformations within skeletal architecture, such as in the cranial formation of the secondary palate (Jiang et al., 1998; Kaartinen et al., 1995).

During normal palate morphogenesis in the embryo the primordial palatal shelves are bilaterally elevated, which is followed by growing towards the above the tongue located midline. In a final step these shelves fuse and form the roof of the oral cavity, the secondary cleft palate (Ferguson, 1988). Examination of the oral cavity revealed a normal formation of secondary palate in Kleip-mutants (Figure 25). Moreover, osseous related abnormalities that impair normal breathing, like rib malformations, were not observed (data not shown). These findings indicated that the respiratory failure is due to either cardiovascular or to lung defects.

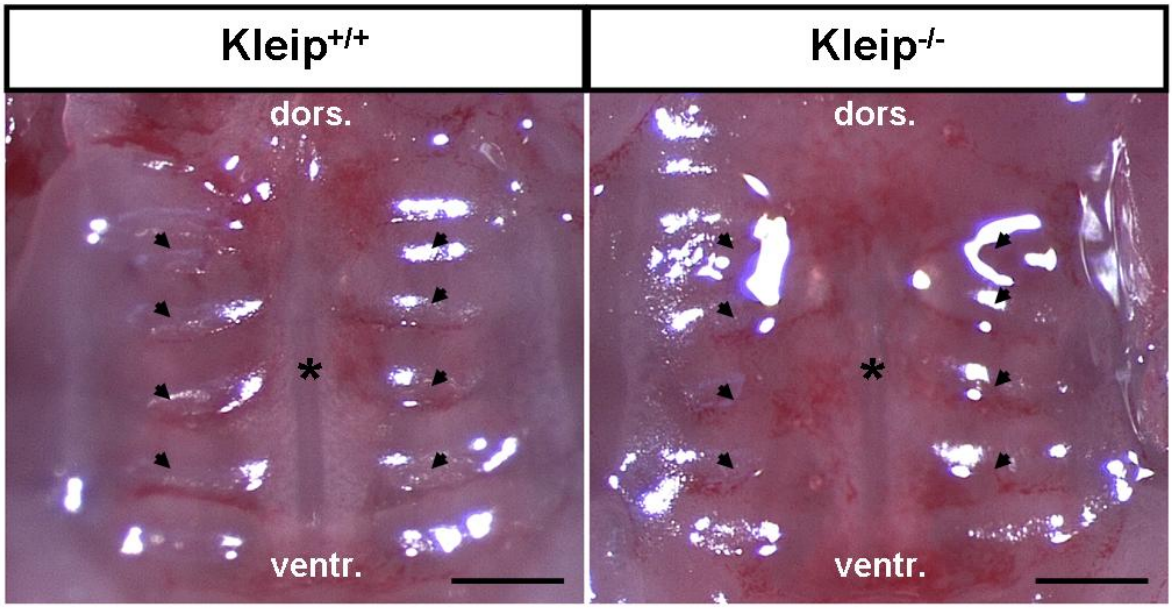

Figure 25: Kleip-mutants display a normal-shaped secondary palate.
Macroscopically analyses exclude possible defects in the formation of the secondary palate as reason for aerophagia. Images represent the caudal view of the secondary palate of a Kleip$^{+/+}$ and Kleip$^{-/-}$ neonate at P0.5.For analyses animals were decapitated and mandible removed. Abbreviation: dors.: dorsal; ventr.: ventral; arrows: plicae palatinae transversae; asterisk: palatine raphe. Scale bars, 500µm.

2.1.2.2 The transition from placental to respiratory circulation is not affected in Kleip$^{-/-}$-neonates

With the onset of breathing after birth dramatic changes occur in the circulatory system of mammalian neonates. The major challenging one is thereby the switch from embryonic, placental to respiratory blood circulation. This process of transition is accomplished by a large specialized vessel, called ductus ateriosus, which connects the pulmonary artery to the aorta. During fetal life the ductus arteriosus bypasses blood flow away from the pulmonary circulation. Simultaneously with the initiation of respiration the thick muscular wall of ductus arteriosus starts to contract and mediates its closure. The initial closure occurs 30 minutes after delivery and is functionally completed after 3 hours (Tada and Kishimoto, 1990). Several studies with transgenic mouse models, as well as in humans, demonstrate that a patent ductus ateriosus implicate live threatening respiratory complications (Coggins et al., 2002; Loftin et al., 2001; Vaughan and Basson, 2000). Examinations of born Kleip-mutants that died less than 3 hours after birth revealed still a fully lumenized ductus arteriosus. However, the majority that died between postnatal stages P0.5 to P1 did not reveal any defects in ductus arteriosus closure mechanism (Figure 26), as well as in the descending congenital vessels. These made findings display that absence of functional Kleip protein to be responsible for rather lung malformations than cardiovascular defects.

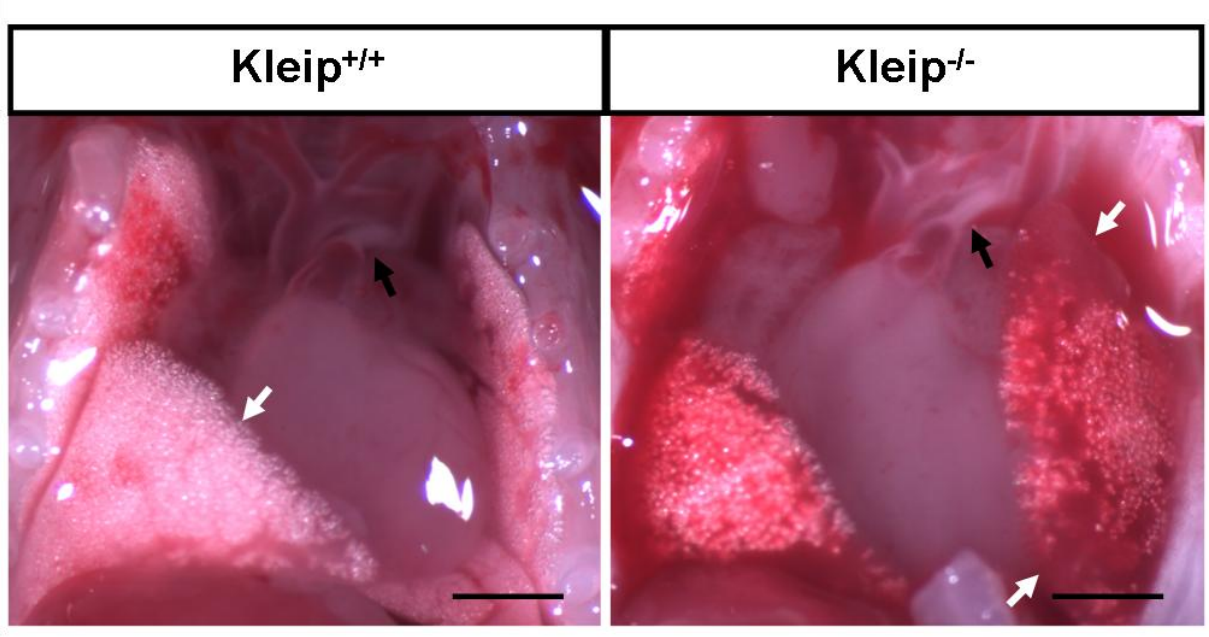

Figure 26: Closure mechanism of ductus arteriosus functions properly in newborn Kleip-deficient neonates.
P0.5 to P1 Kleip-deficient and wild-type puppies were sacrificed. Upon opening of thorax the closure state of ductus arteriosus was examined. Although Kleip-mutants exhibited a closed ductus arteriosus as wild-type animals (black arrow), they displayed lung defects (white arrow). Lungs were hypomorphic and displayed altered branching morphogenesis. Scale bars, 1mm.

2.1.2.3 Lung maturation defects in Kleip-deficient neonates

During mouse development the formation of the lung can be divided into five structural stages (Maeda et al., 2007). Normal developing, healthy newborns should be in the saccular stage (E17.5 to P5) which is characterized by dilation of peripheral airspaces, differentiation of respiratory epithelium, as well as in an increase of vascularization of the saccules. According to the observed postnatal lethality and presumable respiratory distress it is more likely that Kleip-deficient neonates suffer from a delay in lung development. Macroscopic analyses of lungs from newborn Kleip-mutants displayed no obvious gross changes, when compared to wild-type littermates, instead the mutant lungs are inmature. Especially, the branching morphogenesis appeared to be partially inhibited (Figure 26 and 27).

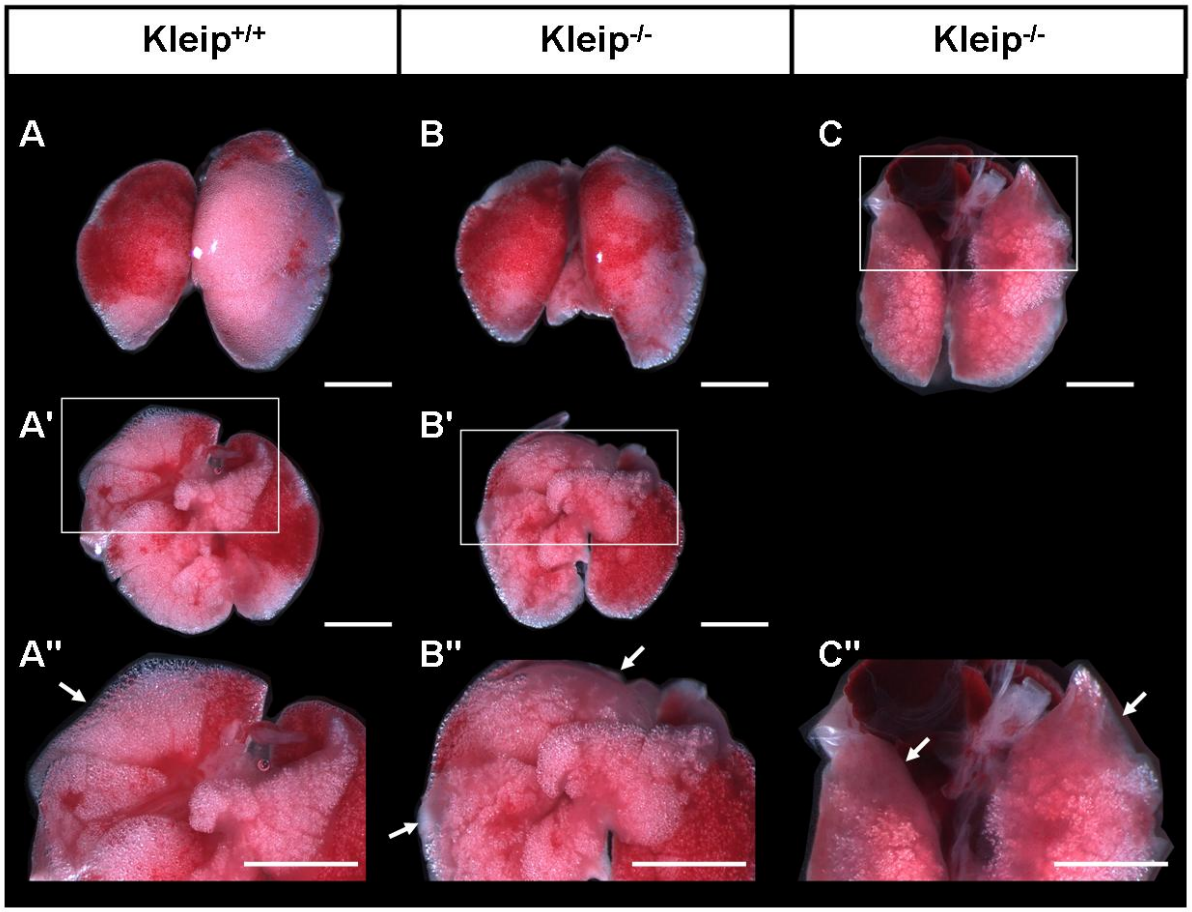

Figure 27: Kleip-mutant neonates display lung maturation deficiencies.
Homozygous lung of P0.5 newborns show after birth less branching morphogenesis and are more hypomorph (Ward et al.), when compared to wild-type littermates. Illustrated are the fresh issected lungs of one wild-type (A) and one homozygous littermate (B), while (C) represents the lung of a perished Kleip$^{-/-}$-neonate (P0.5). Scale bars, 2mm.

Histological examinations of lungs from Kleip-null puppies (P0.5) revealed a lung architecture that was characterized by narrowed alveolar sacs, considerable thickened interalveolar septae and a dense cellularity, when compared to wild-type lungs (Figure 28). To underline the made observations the lung section were metricially quantified. The mean alveolar areas of Kleip-deficient (1988µm^2±109) neonates were in contrast to wild-type animals (5608µm^2±340) significantly reduced. Coincidental the alveolar septae of Kleip$^{-/-}$ lungs were significantly extended (Kleip$^{+/+}$: 9.15µm± 0.12; Kleip$^{-/-}$:13.83µm±0.3). In order to determine whether the greater alveolar septae are the result of hyperproliferation the nuclei were furthermore counted. Comparable analyses elicited that the mean number of counted nuclei was significantly increased in the alveolar wall of Kleip-mutants than in Kleip wild-type animals. In addition to these findings it could be shown that to all analyzed time-points the lungs of both genotypes were not drastically infiltrated by inflammatory cells.

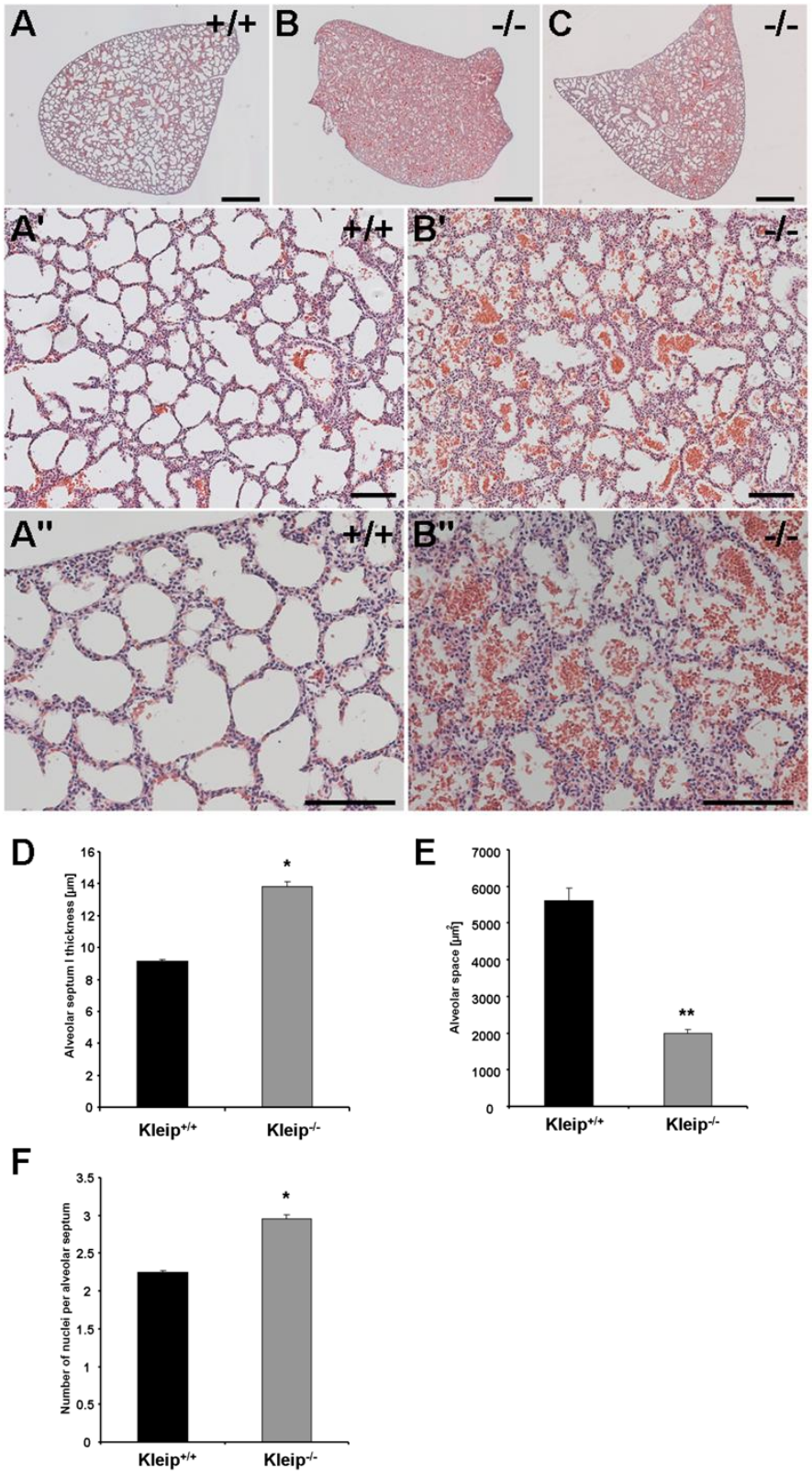

Figure 28: Decreased lung maturation in Kleip-mutant neonates.
Paraffin sections (8µm) of P0-P0.5 lungs after H&E staining. Kleip$^{+/+}$ lungs revealed a normal and ventilated lung morphology (A, A', A''), while Kleip$^{-/-}$ lungs displayed reduced to nearly missing sacculation (B, B', B'', C). Furthermore, comparable analyses of lungs from Kleip$^{+/+}$ and Kleip$^{-/-}$ newborns exhibited significant changes in septal thickening (B''). For quantification the lungs of Kleip$^{+/+}$ (n=5) and Kleip$^{-/-}$ (n=4) newborns were measured in relation to their alveolar area (D), septae thickening (E) and the total number of nuclei per alveolar septum (F). Results are expressed as mean ± s.e.m *p<0.0002;** p<0.005. Scale bars, 500µm (upper row), 100µm (middle and lower row).

2.2 Further G-protein signaling molecules in relation to angiogenesis

2.2.1 ROCK signaling involved in angiogenesis

From the literature it is well known that VEGF triggers upon binding to its VEGFR-2 several downstream signaling cascades. One of its downstream mediators is thereby represented by the small GTPase RhoA, which in turn activates the serine/threonine kinases ROCK I and ROCK II (Fujisawa et al., 1996). Previous reports have demonstrated that endothelial inhibition of these kinases with a relatively unspecific pharmacological inhibitor (Y-27632) led to contrary findings, which are still controversially discussed. While some suggested that *in vitro* inhibition of the serine/threonine kinases ROCK I/II leads to a reduction of endothelial migration and capillary-like tube formation (van Nieuw Amerongen et al., 2003), the same and others have demonstrated that the inhibition induces capillary-like sprout-formation and tube stability (Mavria et al., 2006; van Nieuw Amerongen et al., 2003). For the intrinsic determination of the function of ROCK I and ROCK II in angiogenic processes both kinases were inhibited with the specific inhibitor H-1152 and investigated (Ikenoya et al., 2002).

2.2.1.1 Pharmacological inhibition of ROCK I/ II activates angiogenic signaling.

Based on the results of Jens Kroll and Daniel Epting (both CBTM, Mannheim) which identified the Rho-dependent kinases ROCK I/II to function as negative regulators of in-gel sprouting angiogenesis their role on VEGF-induced signaling was further determined. For the confirmation, that endothelial specific pharmacological inhibition of ROCK I/II increases VEGF-induced angiogenic signaling endothelial cells were treated with the ROCK I/II inhibitor H-1152 and tested for the activation of their downstream targets, such as the extracellular signal-regulated kinase (ERK) 1/2 pathway. The obtained data indicated an increase in the ERK activation upon VEGF-stimulation in H-1152 pretreated endothelial cells than in the control (Figure29).

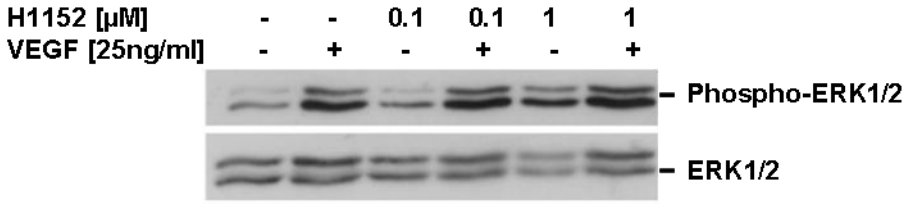

Figure 29: Pharmacological inhibition of ROCK I/II enhances VEGF-induced ERK 1/2 signaling. Pharmacological inhibition of the endothelial ROCK I/II mediator in the VEGF signaling cascade via H-1152 leads to an increased activation of ERK 1/2. For analyses HUVE cells were prior to stimulation with VEGF (25ng/ml) incubated for 30 minutes with H-1152. Subsequent cell lysates were analyzed by Western blotting against phosphorylated ERK 1/2 and total ERK 1/2. Experiments were performed in three independent trials with similar results.

2.2.2 Elmo1/Dock180 complex regulates Rac1-driven vessel formation in zebrafish

Next to the small GTPase RhoA other Rho family members, including the key regulators Rac1 and Cdc42, have been identified to regulate migratory processes during angiogenesis (Dormond et al., 2001; Nacak et al., 2007; Tan et al., 2008). Recently, it has been demonstrated that the endothelial specific disruption of Rac1 in mice result in an early embryonic lethal phenotype effected by an impaired vasculature (Tan et al., 2008). In other model organisms, such as *Caenorhabditis elegans*, *Drosophila melanogaster*, and in human glioblastomas the ELMO1/DOCK180 (engulfment and cell motility 1/ dedicator of cytokinesis 180) complex was identified as a bipartite guanine nucleotide exchange factor regulating the activation of the small GTPase Rac1 and consequently cellular migration (Jarzynka et al., 2007; Lu and Ravichandran, 2006). In order to study elmo1 and dock180 interaction and its function during angiogenesis the expression of both genes were silenced in zebrafish embryos.

2.2.2.1 Dock180 is predominantly expressed in the zebrafish vasculature

Recent findings indicate that dock180 is ubiquitously expressed during early somitogenesis stages of the zebrafish embryo (Moore et al., 2007). For the examination whether dock180 is expressed in the zebrafish vasculature specific immunhistological stainings were performed. Dock180 immunofluorescence stained transverse sections of 48hpf *tg(fli:EGFP)* embryos display a strong expression pattern within the vascular system, such as the dorsal aorta and the posterior cardinal vein (Figure 30).

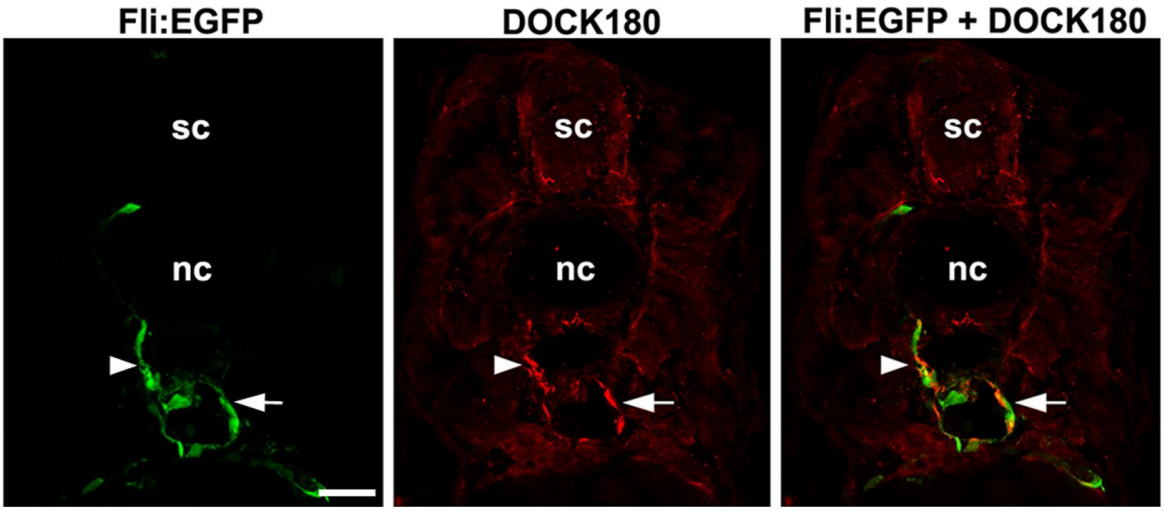

Figure 30: Dock180 is highly expressed in the zebrafish vasculature.
Immunostainings of transverse sections of 48hpf *tg(fli:EGFP)* zebrafish embryos reveal vascular expression of dock180 in the posterior cardinal vein (Ward et al.) and dorsal aorta (arrowhead). Representatively illustrated is the confocal captured fluorescence of endothelial specific EGFP-expression (left), in red the with antibody detected distribution of dock180 (Kleyman et al.)and the merged images (right). Abbreviation: sc: spinal chord, nc: notochord. Scale bar, 25µm.

2.2.2.2 Elmo1 regulates vascular morphogenesis in zebrafish

In further experiments Daniel Epting (CBTM, Mannheim) showed that a global morpholino-based expression silencing of *elmo1* in zebrafish leads to tremendous alterations in the formation of the vasculature, including the intersomitic vessels, the dorsal longitudinal anastomotic vessel (DLAV), the parachordal vessel (PAV), and the development of the thoracic duct (Epting et al., 2010). In order to confirm that the observed vascular phenotype is caused autonomously by endothelial cells and not in response due to other cellular functions in the surrounding tissue, a spatial and temporarily restricted expression silencing of *elmo1* in the ventral mesoderm was performed. For this analysis a photoactivatable morpholino for *elmo1* (PhotoMorph^{elmo1}) was injected into a fertilized egg and activated after 20hpf. Prior to investigation and quantification the experimental settings were tested. In a first step the PhotoMorph^{elmo1} functionality was verified in zebrafish embryos that were globally treated at 20hpf with UV light. After another 28 hours, mRNA was isolated, transcribed and analyzed for Elmo1 expression. Figure 31 represents that UV treatment generated a substantial increase of the morphant splice products, like it was observed in SB-Mo^{elmo1}-injected embryos. As a positive control for spatial restricted irradiation Kaede-mRNA was injected into zebrafish embryos. After light treatment of the embryonic ventral mesoderm at 20hpf only the irradiated field displayed a photoconversion from green to red fluorescence, indicating the functionality of this experimental approach. Hence, the performance of spatial-restricted expression silencing of *elmo1* recapitulates largely a similar vascular phenotype as the global expression silencing. The activation of PhotoMorph^{elmo1} in the ventral mesoderm disrupts the formation of the DLAV, as well as the PAV.

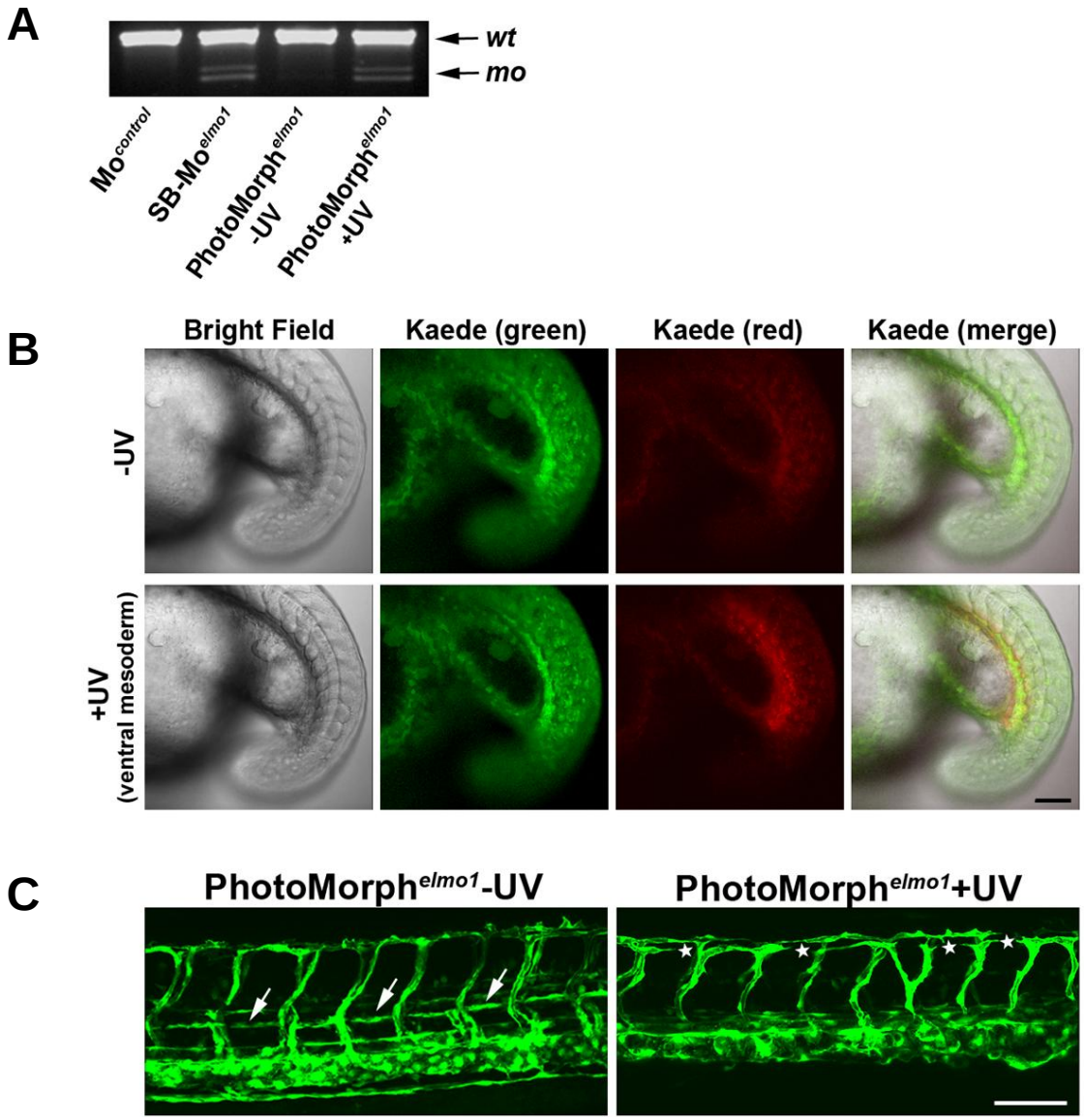

Figure 31: Spatial expression silencing of elmo1 impairs vascular morphogenesis in zebrafish. (A) Expression silencing of *elmo1* in 48hpf *tg(fli1:EGFP)* zebrafish embryos mediated through the injection of an *elmo1* specific photomorph (PhotoMorph^{elmo1}). RT-PCR after global UV irradiation at 20hpf causes a substantial increase of the morphant (mo) splice products at 48hpf. SB-Mo^{elmo1}-injected embryos were utilized as positive control. (B) For the confirmation of spatial-restricted photmorph activation *tg(fli1:EGFP)* zebrafish embryos were injected with Kaede mRNA. Photoconversion from green into red fluorescence due to light treatment, detected by confocal microscopy, indicates the regional activation within the ventral mesoderm of the zebrafish embryos. **Left images**, Bright field images. **Middle images**, green and red fluorescence images of Kaede. **Right images**, merged images. (C) Spatial-restricted expression silencing of *elmo1* reflects a similar vascular phenotype, as the global epression silencing. After light treatment (at 20hpf) the PhotoMorph^{elmo1}-injected embryos display at 48hpf a disrupted formation of the DLAV (asterisks) and the PAV (arrows).Scale bars, 100µm.

3. Discussion

In the last three decades strong efforts have been performed to identify and understand the function and the molecular mechanisms involved in the formation of a proper vascular system. Interestingly, much attention was given thereby to the role of VEGF and its influence on EC migration and proliferation (Ferrara et al., 2003). Beside the discovery of VEGF a large number of further molecules were characterized, which either mediates vessel guidance due to the setting of an attractant or repellent stimulus to ECs, for example, such as the DELTA/NOTCH- or Eph/Ephrin-system (Gerhardt, 2008; Heroult et al., 2006). In contrast other factors were identified to function endothelial cell-autonomously. Many of these cell-autonomous endothelial factors belong to the Rho GTPase family or are involved in the modulation of G-protein signaling. In previous performed *in vitro* studies the Rho GTPase family members were predominantly correlated to basic cellular processes such as cell migration, proliferation and the mediation of cell polarity (Fryer and Field, 2005; Kranenburg et al., 2004; Tan et al., 2008). However, their molecular mechanisms in controlling angiogenesis *in vivo* remain to be determined. Thus, this study was aimed to elucidate the role of G-proteins such as Kleip, elmo1, dock180, and the downstream target of RhoA signaling ROCK in the regulation of angiogenesis *in vivo* in vertebrates.

3.1 Role of *Kleip* during murine development

The first modulator of G protein signaling that is predominantly edited in this thesis comprises the BTB-kelch protein Kleip, which was recently contributed to angiogenesis. In these previous performed studies KLEIP was identified as an actin-binding protein, which is strongly upregulated under hypoxic conditions and acts VEGF-dependent as a functional guanine nucleotide exchange factor for the small GTPase RhoA during *in vitro* angiogenesis. Based on these findings it was suggested that KLEIP function could be essential for physiological and pathological angiogenesis *in vivo* as well as during mouse development (Nacak et al., 2007).

3.1.1 Generation of Kleip deficient mice

In order to explore the role of Kleip during mouse development, especially in the formation of a functional vascular system, the transgenic Kleip embryonic stem cell line XF202 was purchased from the company Baygenomics. This modified ES cell line originates from a gene trap screen, which is characterized by the random insertion of the pGT2LXf construct into the intronic sequence between exon 2 and exon 3 of the mouse *Kleip* gene. In recent years the gene-trapping method has gained more and more prominence among other genome modifying methodologies, such as chemical mutagenesis, and RNA interference-mediated gene silencing chromosome engineering as a high-throughput technology to study the

causes of human diseases. The advantages of this mutagenesis method are beside the gene-orientation the fact that the mutated gene is known from the beginning due to its reverse genetics approaches. Furthermore this cost-effective technology of generating mouse mutants is an unique and effective tool to study the expression pattern of the gene of interest due to the integration of a reporter gene. Especially for genes that are differentially regulated during murine development, as well as for those that are expressed in different cell types and stages. Here in this study the reportergene β-geo was used, which encodes for the fusion protein consisting of the first aminoacids of the Kleip-protein tagged to β-galactosidase and further for neomycin resistance as a by-product. In contrast to gene targeting via homologous recombination this method exhibits yet one noteworthy disadvantage, namely the random insertion of the reporter gene into the genome (Lee et al., 2007; Skarnes, 2005).

3.1.2 Kleip-deficiency leads to a lethal phenotype

In this present study the transgenic founder animals were subsequently crossed after germline transmission into the inbred strain C57BL/6. Due to the establishment of a specific genotyping protocol, as well as the validation of Kleip loss of function via semi quantitative RT-PCR (Figure 12), the transgenic Kleip mice could be used for their further phenotopically characterization. Several rounds of performed heterozygous matings have revealed for the first time that incipient cogenic Kleip-deficient mice die in two waves during their development (Figure 13). A small percentage from around 21% of the homozygous progeny die during embryogenesis between embryonical stage E11.5 and their delivery, whereas nearly half of those that reaches birth die within twenty four hours. In addition, those that survived displayed developmental defects in the eye formation otherwise Kleip-mutants were healthy and fertile (data not shown).

Interestingly, at this point one could argue that there is no real embryonic lethal phenotype. In accordance with Mendel a distribution of 25% homozygous, 50% heterozygous, and 25% wild-type littermates would be normally expected. However, the data from the graphic and table in figure 13 reveal that the percentage of Kleip-mutants at stage E11.5 is slightly increased (25% + 2.9%; n=158). In contrast, at birth (P0) only 22.1% (n=95) of the progeny are homozygous. However, the embryonic lethal phenotype can be furthermore supported by the finding that in nine of thirty nine performed heterozygous intercrosses no homozygous newborns were detectable. Yet, from these findings it was hypothesized that Kleips molecular function is crucial for embryonic and neonatal development which will be further elucidated in the following chapters.

3.1.3 Role of Kleip during embryogenesis

3.1.3.1 Kleip is essential for the maintenance of vascular integrity

To date it is well accepted that the establishment of a functional blood vessel network starts in the mouse embryo around E7.5 with the *de novo* formation of a primitive vascular plexus (Adams and Alitalo, 2007; Risau, 1997). Thereby the process of vasculogenesis is dependent on the growth factor VEGF and endothelial tyrosine kinase receptors, such as VEGFR1 and VEGFR2. The targeted disruption of these genes in mice leads in all three cases to embryonic lethality between E8.5 and E9.5 due to perturbations during the formation of the primitive vasculature (Fong et al., 1995; Shalaby et al., 1995). Between E8.5-E9.5 this initial step is followed by angiogenesis, which is characterized by the remodeling and expansion of the immature and poorly functional vasculature (Adams and Alitalo, 2007). Among the factors involved in angiogenesis the endothelial expressed tyrosine kinase receptor Tie-2 and its ligand adopt a key role. Transgenic mice either for Tie-2 or angiopoetin-1 die around E10.5 because of defects in vessel sprouting, branching, and remodeling (Dumont et al., 1994; Suri et al., 1996). In context to the BTB-kelch protein KLEIP it has been recently shown in *in vitro* analysis with cultured HUVE cells that KLEIP, as a guanine nucleotide exchange factor, plays an important role in the downstream regulation of VEGF-induced endothelial migration and sprouting angiogenesis (Nacak et al., 2007). For this reason, intercrosses of heterozygous Kleip animals were performed and the mouse embryos were to distinct developmental stages first macroscopically and later on microscopically analyzed. On the one hand it has been shown, that some homozygous Kleip-mutants displayed growth morphological differences. However such malformation only became evident at E11.5 (Figure 14A). Prior to this date homozygous embryos were indispensable from their wild-type littermates (Figure 16). Previous performed studies have demonstrated that growth retardation as well as embryonic lethality can be caused by multiple malfunctions. In general, these phenotypes are often correlated with defects during embryonic implantation or cardiovascular development (Conway et al., 2003; Wang and Dey, 2006). Interestingly, beside the growth retardation further analyses have demonstrated that around 16% of the homozygous embryos exhibit at E11.5 life-threatening hemorrhages (Figure 14A). Additionally, such bleedings were mainly located in the embryonic head area. These findings support furthermore the hypothesis that Kleip deficiency during embryonic development leads to a low penetrant, but lethal phenotype. Moreover the made observations emphasize a possible vascular phenotype.

In order to confirm the bleedings first observed in Kleip-mutant mouse embryos another *in vivo* model was chosen to gain further insights into the function of Kleip on vascular integrity. For this purpose the zebrafish model organism with its advantages such as the extra-maternal and rapid development and the embryonic transparency was utilized (Figure 21).

Gene silencing of *Klhl20*, the zebrafish ortholog of murine *Kleip*, was achieved by the injection of a specific splice blocking morpholino into fertilized transgenic fli:EGFP zebrafish eggs. Although high doses of splice blocking morpholino were injected only a partial downregulation of *Klhl20* was reached in the zebrafish embryos (Figure 21C). Nevertheless klhl20 silenced embryos displayed increasing intracranial hemorrhages from 48hpf onward (Figure 21 A&B&D). In summary it has been shown, that the disruption of Kleip in mice, as well as the silencing of Klhl20 in zebrafish, causes in both *in vivo* models life-threatening intracranial hemorrhages.

Furthermore, these findings were reinforced by an additional *in vitro* experiment, the transwell permeability assay. Knock-down of KLEIP in immortalized HUE cells using two specific and independent siRNAs lead in comparison to the scramble control transfected cells to a statistical significant increase in monolayer permeability within the first 120min (Figure 22). Interestingly, even with KLEIP siRNA 1 transfected cells revealed a higher permeability in comparison to the positive control. Taken together, these findings implicate an essential role for Kleip in the maintenance of vascular integrity.

3.1.3.2 Dilatation of cranial vessels in Kleip-null embryos

In general, under normal healthy conditions endothelial cells of the vasculature maintain vascular integrity, as well as permeability, through the regulation of cell-cell and cell-matrix protein interaction (Dejana et al., 2008; Vandenbroucke et al., 2008). In order to identify the reasons for the observed intracranial bleedings *whole-mount* immunofluorescence stainings either with the specific endothelial marker CD31 or endomucin were performed (Figure 14, 15, 16). Kleip-mutants that suffer from hemorrhages revealed ruptured and dilated cranial vessels (Figure 14B), while the greatest possible extent of the body vasculature and the extra-embryonic tissues (Figure 19&20) did not reveal an apparent vascular phenotype. The only exception was exhibited by E10.5 staged Kleip-deficient embryos, which displayed diminished intersomitic vessel sprouting (Figure 16). Moreover, even those Kleip-deficient embryos that displayed no bleedings showed a significant increase in cranial vessel diameter, when compared to wild-type littermates (Figure 15). Although the hemorrhages were first visible at E11.5 such vascular abnormalities were already observed in E10.5 embryos (Figure 16). These made findings are in accordance with those that were previously published by Hellström et al., who showed that mouse mutants either for Pdgf-B or Pdgf receptor-β exhibited a lethal phenotype with widened cranial microvessels and an increase in transendothelial permeability during embryogenesis (Hellstrom et al., 2001). In order to support these findings an additional *ex vivo* p-Sp-explant assay which mimics vasculogenesis and angiogenesis was utilized (Takakura et al., 1998). Surprisingly, this in

collaboration with Anja Runge (DKFZ, Heidelberg) performed assay displayed no similar angiogenic alterations with regard to vessel extention (Figure 17).

In addition, the silencing of *klhl20* in zebrafish *tg(fli:EGFP)* embryos had no effect on the formation of the intersomitic vessels. In contrast, the cranial vessels appeared thinner in the klhl20-silenced embryos than in control-morpholino injected ones (personal communication with Kristina Jörgens, CBTM, Mannheim).

Normally the functional blood vessel is constructed of endothelial tubes surrounded by tightly associated and organized mural cells that mediate vessel stability. However, a dysfunction in the vessel attachment of pericytes and SMCs leads to vessel dilatation and even under worst conditions to the formation of microaneurysms and vessel wall disruption accompanied with hemorrhages (Hellstrom et al., 2001). In the previous mentioned mouse models that either lack Pdgf-B or Pdgfr-β the life-threatening hemorrhages are primarily caused by a diminished pericyte coverage which implicates endothelial cell overproliferation and failure in forming inter-endothelial junctions (von Tell et al., 2006). A similar phenotype is resembled by the G-protein-coupled receptor Edg1 and its ligand shingosine-1-phosphate, indicating that both pathways are closely linked to each other (Kluk and Hla, 2002). Another signaling system involved in vessel growth and stabilization is the angiopoietin/Tie-system. While the binding of Ang-1 to the receptor Tie-2 mediates cell quiescence and vessel stability, the binding of Ang-2 to Tie-2 controls vascular homeostasis through an autocrine loop mechanism (Scharpfenecker et al., 2005). The absence of Ang-2/Tie2 interaction during mouse embryogenesis leads to vessel regression caused by detachment of the endothelium from smooth muscle cells (Maisonpierre et al., 1997; Visconti et al., 2002). From these described mouse models and our obtained *in vivo* data the question arose whether the served hemorrhages are also caused by the loss or disorganization of mural cell attachment to the affected vessels. Interestingly, *whole-mount* double immunofluorescence stainings for endomucin and the pericyte marker NG2 did not display major changes in the attachment of mural cells to the nascent vessels in the cranium of Kleip deficient embryos (Figure 18), arguing against defective migration and recruitment of pericytes as a cause for the leaky vascular phenotype.

3.1.3.3 Possible role of Kleip during prenatal angiogenesis

Taken together, the findings of the present study implicate so far a pivotal role for Kleip's function during prenatal angiogenesis. Although the microvasculature of the central nervous system in Kleip-deficient embryos appears to be normally covered and stabilized by pericytes the observed cranial hemorrhages might be rather caused due to defects in the assembly of adhesive junctions between endothelial cells or between endothelial cells and the extracellular matrix. Nevertheless, it has to be considered that the observed vascular

leakiness is presumably caused by defective association of endothelial cells with pericytes and extracellular matrix like it is described for T-synthase-deficient embryos (Xia et al., 2004). Another example for embryonic lethal hemorrhages with non-impaired pericyte recruitment is provided by the orphan G protein-coupled receptor GPR124. LacZ knock-in null embryos for GPR124 rather reveal numerous packed endothelial cells with diminished cytoplasm (Kuhnert et al., 2010). Based on these two phenotypes we suggest performing comparative ultrastructural analyses, using electron microscopy.

As mentioned above it is more likely that the observed vascular phenotype results of defects in the molecular organization of adhesive junctions. Defects in the organization of these endothelial junctions are often associated with human pathologies, such as vascular malformations, hemorrhagic stroke or edema (Dejana et al., 2009). The inter-endothelial adhesion is thereby mediated by adherens junctions, whereas the adhesive properties to the extracellular matrix are known as tight junctions (Nyqvist et al., 2008; Vandenbroucke et al., 2008). In a previous work Hara and co-workers already identified KLEIP to be involved in actin remodeling at new forming cell-cell contact sites of epithelial cells in a calcium-dependent manner. From these data it was proposed that KLEIP functions as an actin-cross-linker at E-cadherin mediated adherens junctions during the initiation of cell-cell adhesion (Hara et al., 2004). Furthermore, our group could verify in HUVE cells that KLEIP is located in the cytoplasm, however upon VEGF stimulation it translocates to the cell membrane (Nacak et al., 2007). Moreover, based on the fact that the immortalized HUE cells used here in the *in vitro* permeability assay were not co-cultured with mural cells we rather propose defects in the assembly of inter-endothelial junctions or within the focal adhesions between the endothelial cells with the surrounding cell-matrix. A starting point for further experiments will be the examination of several components that are associated to the assembly of adhesive junctions. For instance, endothelial adherens junctions predominantly consist of VE-cadherin a molecule that mechanically connects neighboring endothelial cells by linking α-, β- and γ-catenin to the cytoskeleton (Mehta and Malik, 2006). However, a direct association of both β-catenin and actin to α-catenin has not been reported (Weis and Nelson, 2006). Another important interaction partner is represented by p120, which binds to a juxtamembrane domain of VE-cadherin (Xia et al., 2003). In addition, it is well known that p120 functions as an inhibitor of Rho family GTPases (Anastasiadis et al., 2000). A deletion of these genes during mouse development results in all these cases in an embryonic lethal phenotype with vascular leakiness and severe hemorrhages (Nyqvist et al., 2008; Oas et al., 2010). In contrast to the interendothelial junctions the cell-matrix contacts are primarily composed of integrins. Mice lacking the α_5 subunit of integrins display severe vascular defects, such as leaky and distended blood vessels (Yang et al., 1993). In addition, others implicated for the integrin $\alpha_5\beta_1$ rather to be required for the proper formation and

maintenance of blood vessels than in initial vasculogenesis (Bouvard et al., 2001). Furthermore, it has been shown for the αv subunit of integrins that its absence during murine development is consistent with intracerebral and intestinal hemorrhages (Bader et al., 1998). In summary, alterations within these signaling pathways have an impact in the organization of cytoskeleton which furthermore results in the modification of endothelial cell-cell contact and vessel integrity. Furthermore, a helpful tool to study the role of Kleip in maintaining vascular integrity would be the usage of a conditional knockout mouse model, which allows site-specific recombinase (such as Cre and Flp) to inactivate genes in a spatial and temporally controlled manner during mouse development (Garcia-Otin and Guillou, 2006; Nagy, 2000).

Yet, prior to the performance of the mentioned experimental approaches the identification of Kleip's expression pattern during murine development is still of exceptional importance. In spite of several attempts with several commercially available antibodies directed against the Kleip protein, it was not possible to perform expression studies. None of the tested antibodies were useful for biochemical or immunofluoresence stainings due to the lack of acceptable antibody sensitivity and/or specificity. Similarly and unsatisfactorily results were obtained after specific X-Gal staining (data not shown). Only the endothelial RT-PCR analyses in this study (Figure 23), as well as in those performed by Nacak et al. demonstrate its expression in endothelial cells (Nacak et al., 2007). To solve this problem several antibodies have been generated and tested currently for their specificity. Another approach to overcome such deficits would be the performance of in situ hybridization experiments.

3.1.4 Role of Kleip during neonatal development

3.1.4.1 Kleip-null mutant neonates die presumably due to respiratory distress

At the edge of embryogenesis and neonatal development diverse life-challenging events occur in the neonates after parturition. Beside the birth process itself, other abnormalities in breathing, suckling and homeostasis, as well as the resulting perturbations of these physiological processes can affect neonatal survival (Turgeon and Meloche, 2009). As previously described above, we could show within the scope of this thesis that only a few number of homozygous Kleip embryos die during embryonic development, whereas the majority of those that reaches birth die shortly after within one day (Figure 13). This made observation implies that Kleip is of essential importance for neonatal survival. The first extrauterine and most important challenge of newborns is thereby probably the switch from embryonic oxygen supply accomplished by the mother to independent breathing. Detailed macroscopically examination of perished Kleip-mutant neonates pointed out that neonatal lethality is presumably caused by respiratory distress, because some Kleip-deficient puppies suffered form with air extended stomachs (Figure 24).

Strongly associated to breathing is the closure of a specialized vessel called ductus arteriosus that mediates the connection between the pulmonary artery and the aorta. During embryogenesis the blood circulation is shunted from the developing lungs. However with the onset of breathing the closure mechanism gets initialized that furthermore implies the switch form fetal circulation to pulmonary circulation. Failure in this closing process threatens the health status of neonates as shown by respiratory complications in human newborns presenting a patent ductus arteriosus (Vaughan and Basson, 2000). While the closure mechanism of the ductus arteriosus as well as the morphology of the congenital vessels is persistently not impaired in Kleip-deficient newborns (Figure 26) we rather suggested morphological alterations in the formation of the respiratory tract. Several reports have demonstrated before that asphyxia can be caused by craniofacial defects. Especially alterations in the forming of the secondary plate, which separates the nasal cavity form the oral cavity (Jiang et al., 1998; Kaartinen et al., 1995). Its absence leads to a defective suckling because of the lacking of negative pressure that is normally build up during this process (Turgeon and Meloche, 2009). However, our studies have shown that the by respiratory distress caused alterations in homozygous Kleip neonates are rather caused by a failure in lung morphogenesis and not due craniofacial defects (Figure 25). Yet, it should be noted that asphyxia can be also a result of obstruction in the upper airways like it was previously described for retinalaldehyde dehydrogenase type 3 (Aldh1a3) mouse mutants (Dupe et al., 2003). During the attempt to breathe nasal malformations in these mouse mutants lead to the pulling of the tongue to the palate, thereby resulting in obstruction of the upper respiratory tract and neonatal lethality within 10 hours after birth. Yet, this was not investigated in Kleip-mutants so far.

3.1.4.2 Kleip-mutants exhibit retarded pulmonary development

During the late embryonic phase of lung development, the saccular stage, the fetal lung undergoes structural and functional maturation processes that are required for adaptation to air breathing at birth. The main characteristics of this stage are in particular the formation of terminal lung saccules accompanied with a differentiation process of type I and type II pneumocytes. Prior to parturition lung saccules dilatation mediates the thinning of the pulmonary mesenchyme in the periphery. In parallel apposition of juxtaposed capillaries and saccules facilitates the forthcoming gas exchange. With the first attempts of breathing the pulmonary blood flow increases in the neonates while the in the lung remaining fluid is getting resorbed. In contrast the *de novo* pulmonary surfactant protein/lipid biosynthesis and secretion in the peripheral saccules is activated. A dysregulation of these processes result in pulmonary immaturity and surfactant deficiency accompanied with the respiratory distress syndrome (RDS), which is likely the most important disorder for morbidity and mortality in

human newborns (Jobe, 2010). Based on the previous made findings the lungs of homozygous Kleip neonates were intensively analyzed. Lungs of Kleip-deficient newborns did neither exhibit an abnormal lobulation pattern nor gross morphological alterations (Figure 27). In contrast, histological examinations displayed strikingly changes in the pulmonary tissue structure. Lungs of Kleip-mutants revealed in comparison to wild-type littermates significantly reduced airspace, and marked thickening of alveoloar septae (Figure 28). Although branching morphogenesis was slightly inhibited (Figure 26 & 27), the observed neonatal alveolar hypoplasia implicates rather a developmental arrest at the beginning of the saccular stage. All of our made findings are thereby in accordance to previously published mouse studies, such as the specific respiratory epithelial disruption of the transcription factor FOXA2 (Wan et al., 2004), calcineurin b1 (Cnb1) (Dave et al., 2006) or the global deletion of glucocorticoid receptor (GRα) (Cole et al., 1995). Mutation of FOXA2 and Cnb1 in mice also did not substantially affect early lung branching morphogenesis, instead the lungs showed altered sacculation consistent with a generalized maturation arrest. Expression studies in theses mouse mutants revealed that the respiratory distress is induced by an impaired regulation of surfactant metabolism. Surfactant proteins are known to prevent the collapse of with air-filled alveoli due to the reduction of surface tension.

During the saccular stage lung maturation is closely linked to the differentiation of the lung epithelium into type I and type II pneumocytes. Further the surfactant is synthesized by type II pneumocytes and intracellularly stored by lamellar bodies. In order to identify such a failure in epithelial differentiation or lung maturation it would be helpful to study the expression of several genes that are tightly associated to these processes in Kleip-mutant lungs. For instance the carboxypeptidase M (Nagae et al., 1993) and Aqp-5 (Funaki et al., 1998) genes are expressed in type I pneumocytes, whereas the four main surfactant proteins (SP-A to –D), and VEGF (Bhatt et al., 2000) are expressed in type II pneumocytes and the epithelial progenitor cells (Clara cells) of small bronchioles. In addition, we suggest performing electron microscopy analysis to unravel potential cellular alteration in the differentiation process.

Next to defective maintenance of surfactant synthesis the inadequate lung clearance of remaining embryonic fluids after birth can also affect breathing and neonatal survival. This vital process is dependent on Na^+ absorption (Olver et al., 2004). Mouse mutants for the α-subunit of the epithelial sodium channel (αENaC) displayed an abolished Na^+ transport and developed RDS. Although αENaC mutants were initially able to breathe and inflate their lungs the increasing accumulation of liquid in the pulmonary system caused neonatal death within 40 hours after birth (Hummler et al., 1996). In context, mortality of Kleip-deficient neonates was obvious visible around ten hours after birth. An important tool to determine whether liquid accumulation is responsible for the neonatal lethal phenotype in Kleip-mutants is thereby presumably the weighing of the freshly isolated wet lung.

Another feature that is necessary for transition to air breathing at birth is the increasing vascularity of the saccules that ensures proper respiratory gas exchange. Recently it has been demonstrated by Han et al. that the majority of eNOS-deficient mice die neonatal due to alveolar capillary dyplasia. Next to a marked thickening of saccular septae and reduced surfactant the lungs of mutant newborns exhibited reduced distal arteriol branches accompanied with hypoperfused capillary regions (Han et al., 2004). However, preliminary experiments with after birth isolated Kleip$^{-/-}$-lungs displayed no alterations in the vascular network in comparison to those of wild-type littermates (data not shown), suggesting that the observed lethal phenotype is rather a result of defects in the previous mentioned lung maturation or clearance.

Although our data hitherto only describes morphological changes during the saccular stage of lung development, we conclude that Kleip is indispensable for lung maturation. Transgenic Kleip mice may provide a useful model to investigate the processes and signaling pathways of late gestational and neonatal lung maturation more in detail. In addition heterozygous as well as some homozygous Kleip mice that do not display any viability defects are presumably more susceptible to pathophysiological lung alterations in consequence of stress conditions or to pulmonary infections.

3.2 Further G-protein proteins and their role in angiogenesis

Beside the BTB-kelch protein Kleip, our group is also interessted in other G-proteins that play a putative role during angiogenesis, such as ROCKI/II, and the DOCK180/ELMO1 complex that modulates directly the activation of the small GTPase Rac1. In the scope of this thesis I was able to substantiate the findings of Daniel Epting who was primarily working on these two last mentioned G-proteins.

3.2.1 ROCK I/II functions as negative regulators of VEGF-induced angiogenesis

The first side project deals with the downstream targets of RhoA signaling during angiogenesis-related processes, namely the two highly related Rho-associated coiled-coil forming protein kinases ROCK I and ROCK II. To date it is well known that upon VEGF stimulation RhoA signaling is partially mediated by the activation of ROCK I/II, which in turn promotes actomyosin mediated contractile force generation through the phosphorylation of numerous downstream target proteins. Based on its essential functions during endothelial migration and other angiogenic processes, ROCK I/II become more and more attractive as a therapeutic target for several cardiovascular diseases. Yet, previous studies have demonstrated that the pharmacological inhibition of ROCK I/II apparently led to conflicting results with respect to regulation of angiogenic processes and thereby relying mainly on the usage of the inhibitors Y-27632 and fasudil. For Y-27632 it has been shown that even with

the use of the same concentrations the inhibition of ROCK I/II can affect endothelial migration and sprouting positively (Mavria et al., 2006) as well as negatively (van Nieuw Amerongen et al., 2003). Furthermore, on the one hand the usage of fasudil was reported to inhibit angiogenesis (Yin et al., 2007), whereas on the other hand fasudil was identified to improve endothelial function in patients (Nohria et al., 2006). In order to shed some light on theses discrepancies, we used the supposed specific pharmacological inhibitor H-1152 (Davies et al., 2000) for *in vivo* as well as for *in vitro* studies. Interestingly it could be shown that the blockade of ROCK I/II led to an activation of VEGF-driven retinal neovascularization and sprouting angiogenesis (Kroll et al., 2009). Moreover, these data could be verified by biochemical experiments. While Daniel Epting demonstrated that inhibition of ROCK I/II with the help of H-1152 or ROCK I/II-specific siRNAs resulted in an enhanced VEGF-induced VEGF-receptor kinase domain receptor- or ERK1/2-phosphorylation respectively, I could reinforce these findings by showing that the activation status of ERK1/2 is dependent on the used H-1152 concentration (Figure 29). Taken together, our data identify the inhibition of ROCK I/II activity in endothelial cells as an interesting therapeutic target to enhance angiogenesis. Yet, it cannot be ruled out that H-1152 inhibit additional kinases. For this reason it becomes more and more important to identify further specific inhibitors, which either block ROCK I or ROCK II alone or both of them. Furthermore, the generation of conditional knockout mice for ROCK I and/or ROCK II would be helpful to decipher the specific roles of these two Rho-associated kinases in the cardiovascular system.

3.2.2 The Rac1 regulator elmo1 controls vascular morphogenesis in zebrafish

The last part of this thesis deals with the Dock180/Elmo1 complex, a nucleotide exchange factor for the small GTPase Rac1, which was also investigated in our group. The small GTPase Rac1 is beside RhoA and Cdc42 a major regulator of endothelial cell migration during angiogenesis (Tan et al., 2008) and in other biological systems (Sugihara et al., 1998). Initially the ELMO1/DOCK180 complex has been described as a bipartite guanine nucleotide exchange factor regulating Rac1 activation (Lu and Ravichandran, 2006). The data presented herein show for the first time that the interaction of elmo1 and dock180 is also important for the formation of the zebrafish vasculature *in vivo*. Dock180 as well as Elmo1 were identified to be expressed in the endothelium (Figure 30 and data from (Epting et al., 2010)). Further Daniel Epting has shown that morpholino based silencing of dock180 alone did not affect vessel formation in zebrafish while the downregulation of elmo1 resulted in an aberrant vessel morphogenesis (Epting et al., 2010). Especially the intersomitic vessels displayed morphological alterations and were unable to shape the dorsal longitudinal anastomotic vessel. Most strikingly,*elmo1* morpholino-injected embryos were unable to form the parachordal vessel. Based on the findings that the parachordal vessel is the origin of the

thoracic duct and the future lymphatic system (Isogai et al., 2003; Yaniv et al., 2006), it was implied that the formation of the lymphatics may also be affected.

During the paper revision process the question arose whether the observed phenotype is caused autonomously by endothelial cells or in response due to other cellular functions in the surrounding tissue. In order to address this question a spatial and temporarily restricted expression silencing of *elmo1* was performed by myself using a photoactivatable morpholino (PhotoMorph^{elmo1}) (Shestopalov et al., 2007). Inactivation of elmo1 in the ventral mesoderm at 20hpf recapitulated largely a similar vascular phenotype at 48hpf (Figure 31) as the global expression silencing of *elmo1* suggesting a cell-autonomous function of elmo1 in the vasculature.

4. Materials and Methods

4.1 Materials

4.1.1 Equipment

Equipment	Company
Agarose gel documentation system	Intas
Analytical balance (ABS)	Kern
Cell Counting Chamber	Neolab
Centrifuge (Rotina™ 420R)	Hettich
Chemiluminescence-imaging system	Peqlab Biotechnology GmbH
CO_2 cell culture incubator (HERA cell 150®)	Thermo Scientific
Confocal microscope (A1R)	Nikon
Cryostat (CM1900)	Leica
Electrophoresis power supply	Consort
FACSAria cell sorter	BD
Fluorescence microscope Axio Imager 2	Zeiss
Incubator	Memmert
Inverted fluorescence microscope (DMI 6000B)	Leica
Inverted light microscope (Type 090-135.001)	Leica
Magnetic stirrer	IKA
Microbiological Safety Cabinets (HERAsafe®)	Thermo Scientific
Microplate reader (Infinite® 200 Pro)	Tecan
Microcentrifuge (Mikro™ 200R)	Hettich
Microtome (HM 355S)	Microm
Microwave	LG
Minicentrifuge (Rotilabo® Uni-fuge)	Carl Roth
Paraffin Embedding machine	Sakura
PCR Cycler (MyCycler™, MJ Mini)	Bio-Rad
pH-meter	WTW
Photometer (NanoDrop 8000)	Thermo Scientific
Precision balance (PC2200)	Mettler
Rocking shaker	Neolab
Section flattening plate (SW 85)	Adamas Instrumenten bv
Stereomicroscope (MZ 9.5)	Leica
Thermo Mixer (MHR11)	HLC BioTech
Vacuum pump	Integra Biosciences
Vortex Mixer	Scientific Industries
Water bath	Julabo

4.1.2 Chemicals

Bulk chemicals were obtained from the following companies:

- AppliChem (www.applichem.com)
- Carl Roth (www.carl-roth.de)
- Fermentas (www.fermentas.de)
- Merck (www.merck.de)
- Roche (www.roche-applied-science.com)
- Sigma-Aldrich (www.sigma-aldrich.com)

4.1.3 Primers

All used primers were purchased from MWG (www.mwg-biotech.com)

Table 2: Regular used primers

Target gene	species	name	sequence	estimated product seize
Kleip	mouse	Pr.20	5'- CAA GTG CGA TTG AAG CAT CC-3'	1349bp
		Pr.22	5'- AAA CAT TGC TCG GAA GTA GG-3'	
Kleip	mouse	Pr.20	5'- CAA GTG CGA TTG AAG CAT CC-3'	591bp
		Pr.21	5'-ACC TGG CTC CTA TGG GAT AG-3'	
Kleip	mouse	sense	5'-GTG ATG GCC TGG GTC AAA TAC-3'	428bp
		antisense	5'-GAG GAT CCA TCA TGG CCG CCT AC-3'	
KLEIP	human	sense	5'-GTG ATG GCC TGG GTC AAA TAC-3'	428bp
		antisense	5'-GAG GAT CCA TCA TGG CCT CCT AC-3'	
TBP	mouse	sense	5'-GGA CCA GAA CAA CAG CCT TCC-3'	535bp
		antisense	5'-CAT GAT GAC TGC AGC AAA TCG-3'	
TBP	human	sense	5'-GGA TCA GAA CAA CAG CCT GCC-3'	335bp
		antisense	5'-CCT GTG TTG CCT GCT GGG ACG-3'	
klhl20	zebrafish	sense	5'-CTG TTA ACC CAG CGG TTG TA-3'	1202bp
		antisense	5'-TTG AGA TAA GAC GAG CCG TC-3'	

Table 3: Irregular used primers

Target gene	Identification	sense (S) antisense (AS)	primer sequence
Kleip	S1	S	5'-GTA AAG AGT GAG AAT CGA TG-3'
Kleip	S2	S	5'-GTC AGA AAG TCA AGG TCC ATC-3'
Kleip	S3	S	5'-CAC TGT TAG GAG TCT CAC AAG-3'
Kleip	S4	S	5'-CAG GAG ACC TCT TCA GAA AG-3'
Kleip	S5	S	5'-GAC CAC ATG TTG AGA GAA CC-3'
Kleip	S6	S	5'-CAC AGA CTC ACT CAA TGC CAG-3'
Kleip	S7	S	5'-GAG ATT CCT GTC CTA CTA TG-3'
Kleip	S8	S	5'-CAG AAG CCA AAT GCT TCA-3'
Kleip	S9	S	5'-GTT GTG CAG AAC CAG CAC TG-3'
Kleip	S10	S	5'-CTA GGG TAG TGA GTA TTG TC-3'
Kleip	S11	S	5'-GAA GTA AGC ACA CTT GTC CC -3'
Kleip	S12	S	5'-GAC TCT AGG AGT TTT GGA TG-3'
Kleip	S13	S	5'-GAT CTG GTT CCT TCT GGT CT-3'
Kleip	S14	S	5'-GAC ATT TTT GAT ATT AGG AC-3'
Kleip	S15	S	5'-CAC CAG TCA GAA TGT CTA AG-3'
Kleip	S16	S	5'-CTG ACC CAG TGA ACA GAA TG-3'
Kleip	S17	S	5'-GTC ACT GAG TTA GCC TCA AG-3'
Kleip	S18	S	5'-CAC ATG GTT CAC ATG CTG AC-3'
Kleip	S19	S	5'-CTC GAT CCA GAT TTA GCA GG-3'
LacZ	LacZ	S	5'-TAT CGA TGA GCG TGG TGG TTA TGC C-3'
LacZ	LacZ	AS	5'-GCG CGT ACA TCG GGC AAA TAA TAT C-3'

4.1.4 Small interfering RNA (siRNA)

Knock-down of KLEIP via siRNA was achieved using Silencer® pre-designed siRNA purchased from Ambion (www.ambion.com):

Table 4: Used siRNA

Target gene	siRNA	sequence sense (above) sequence antisense (below)
KLEIP (human)	siRNA 1 (ID: 21286)	5'-GGG CUA UGG AAU UAC UGA Utt-3' 5'-AUC AGU AAU UCC AUA GCC Ctc-3'
KLEIP (human)	siRNA 2 (ID:21381)	5'-GGG CAA UGU UCA GAC UCU Utt-3' 5'-AAG AGU CUG AAC AUU GCC Ctc-3'

As a negative control the Ambion Silencer® Negative Control siRNA #1 (AM4635) was used.

4.1.5 Splice-site blocking morpholinos

Splice-site blocking (SB) morpholinos for silencing of *klhl20* and *elmo1* in zebrafish were purchased from GeneTools (www.gene-tools.com).

4.1.6 RT-PCR and PCR reagents, buffers, nucleotides

The following reagents were used for RT-PCR and PCR

Reagents	source of supply
E.coli RNase H, 2U/µl	Invitrogen
DEPC-treated water	Invitrogen
dNTP mix, 10mM each	Invitrogen & Peqlab
DTT, 0.1M	Invitrogen
Magnesium chloride, 25mM	Invitrogen
random hexamers, 50ng/µl	Invitrogen
10x Reaction buffer S	Peqlab
Ribonuclease inhibitor, 40 U/µl	Invitrogen
RNaseOUT™ recombinant	Invitrogen
10x RT buffer	Invitrogen
SuperScript™ II reverse transcriptase, 50U/µl	Invitrogen
Taq DNA polymerase 5U/µl	Peqlab

4.1.7 Kits

Kits	source of supply
DAB Peroxidase Substrate Kit	Vector Laboratories
RNeasy® Micro Kit	Qiagen
RNeasy® Mini Kit	Qiagen
SuperScript™ First-Strand Synthesis System for RT-PCR	Invitrogen
VECTASTAIN Elite ABC Kit (Rabbit IgG)	Vector Laboratories

4.1.8 Transfection reagents

Reagents	source of supply
Oligofectamine™	Invitrogen

4.1.9 Antibodies

4.1.9.1 Primary antibodies

Specification	Host	source of supply
anti-mouse CD31 (MEC 13.3), monoclonal	rat	BD Pharmingen (553370)
anti-mouse CD31 (MEC 13.3), monoclonal, FITC-conjugated	rat	BD Pharmingen (553372)
anti-human CD31 (JC70A), monoclonal	mouse	Dako (M0823)
anti-mouse CD34 (RAM 34), monoclonal, Alexa 647-conjugated	rat	BD Pharmingen (560230)
anti-DOCK 180 (H-70), polyclonal	rabbit	Santa Cruz (sc-5625)
anti-mouse Endomucin (V.1A7), monoclonal	rat	Santa Cruz (sc-53940)
anti-ERK1/2 (K-23), polyclonal	rabbit	Santa Cruz (sc-94)
anti-NG2, polyclonal	rabbit	Milipore (AB5320)
anti-phospho-ERK1/2 (E-4), monoclonal	mouse	Santa Cruz (sc-7383)
anti-human SMA (1A4), monoclonal	mouse	Dako (M0851)

4.1.9.2 Secondary antibodies

Specification	Host	source of supply
anti-mouse IgG, HRP	rabbit	Dako (P0260)
anti-mouse IgG, Alexa 546	goat	Molecular Probes (A-11003)
anti-rabbit IgG, Alexa 488	donkey	Molecular Probes (A-21206)
anti-rabbit IgG, Alexa 546	goat	Molecular Probes (A-11071)
anti-rabbit IgG, HRP	goat	Dako (P0448)
anti-rat IgG, Alexa 546	goat	Molecular Probes (A-11081)
anti-rat IgG, biotin	rabbit	Dako (E0468)
anti-rat IgG, HRP	rabbit	Dako (P0450)

4.1.10 Nuclei Staining reagents

Specification	source of supply
Hoechst Dye (DAPI; 33258) 10mg/ml	Sigma Aldrich

4.1.11 Additional staining reagents

Specification	source of supply
CAS Block	Invitrogen
DAB-tablet, 10mg	Sigma Aldrich
Pap Pen	Dako
DPX mounting medium	Sigma Aldrich
Eosin Y Solution	Sigma Aldrich
FITC-dextran	Sigma Aldrich
Fluorescent Mounting Medium	Dako
Hydrogen peroxide, 30%	Roth
Kaiser's glycerol gelatine	Merck
Mayer`s Hematoxylin solution	Roth
Mouse BD Fc Block™ (rat anti-mouse CD16/CD32; clone 2.4G2)	BD Pharmingen
Nickel chloride	Sigma Aldrich

4.1.12 Markers

Specification	source of supply
GeneRuler™ DNA Ladder Mix	Fermentas (SM0331)
PagerRuler™ Protein Ladder	Fermentas (SM1811)

4.1.13 Miscellaneous

Specification	source of supply
Blotting Papers (Grade GB003)	Whatman
Fibronectin	Sigma-Aldrich
Injection needles	
(0.4 x 19mm, 27G ¾" – Nr.20)	BD
(0.7 x 30mm, 22G 1¼" – Nr.12)	BD
Lab-Tek chambered coverglass	Nunc
Low Melting Agarose	Promega
Microscope coverglasses	Thermo Scientific / Langenbrinck
Microscope glass slides	Thermo Scientific / Langenbrinck
Microtome blades (S35)	Feather
Optitran Nitrocellulose membrane (0.2µm)	Whatman
Paraplast	McCormick
PBS (powder)	Sigma
PCR-Tubes	Starlab
Pierce ECL Western Blotting Substrate	Thermo Scientific
Proteinase K	Roche
RNase-Free DNase Set	Qiagen
Syringe (1ml and 30ml)	BD
Tissue embedding cassettes	Langenbrinck
Tissue embedding molds	Polysciences
Tissue-Tek O.C.T. Compound	Sakura

4.1.14 Cell culture

4.1.14.1 Cell culture consumables

Specification	source of supply
Cell scraper	Greiner
Cell strainer (70µm)	BD
FACS Tubes	BD
Pasteur pipettes	Buddeberg
Plastic cell culture flasks, T75	Greiner
Safe-Lock Tubes (1.5ml, 2.0ml)	Eppendorf
Sterile filters (0.22µm and 0.45 µm)	Roth
Sterile pipettes	BD
Tissue culture and suspension plates	
6-, 24-, 96-well	Greiner
4-well	Nunc
Transwell®, 6.5mm insert, 0.4µm pore seize	Corning
Tubes: 15ml and 50ml	BD

4.1.14.2 Cells

Specification	source of supply
Human umbilical vein endothelial cells (HUE cells)	freshly isolated
Immortalized human umbilical vein endothelial cells (HUE cells)	Ulrike Fiedler Freiburg
OP9 feeder cells (CRL-2749™)	ATCC

4.1.14.3 Cell Culture Media

Specification	source of supply
RPMI 1640	Gibco
Endothelial Cell Growth Medium	Promocell
Endothelial Cell Basal Medium	Promocell

4.1.14.4 Supplements and antibiotics

Specification	source of supply
Fetal bovine serum (FCS), heat inactivated	PAA Laboratories
Penicillin/Streptomycin, 100x	PAA Laboratories

4.1.14.5 Miscellaneous

Specification	source of supply
β-mercaptoethanol (tissue culture tested)	Sigma
Collagen	Wothington
Dimethlysulfoxide (DMSO)	Roth
Dulbecco's phosphate buffered saline (PBS), -Ca^{2+},-Mg^{2+}	Gibco
Opti-MEM® Gluta max	Invitrogen
Trypsin-EDTA solution (25%)	Gibco

4.1.15 Growth factors and inhibitors

Growth factors and inhibitors	source of supply
Recombinant human Erythropoietin	R&D systems
Recombinat human VEGF-A_{165}	R&D systems
Recombinant mouse Interleukin 6	R&D systems
Recombinant mouse SCF	R&D systems
ROCK I/II inhibitor H1152	Calbiochem

4.1.16 Solutions and buffers

Solutions and buffers for agarose-gels, SDS-PAGE and Western blotting were prepared according to standard methods (Sambrook and Russell, 2001)

4.1.16.1 Lysis buffer

Lysis buffer	Components
10x Erythrocytes lysis buffer	1.55mM NH_4Cl 0.1M NH_4HCO_3 1mM EDTA aqua dest. ad 1000ml
Mouse tail lysis buffer	100mM Tris / HCl pH8.5 5mM EDTA 0.2% SDS 200mM NaCl Proteinase K (final concentration 100µg/ml)
Nonidet P-40 (NP-40) cell lysis buffer	150mM NaCl 50mM Tris / HCl pH 7.4 10mM EDTA 1% NP-40 (v/v) 10% Glycerol (v/v) 1% Protease Inhibitor Cocktail (Sigma-Aldrich) (v/v)
Sodium vanadate (Na_3VO_4) lysis buffer	NP-40 Lysis buffer 1% Vanadate (v/v)

4.1.16.2 Staining solution

Staining solution	Components
3,3'-Diaminobenzidine (DAB) staining solution	1.step: dissolving 10mg DAB tablet (Sigma-Aldrich) 10ml 1x PBS (w/o Ca^{2+} and Mg^{2+}) 2.step: dilution 3ml DAB/PBS 7ml 1x PBS (w/o Ca^{2+} and Mg^{2+}) (final concentration 0.3mg/ml)

4.1.16.3 Tissue fixation solutions

Tissue fixation solutions	Components
4% PFA/PBS	0.2g Sodium hydroxide (NaOH) 4g Paraformaldehyde 0.84g Sodium di hydrogen phosphate (NaH_2PO_4) pH 7.2 aqua dest. ad 100ml
Zinc fixative	1l 0.1M TRIS, pH 7.4 0.5g Calcium acetate ($C_4H_6O_4Ca$) 3.2mM 5g Zinc acetate ($Zn(CH_3CO_2)_2$) 27.3mM 5g Zinc chloride ($ZnCl_2$) 36.7mM

4.1.16.4 Washing buffer

Washing buffer	Components
PBSMT	3% instant milk powder (w/v) 0.1% Triton X-100 (v/v) 1x PBS (w/o Ca^{2+} and Mg^{2+})
PBST 0.1%	0.1% Tween 20 (v/v) 1x PBS (w/o Ca^{2+} and Mg^{2+})

Washing buffer	Components
FACS buffer	0.5% FCS (v/v) 1x PBS (w/o Ca^{2+} and Mg^{2+})
FACS washing buffer	2.5% FCS (v/v) 1x PBS (w/o Ca^{2+} and Mg^{2+})

4.1.16.5 Miscellaneous buffer

Miscellaneousbuffer	Components
PBT	0.2% BSA (w/v) 0.1% Triton X-100 (v/v) 1x PBS (w/o Ca^{2+} and Mg^{2+})
Stripping buffer	0.375g Glycine 500µl fuming HCl aqua dest. ad 50ml
50x TAE	242g Tris 57.1ml Acetic acid 100ml 0.5 EDTA pH 8.5 aqua dest. ad 1000ml
10x TE buffer	100ml 1M Tris / HCl, pH 7.5 20ml 500mM EDTA, pH 8.0 aqua dest. ad 1000ml

4.1.16.6 Blocking solutions

Blocking solutions	Components
3%BSA/PBS	3% Bovine Serum Albumin (w/v) 1x PBS (w/o Ca^{2+} and Mg^{2+})
5% milk powder/PBST	5% instant milk powder (w/v) 1x PBST 0.1% (w/o Ca^{2+} and Mg^{2+})

4.1.16.7 Sample buffers

Sample buffers	Components
5x protein sample buffer	250mM Tris / HCl, pH 6.8
	0.5M DTT (1.4-Dithiothreitol)
	10% SDS(v/v)
	0.5% Bromphenol Blue solution (v/v)
	50% Glycerol (v/v)
5x DNA sample buffer	0.2% Bromphenol Blue solution (v/v)
	50% Glycerol (v/v)
	10mM EDTA

4.2 Methods

4.2.1 Molecular Biology

4.2.1.1 RNA isolation

For RNA isolation of animal cells the cell suspension was centrifuged (198 x g, 5min, 4°C; Hettich) and the supernatant aspirated. 350µl RLT buffer (RNeasy® Mini Kit or RNeasy® Micro Kit) were mixed with β-Mercaptoethanol (10µl β-Mercaptoethanol/1ml RLT buffer) and added to the cell pellet. After incubation at -20°C the RLT buffer was defrosted and the cell lysate was homogenized by passing through a 22-gauge (0.9mm) needle attached to a 1ml syringe for at least 15 times. The following RNA isolations steps, as well as the optional DNAse digestion, were performed according to the manufacturer's instructions. The RNA was eluted in 14-30µl RNase-free water and stored at -80°C. The RNA concentration was measured photometrically with NanoDrop (Thermo Scientific). For the RNA isolation of human cells the procedure from above were used with the following modifications. Prior to cell lysis with 600µl RLT buffer the adherent growing cells were washed twice with PBS to remove the culture medium. Furthermore, for RNA elution 30-50µl RNase-free water was used.

4.2.2 Reverse transcription and Polymerase Chain Reaction (RT-PCR)

4.2.2.1 Reverse Transcription

RT-PCR was performed to detect the expression levels of *Kleip* (*Klhl20*) in vertebrates, such as zebrafish, human or mice, as well as zebrafish elmo1. As control the analogous housekeeping gene tata box binding protein (TBP) was used. The transcription from mRNA into copy DNA (cDNA) was performed according to the SuperScript™ First-Strand Synthesis System for RT-PCR (invitrogen) instruction manual. For reverse transcription 1 to 5µg total cellular RNA was transferred into a PCR tube and mixed with 3µl random hexamer primer (50ng/µl) and 1µl of dNTP mix (10mM each). The total volume of 10µl was adjusted by adding DEPC-treated water. After incubation at 65°C for 5 minutes the reaction unit was chilled on ice, before the following RT-reaction buffers and nucleotides were added: 2µl 10x RT buffer, 4µl $MgCl_2$ (25mM), 2µl DTT (0.1M) and 1µl RNaseOUT recombinant ribonuclease inhibitor. The components were collected by a brief centrifugation step with the minicentrifuge (Carl Roth) and incubated at 25°C for 2 minutes. After addition of 1µl SuperScript™ II RT (50U/µl) further incubation steps followed: 25°C for 10min, 42°C for 50min. The reverse transcription reaction was stopped by heating to 70°C for 15min, followed by a short cooling on ice. Before the cDNA was used for expression analysis, the RNA was digested in a final step by adding 1µl of RNaseH (2U/µl) with an additional incubation for 20min at 37°C. Excessive cDNA was stored at -20°C.

4.2.2.2 Polymerase Chain Reaction (PCR)

In general, PCR was performed using 1-2µl cDNA / DNA, 0.04µl of the corresponding primers (4pmol), 2µl 10x reaction buffer S, 0.4µl dNTP-mix (10mM each), and 0.2µl Taq DNA polymerase (5U/µl). The reaction volume was adjusted to 20µl with water. For genotyping of mouse tails the amplification reaction was performed as follows:

First denaturation: 94°C, 3min
Denaturation: 94°C, 45sec
Annealing: 58°C, 30sec
Extension: 72°C, 1min 30sec
Final extension: 72°C, 10min

The reaction ran for 32 cycles in a Bio-Rad PCR Cycler. Amplification of the product was confirmed by 1% - 2% gel electrophoresis (Sambrook and Russell, 2001). For RT-PCR analysis the running conditions were slightly modified. The extension time was reduced to 45-60 sec and the number of cycles was increased to 34 cycles.

4.2.3 Cell culture and transfection

4.2.3.1 Cell culture conditions

Normal and immortalized human vein endothelial cells were cultivated in endothelial cell growth medium containing 10% FCS, 1% Penicilin/Streptomycin and the corresponding supplements. OP-9 feeder cells were cultured in RPMI charged with 10% FCS and 1% Penicilin/Streptomycin. All used cells were cultured in a humidified incubator with constant conditions of 37°C and 5% CO_2. HUVE cells were used for experiments between passage 2 and 5. For stimulation experiments cells were starved in endothelial basal medium containing 2.5% FCS overnight followed by stimulation with VEGF (25ng/ml).

4.2.3.2 Isolation of endothelial cells from umbilical chord

For the isolation of endothelial cells from a fresh umbilical chord a buttoned cannula was inserted into the vein and fixed with a vascular clamp. After a washing step to remove excessive blood the umbilical chord was closed with another clamp at the opposite end. Subsequently, vein got filled with a solution containing PBS (with Ca^{2+} and Mg^{2+}) and collagenase (1mg/ml; Worthington). To detach the endothelial cells from the venous vessel wall the buttoned cannula was carefully removed and the umbilical chord was incubated for 15 minutes at 37°C. Next the venous vessel was flushed with PBS and isolated endothelial cells were collected. After centrifugation (198 x g, 5min, 4°C; Hettich) the HUVE cells were resuspended in fresh growth medium and plated on a flask. In addition medium was changed

twice after an incubation period of 3 hours. At passage 1 endothelial identity was verified by CD31 (JC70A, DAKO) and αSMA (1A4, DAKO) single immunofluorescence stainings. Cells were first fixed with 4% phosphate buffered paraformaldehyde for 30min and than stained with primary antibodies (1:25) for 1h. Labelling of the primary antibodies was accompanied by the incubation with anti-mouse secondary Alexa 546 coupled antibodies (1:250, Molecular Probes) for 30min. After nuclei staining with DAPI (1:5000) for 10min cells were embedded in Kaiser's glycerol gelatine (Merck).

4.2.3.3 Passaging, freezing and thawing of cells

Confluent cells were splitted to mediate cellular expansion. Therefore exhausted growth medium was removed by aspiration and the cell layer was washed once with PBS (w/o Ca and Mg). To detach the cells from the flask a trypsin solution (25%; Gibco) was added and incubated at 37°C for several minutes. Trypsin-dependent digestion was stopped by 10% serum containing medium, followed by a centrifugation step (198 x g, 5min at 4°C; Hettich) to collect the cells. Subsequently, the cells were resuspended in fresh culture medium and splitted on new flasks.

For storage the cells were detached from the flask as described above. After and careful aspiration of the supernatant the cells were resuspended in freezing medium, consisting of endothelial growth medium charged with 10% DMSO and 10% FCS. Next, the cell-freezing medium suspension was transferred to cryostatic vials, which got rapidly frozen in an isopropanol containing box at -80°C overnight. Cells were then stored in liquid nitrogen at -165°C.

For thawing vials were transferred in a 37°C pre-warmed water bath and immediately mixed with culture medium. After a centrifugation step supernatant was discarded and replaced against fresh medium. The resuspended cells were then plated onto a flask.

4.2.3.4 Seeding of cells

For the maintenance of stable conditions during *in vitro* experiments a certain amount of cells was utilized. Prior to determination cells were first detached from the flask bottom by trypsinization, centrifuged and resuspended as described above. For enumeration 10µl of the cell suspension was transferred into a Neubauer counting chamber. After counting from at least on large square by using an inverted light microsope (Leica), the total cell number was calculated according to the following formula.

Total cell number = number of cells per square x volume x chamber factor x dilution.

The chamber factor is 10^4 due to the dimension of the counting chamber. Subsequently the required cell number was adjusted with culture medium and distributed either in 6-well plate or transwell inserts.

4.2.3.5 Transfection of HUE cells with siRNA

HUE cells were seeded in a 6-well plate at a density of $12x10^4$ cells per well 24 hours prior to transfection and were grown to 70-80% confluence. Knock-down of KLEIP was thereby achieved by using pre-designed annealed siRNA from ambion. Per 6-well, 10µl pre-designed specific siRNA against KLEIP (20µM) were mixed with 90µl Opti-MEM (solution A) and 6µl Oligofectamine were mixed with 94µl Opti-MEM (solution B). As negative control 5µl scrambled siRNA #1 (40µM) was mixed with 95µl Opti-MEM, respectively. Both solutions were incubated for 10min at RT, afterwards mixed and incubated for further 30min. In the meantime, cells were washed twice with Opti-MEM. Subsequently, 800µl of Opti-MEM were added to the siRNA-Oligofectamine mixture, which in turn was given drop-wise to the cells. After 4hours of incubation the mixture was changed to normal growth medium. Transfected HUE cells were than cultured for additional 24 hours before they were used for the permeability assay. Knock-down efficiency was determined by mRNA isolation and following semi-quantitative RT-PCR. PCR signals were quantified using Gel-Pro Analyzer 6.0 (Intas) and normalized to its respective loading controls.

4.2.4 Cellular assays

4.2.4.1 Endothelial cell permeability assay

Insert membrane of a transwell unit were coated with fibronectin (10µg/ml in PBS with Ca^{2+} and Mg^{2+}) for at least 1h at RT. Meanwhile, the transfected HUE cells were trypsinized and collected by centrifugation as described in 4.2.3.3. After removing fibronectin and washing of the insert membrane with 100µl serum-free culture medium transfected HUE cells were diluted to the required cell concentration (30×10^4 cells/ml) and 100µl of the cell suspension was pipetted on top of the membrane in the upper compartment. In parallel 600µl of endothelial growth medium were added into the lower compartment. For each condition triplicates were performed. After another 72 hours of cultivation 2.5µl of FITC-dextran (20mg/ml in PBS w/o Ca and Mg) was added in the upper compartment. To distinct time-points 50µl were sampled from the lower compartment, without removing the upper unit. To maintain hydrostatic equilibrium, the volume sample was replaced against 50µl fresh culture medium. For measuring with a microplate reader at 492nm (absorbance) and 520nm (emission) samples were diluted 1:20 in PBS (w/o Ca^{2+} and Mg^{2+}). From each dilution the volume of 100µl was pipetted to a 96-well microtiter plate in triplicates. As positive control transfected HUE cells were starved overnight and shortly before sampling stimulated with

VEGF (25ng/ml). For starvation the media in both compartments were exchanged, while for stimulation VEGF was added only to the upper one.

4.2.5 *In vivo* and *ex vivo* assays

4.2.5.1 Animals

Transgenic mice were housed in a climatic controlled room under specific pathogen-free conditions according to the animal facility regulations of "Zentrum für Medizinische Forschung". Mice were quarterly checked for their state of health according to FELASA guidelines. All animal experiments, either with mice or zebrafish, were conducted in accordance with guidelines outlined by the Regierungspräsidium Karlsruhe (approved protocol number: 35-9185.64). For the investigation of the role of *Kleip* during embryonic development intercrosses of 8 week old heterozygous mice were performed. Females were checked each morning and the presence of a vaginal plug was considered to be E0.5. To certain embryonic stages pregnant females were killed by cervical dislocation and the uterus was removed and placed into PBS. Embryos were dissected and parts of the yolk sac or of the embryonic tail were used for genotyping. State of being alive or dead was determined by the presence or absence of heart beat. Neonates were sacrificed by decapitation.

For zebrafish experiments the published transgenic zebrafish line *tg(fli:EGFP)* was raised under animal husbandry conditions (Lawson and Weinstein, 2002). Zebrafish embryos were kept in E3 solution at 28.5°C with or without 0.003% 1-phenyl-2-thiourea (Sigma) to suppress pigmentation and staged according to somite number or hours post-fertilization (hpf)(Kimmel et al., 1995).

4.2.5.2 Generation of transgenic *Kleip* mice

In order to analyze the function of *Kleip* during mouse development, especially in angiogenic processes, transgenic knockout mice were generated with the help of the gene-trap technology. In brief, the β-geo encoding vector pGT2Lxf was integrated into the *Kleip* gene of mouse embryonic stem cells originating from the mouse inbred strain 129SvEv. The company Baygenomics (http://baygenomics.ucsf.edu/) confirmed the integration molecularly via 5'-RACE. The embryonic stem cell clone XF202 was then injected into a blastocyst of the C57BL/6 inbred strain and furthermore implanted in a CD1 (outbred strain) foster mother. After germline transmission progeny was first crossed onto a CD1 background. Later on heterozygous *Kleip* animals were backcrossed onto a pure C57BL/6 background. For analysis only the mice from the F6 and following generations were used. Currently the mice are in the F9 generation and are nomenclatured as B6.129SvEv-*Klhl20*^{tm1}/Mhm.

4.2.5.3 DNA isolation of mouse tissue

Embryonic tissues and tail biopsies of 4 to 10 week old mice were transferred in safe-lock tubes. Per each tube up to 500µl mouse tail lysis buffer were added and transferred on a rotating thermo mixer (HLC BioTech) at 55°C overnight. The consistent agitation is necessary for complete tissue lysis. Subsequently, samples were centrifuged with a microcentrifuge (18.625 x g, 10min, RT; Hettich) and the supernatant was transferred into with equal volumes of isopropanol filled tube. After homogenization of the lysate on a vortex mixer (Scientific Industries) the visual appearing precipitate got centrifuged (18.625 x g, 5min, RT; Hettich). The supernatant was removed and the DNA pellet washed with 70% ethanol prior to a final centrifugation step. In addition the pellet was dried at 37°C and then dispersed in 20-500µl elution buffer (5mM Tris/HCl, pH 8.5; Marcherey-Nagel).

4.2.5.4 Gene silencing in zebrafish

Klhl20 gene silencing in zebrafish was performed through splice blocking morpholino injection. Before 1µl of the specific splice blocking morpholinos (Gene Tools) were injected through the chorion of a 1-cell or 2-cell embryo the morpholinos were diluted in 0.1M KCl to concentrations of 8µg/µl. For the determination of splice blocking morpholino induced gene silencing efficiency RNA was isolated at 48 or 72hpf, transcribed and checked for expression by RT-PCR analysis. As control zebrafish embryos were injected with a standard control morpholino.

4.2.5.5 Caged Morpholino/PhotoMorph experiments

The PhotoMorph (Shestopalov et al., 2007; Tomasini et al., 2009) caging strand for *elmo1* was synthesized by SuperNova Life Science and annealed to the SB-Mo*elmo1* according to the supplier's protocol in a ratio of 1:5 (SB-Mo^{elmo1} : PhotoMorph). One nanoliter of this dilution (PhotoMorph^{elmo1}) was injected through the chorion of 1-cell or 2-cell stage t*g(fli1:EGFP)* embryos reaching an effective concentration for the SB-Mo^{elmo1} of 2ng. To test the functionality of the PhotoMorph*elmo1* the injected 20hpf embryos were globally treated with UV light for 30min and analyzed by RT-PCR at 48hpf. In addition, UV treated *tg(fli1:EGFP)* embryos were analyzed at different developmental stages until 48hpf regarding morphology and EGFP fluorescence intensity. Yet, no differences were visible as compared to non UV treated *tg(fli1:EGFP)* embryos. For activation of the PhotoMorph^{elmo1}, the ventral mesoderm of dechorionated 20hpf old PhotoMorph^{elmo1} injected *tg(fli1:EGFP)* embryos was irradiated using the confocal microscope for 20 seconds and analyzed and quantified for vascular defects at 48hpf. Spatial restricted irradiation in 20hpf *tg(fli1:EGFP)* embryos was controlled by investigation of Kaede protein photoconversion from green to red fluorescence (150pg *kaede* mRNA injection, 1 min UV irradiation by confocal microscope). For confocal

image capturing and irradiation zebrafish embryos were anesthetized with 0.003% tricaine. Moreover, 48hpf embryos were embedded in 1% low melting agarose prior to confocal imaging.

4.2.5.6 Isolation and cultivation of p-Sp-explants

P-Sp-explants were generally isolated and cultivated from E9.5 embryos according to the described protocol in the Takakura paper (Takakura et al., 1998). Modifications are described in the following. After isolation of the embryonic AMG region the explant was transferred to the center of a 4-well plate and cocultured on a cell layer of OP-9 stromal cells (ATCC). Explants were cultured for 14 days in RPMI 1640 (Gibco) with 10% cell culture tested FCS (a gift from the transgenic service unit at the DKFZ) supplemented with IL-6 (20ng/ml), EPO (2U/ml), mSCF (50ng/ml), and tissue culture graded β-mercaptoethanol (10^{-5} M). Every second day media was replaced. Assay was stopped by overnight fixation with 4% formaldehyde at 4°C.

4.2.5.7 Isolation of embryonic endothelial cells via FACS sorting

From heterozygous *Kleip* intercrosses E11.5 embryos were dissected and transferred individually into with ice cold PBS filled 50ml tubes. In parallel the yolk sac from each embryo was removed for genotyping. Embryos were washed several times in PBS before they were mechanically shredded in 5ml digest solution (PBS with Ca^{2+} and Mg^{2+}, collagenase 2mg/ml, dispase 0.5U/ml) and incubated at 37°C for 30 minutes. After homogenization each cell suspension was filtered with a 70µm cellstrainer (BD) and washed several times with PBS (w/o Ca^{2+} and Mg^{2+}) supplemented with 2.5% FCS (FACS washing buffer). Next the in 2ml PBS resuspended pellet was mixed with 18ml erythrocytes lysis buffer (1x) and incubated for additional 10 minutes at RT. Lysis was stopped by adding PBS supplemented with 0.5% FCS (FACS buffer). For cell labeling embryonic cells were transferred in a 15ml tube and blocked with FACS buffer containing 1% mouse BD Fc Block™. Afterwards cells were incubated with direct-labeled CD31-FITC and CD34-APC antibodies for 30 minutes at 4°C in the dark. In addition the cells were washed twice with FACS buffer to remove all non-binding antibodies. At the end the cells were resuspended in 250µl FACS buffer. Only the $CD31^{+}CD34^{+}$ endothelial cells were isolated in the in-house FACS core facility with FACS Aria sorter. Finally RNA was isolated with the RNeasy® Micro Kit.

4.2.5.8 Microarray

For transcript expression profiling studies a whole genome BeadChip® microarray was performed. After RNA isolation the RNA amount of the triplicates for *Kleip*-deficient or wild-type embryos was photometrically determined (Nano Drop 8000). Hybridization of the processed samples on Illumina MouseWG-6 v2.0 Sentrix BeadChip® arrays was performed by the Genomics and Proteomics Core Facility at the DKFZ, Heidelberg according to the manufacturer's protocol.

4.2.6 Immunohistochemistry

4.2.6.1 Processing of extraembryonic tissue and neonatal lungs for paraffin sections

Immediately after dissection of the placenta and neonatal lungs, the tissues were fixed in zinc fixative overnight at 4°C. The next day, tissues were washed several times to get rid of excess fixation solution. Afterwards, the samples were dehydrated in an ascending alcohol series (table 5) before they were manual embedded in paraffin.

Table 5: Dehydration of tissue samples for paraffin embedding

		Placenta (E13.5)	Lung (neonatal)
1.)	70% Ethanol	0:45 h	1:00 h
2.)	80% Ethanol	0:45 h	1:00 h
3.)	90% Ethanol	0:45 h	1:00 h
4.)	100% Ethanol	0:45 h	1:00 h
5.)	100% Ethanol	0:45 h	1:00 h
6.)	100% Ethanol	0:45 h	1:00 h
7.)	Xylol	0:10 h	0:15 h
8.)	Xylol	0:10 h	0:15 h
9.)	Xylol	0:10 h	0:15 h
10.)	Paraffin	0:30 h	0:45 h
11.)	Paraffin	0:30 h	0:45 h

In the following step serial sections (8µm) were performed with a microtome (Microm), whereby the sections were mounted on glass slides. The sections were smoothened on a 42°C warm plate. Finally sections were deparaffinized and reyhdrated in a descending alcohol series as indicated in table 6.

Table 6: Rehydration of tissue samples for different staining

1.)	Xylol	3 min
2.)	Xylol	3 min
3.)	Xylol	3 min
4.)	100% Ethanol	5 min
5.)	100% Ethanol	5 min
6.)	100% Ethanol	5 min
7.)	90% Ethanol	5 min
8.)	80% Ethanol	5 min
9.)	70% Ethanol	5 min
10.)	ddH_2O	≥ 5 min

4.2.6.2 H&E staining

For hematoxylin and eosin staining lung or placenta paraffin sections (8µm) of murine neonates were deparaffinized and rehydrated in a descending alcohol series as described above. Nuclei were then stained with freshly filtered Mayer's haemalaun for 2min and washed for 3min in tap water. In contrast the cytoplasm was stained with Eosin Y for 1min. Afterwards the sections were washed in tap water for 3min, followed by dehydration with sequential increasing ethanol washing steps (table 6 in reverse order; each step 2min) and mounted in DPX. Lung tissue morphology was analyzed with the Axio Imager 2 (Zeiss) and quantified with the axiovision software.

4.2.6.3 CD31 DAB staining on paraffin sections

Paraffin sections were deparaffinized and rehydrated as described above. In order to prevent the sections from dehydration the following steps were performed in a humid chamber. After rehydration sections were framed by the usage of a pap pen (Dako). Tissue antigen retrieval was accompanied by incubation with in 1x TE buffer diluted Proteinase K (20µg/ml) for up to 8min at 37°C. This step was followed by three PBS washing steps (5min each). For blocking of the endogenous peroxidase the on slides-mounted sections were incubated in 3% H_2O_2 for 12min. Thereafter slights were washed several times with PBST and unspecific binding was blocked for 30min at RT with 1%BSA/ 8%FCS/ PBST. The primary rat anti-mouse CD31 (MEC13.3) antibody was diluted 1:100 in the previous blocking solution and incubated over night at 4°C. Next day, slides were washed three times with PBST before the placental tissue was incubated with the corresponding biotin-labelled secondary antibody (1:100) for 45min at RT. During secondary antibody incubation the VECTASTAIN- and DAB- solutions were prepared. For the VECTASTAIN-solution 2.5ml PBS was respectively charged with one drop

of reagent A and B of the VECTASTAIN Elite ABC Kit (Vector Laboratories). After a short accumulation phase from around 15-20min the in the meanwhile with PBS washed sections (3x 5min) were incubated with this solution for additional 20min. Subsequently the slides were transferred into with DAB-solution filled cuvette. For color development 1µl of 30% hydrogen peroxide (0.03% final concentration) was added to the DAB-solution. Prior to analysis with the inverted DMI 6000B fluorescence microscope (Leica) slides were intensively washed with PBS and mounted with fluorescent mounting medium (Dako).

4.2.6.4 Dock-180 immunfluorescence staining on zebrafish cryo-sections

For immunhistological Dock-180 staining 48hpf t*g(fli1:EGFP)* zebrafish embryos were first fixed in phosphate buffered paraformaldehyde for 2h at 4°C. This step was continued by intensive washing in PBS. Subsequently embryos were dehydrated in 18% sucrose/PBS overnight at 4°C. The following day embryos were embedded in O.C.T medium (Sakura) and cut into 20µm sections. In order to guarantee the investigation of intersomitic vessels only the cross-sections in the area of the yolk extension were further processed. Cryo-sections were initially rehydrated with PBS under humid conditions before the samples were pretreated with 0.3% Triton-X for up to 8min. After a 30min blocking step with CAS-Block slides were incubated with primary Dock-180 antibody (Santa Cruz; 1:50) over night at 4°C. Next, excess and unbound primary antibodies were removed by washing with PBS. This step was followed by incubation with the recommended secondary Alexa 546 labeled antibody (Molecular Probes; 1:500) for 45min at RT. Finally zebrafish sections were washed again and mounted with fluorescent mounting medium (Dako). Confocal images were taken with the A1R (Nikon) at the Nikon imaging center in Heidelberg.

4.2.6.5 *Whole-mount* CD31 DAB staining

The *whole-mount* CD31 staining was performed based on the protocol of (Sato and Bartunkova, 2000). In brief, embryos (E10.5) or yolk sacs were fixed in 4% PFA in PBS at 4°C overnight and washed in PBS several times. Prior to dehydration through graded methanol series, a sharp incision was made along the dorsal midline of the embryonic hindbrain with the help of a pulled injection needle. This step was followed by tissue bleaching of and blocking of the endogenous peroxidase via the usage of 5% H_2O_2/ methanol (4-5 hours). Bleaching was stopped by rinsing the embryos or yolk sacs in methanol for two times. At this time-point samples can be stored at -20°C. After rehydration and blocking in PBSMT embryos or yolk sacs were incubated with rat anti-mouse CD31 (Mec13.3) antibody diluted 1:50 in blocking buffer at 4°C overnight. Followed by extensive washing embryos were incubated furthermore with the secondary rabbit anti-rat, HRP conjugated antibody (1:100) at 4° overnight. Instead yolk sacs were incubated with a rabbit

anti-rat, biotin conjugated antibody (1:100). Before color development yolks sacs were furthermore incubated for 20minutes with a solution consisting of PBT and the A&B reagents of the VECTASTAIN Elite ABC Kit (Vector Laboratories). For color development embryos and yolk sacs were incubated with a DAB-PBT solution for 20min before the reaction was started by adding 1µl of 30% hydrogen peroxide. Afterwards samples were rinsed and post-fixed in 2%PFA / 0.1% glutaraldehyde / PBS overnight at 4°C. Before stereomicroscopic (Leica) analysis stained samples were equilibrated in 50% and 70% glycerol for one hour each.

For staining of p-Sp explants the protocol for yolk sacs was modified. P-Sp-explants were washed with PBST (0.1% Tween) after fixation and bleaching lasted only 30 minutes. Primary CD31 antibody was diluted 1:300 in PBST supplemented with 2% instant milk powder. The secondary HRP conjugated antibody was used in the dilution of 1:1000. Visualization was enhanced by the incubation with the reagents of the DAB Peroxidase Substrate Kit (Vector Laboratories). Therefore, 2.5ml distilled water was charged with one drop of buffer stock solution (pH7.5), two drops of DAB substrate reagent and one drop of hydrogen peroxide. After approximately 10min the color developed and the staining solution was replaced with PBS. Finally, the CD31 stained p-Sp-explants of somite-matched wild-type and homozygous *Kleip* embryos were compared and recorded under a stereomicroscope (Leica) with a Leica camera.

4.2.6.6 *Whole-mount* immunofluorescence staining

For *whole-mount* CD31 and NG2 immunufluorescence staining, the heads of E11.5 embryos were fixed in 4% paraformaldehyde/PBS at 4°C overnight. The following steps were performed at room temperature. Subsequently after washing with PBS for three times, heads were dehydrated through graded methanol series (50%, 80%, 100%, freezing and storage at -20°C possible). After rehydration embryonic heads were blocked with 1% BSA, 0.5% Triton-X 100 in PBS for at least two hours. Afterwards the heads were cut along the ventral midline and incubated over night at 4°C in presence of rat anti-mouse endomucin (1:20) and rabbit anti-NG2 (1:100) antibodies diluted in the blocking buffer. Prior to incubation with the fluorescent-labeled secondary antibodies (1:200) the halves were washed extensively with PBS for one hour each. After washing off the secondary antibody with PBS the next day, as described before, the heads were equilibrated in 50% and 70% glycerol. For confocal imaging with the A1R (Nikon) the halves were embedded in 1% low melting point agarose (Promega) on a chambered coverglass (Nunc). Quantification of the widening of the cranial vessels was achieved by the usage of the NIS-Elements Imaging software.

4.2.7 Biochemical analysis

4.2.7.1 Inhibition of ROCK signaling in HUVE cells

For inhibitor experiments HUVE cells were seeded in 6-well dishes at a density of $15x10^4$ per well 24h prior to overnight starvation with 2.5% FCS supplemented endothelial growth medium. Next day starving medium was collected and supplemented with either 0.1µM or 1µM of the specific ROCK H-1152 inhibitor. Cells were than incubated with this modified culture medium for 25min at 37°C. Shortly before stimulation with VEGF (25ng/ml) cells were incubated for additional 5min with a mixture composed of exhausted starving medium and the phosphatase inhibitor vanadate (Na_3VO_4). After VEGF stimulation for 5 min HUVE cells were washed with ice-cold PBS and finally lysed with a NP40 lysis buffer-vanadate-mixture. Cell lysates were than stored at -20°C. For gel electrophoresis cell lysates were thawed on ice and subsequently transferred to 1.5ml reaction tubes. In order to remove cellular debris, lysates were centrifuged for 5min at 18.625 x g and 4°C. Pellet was removed and the supernatant was boiled at 95°C in 5x protein sample buffer for 10min and were separated by 10% SDS-PAGE. After Western blotting the membrane was blocked for 1h at RT with 5% milk powder in PBST. The membrane was incubated with a mouse anti-phosphorylated ERK1/2 antibody (clone E4, 1:200) overnight at 4°C. Next, the membrane was washed three times with PBST. The membrane was then incubated with the corresponding HRP-labelled secondary antibody (1:3000) for 1h at RT. Detection of chemiluminescence was performed with the CHEMI-SMART 5100 system (Peqlab). For reprobing membrane was washed three times with PBST and stripped for 30min at RT. To detect total ERK, membrane was extensively washed followed by overnight incubation with a rabbit anti-ERK1/2 antibody (clone K-23,1:500) at 4°C. Subsequent membrane was rinsed again, followed by incubation with the secondary anti-rabbit HRP (1:3000) conjugated antibody for 1h at RT. Visualization of bound antibody was repeated as described before. All incubation and washing steps were performed on rocking shaker. Western blot signals were first quantified using Gel-Pro Analyzer 6.0 (INTAS) and then normalized to its respective loading control.

4.2.8 Statistical analysis

All results are expressed as mean ± standard error of the mean (SEM). To define significant differences of experimental groups, the two-tailed student t-test was used. $p<0.05$ was considered as statistically significant.

4.2.9 Phylogenetic analysis

For phylogenetic relationship and protein alignment analysis the sequences of KLEIP-related proteins from invertebrates and vertebrates the bioinformatic program ClustalW was used (Thompson et al., 2002).

5. Abbreviations

A

AJ	adherens junction(s)
AMG	dorsal aorta, genital ridge/gonad, and pro/mesonephros-region
Ang	angiopoietin

B

β-gal	beta-galactosidase (Szatmari et al.)
β-geo	fusion gene of beta-galactosidase and neomycin resistance
BACK	BTB and C-terminal Kelch repeat
bFGF	basic fibroblast growth factor
bp	base pairs
BSA	bovine serum albumin
BTB	broad-complex, tramtrack and bric-a-brac

C

C	Celsius
cAMP	cyclic adenosine monophosphate
CD	cluster of differentiation
Cdc42	cell division cycle 42
cDNA	complementary DNA
ch	chorion
co	control
CO_2	carbon dioxide
COUP-TFII	chicken ovalbumin upstream promoter-transcription factor II
Crebbp	CREB binding protein
Cul	cullin

D

DAB	3,3'-Diaminobenzidine
DAPK	death-associated protein kinase
DLAV	dorsal longitudinal anastomotic vessel
Dll4	delta-like 4
DMSO	dimethylsulfoxide
DNA	deoxyribonucleic acid
dNTP	equal molar mix of the deoxy-nucleotides dATP, dCTP, dGTP and dTTP

DTT	dithiothreitol
DOCK	dedicator of cytokinesis
dors	dorsal

E

E	embryonic day
EC	endothelial cell(s)
ECL	enhanced chemoluminescence
ECM	extracellular matrix
Ect-2	epithelial cell transforming gene 2
EDTA	ethylendiamine-tetraacetic acid
EGF	epidermal growth factor
eGFP	enhanced green fluorescent protein
ELMO	engulfment and cell motility protein
En	engrailed
eNOS	endothelial nitric oxide synthase
EPO	erythropoietin
ERK	extracellular signal-regulated kinase
ESAM	endothelial cell selective adhesion molecule

F

F-actin	filamentous actin
Fc	Fc end of immunoglobulin
FCS	fetal calf serum
FITC	fluorescein thioisocyanate
Flk-1	fetal liver kinase 1
Flt-1	fms-like tyrosine kinase
FOXC2	Forkhead box C2 transcription factor

G

g	gram
gc	giant cell
GDI	guanine dissociation inhibitor
GDP	guanosine diphosphate
GEF	guanine exchange factor
GTP	guanosine triphosphate
GTPase	guanosine triphosphatase

H

h	hour(s)
H_2O	water
HCl	hydrochloric acid
HIF	hypoxia-inducible factor
hpf	hours post fertilization
HRP	horse radish peroxidase
HUEC	immortalized human umbilical vein endothelial cell(s)
HUVEC	human umbilical vein endothelial cell(s)

I

ICD	intracellular domain
Ig	immunoglobulin
IL	interleukin

J

Jag	jagged
JAM	junctional adhesion molecule

K

kb	kilo base pairs
kDa	kilo Dalton
KDR	insert kinase domain receptor
KLEIP	Kelch-like Ect-2 interacting protein
Klhl	kelch-like

L

L	liter
La	labyrinth
LacZ	beta-galactosidase
LIMK	limk domain containing kinase

M

µ	micro
M	molar
MAP1B	microtubule-associated protein 1B
MAPK	mitogen-activated protein kinase

min	minute(s)
MLC	myosin light chain
MLCK	myosin light chain kinase
MMP	matrix metalloproteinase
Mo	morpholino antisense oligonucleotide
mRNA	messenger RNA

N

n	nano
nc	notochord
N-cadherin	neuronal cadherin
No	nitric oxide
NP40	Nonidet P-40
Nrp	neuropilin

P

P	postnatal
pA	polyadenylation signal
PAGE	polyacrylamid gel electrophoresis
PAK	p21-activated protein kinase
PAV	parachordal vessel
PBS	phosphate buffered saline
PBST	Phosphate buffered saline with 0.1 % Tween 20
PCR	polymerase chain reaction
PCT	pericyte
PDGF	platelet derived growth factor
PDGFR	platelet derived growth factor receptor
PECAM	platelet endothelial cell adhesion molecule
PFA	Paraformaldehyde
pH	pH value
PhotoMorph	photoactivatable morpholino
PlGF	placental growth factor
POZ	poxvirus and zinc-finger
p-Sp	paraaortic-splanchnopleural

R

RAC1	ras-related C3 botulinum toxin substrate-1
RACE	rapid amplification of cDNA ends
RDS	respiratory distress syndrome
Rho	ras homologous
RNA	ribonucleic acid
RNase	Ribonuclease
ROCK	Rho-associated coiled-coil forming protein kinases
RT	room temperature
RT-PCR	reverse transcription PCR

S

S	synthesis
SA	splice acceptor
SB	splice blocking
sc	spinal chord
SCF	stem cell factor
SD	splice donor
SDS	sodium dodecyl sulphate
sec	second(s)
s.e.m	standard error of the mean
siRNA	small interfering RNA
SMA	smooth muscle actin
SMC	smooth muscle cell(s)
sp	spongiotrophoblast

T

TBP	TATA box-binding protein
tg	transgenic
TGF-ß	transforming growth factor-beta
Tie	tyrosine kinase with immunoglobulin and epidermal growth factor (EGF) homology domains
TIMP	tissue inhibitors of MMPs
TJ	tight junction(s)

U

UV	ultra violet

V

VE-Cadherin	vascular endothelial cadherin
VEGF	vascular endothelial growth factor
VEGFR	vascular endothelial growth factor receptor
ventr	ventral

Z

ZO	zona occludens

6. References

Abecassis, I., Olofsson, B., Schmid, M., Zalcman, G., and Karniguian, A. (2003). RhoA induces MMP-9 expression at CD44 lamellipodial focal complexes and promotes HMEC-1 cell invasion. Exp Cell Res *291*, 363-376.

Adams, J., Kelso, R., and Cooley, L. (2000). The kelch repeat superfamily of proteins: propellers of cell function. Trends in Cell Biology *10*, 17-24.

Adams, R.H., and Alitalo, K. (2007). Molecular regulation of angiogenesis and lymphangiogenesis. Nat Rev Mol Cell Biol *8*, 464-478.

Adams, R.H., Wilkinson, G.A., Weiss, C., Diella, F., Gale, N.W., Deutsch, U., Risau, W., and Klein, R. (1999). Roles of ephrinB ligands and EphB receptors in cardiovascular development: demarcation of arterial/venous domains, vascular morphogenesis, and sprouting angiogenesis. Gene Dev *13*, 295-306.

Adelman, D.M., Gertsenstein, M., Nagy, A., Simon, M.C., and Maltepe, E. (2000). Placental cell fates are regulated in vivo by HIF-mediated hypoxia responses. Gene Dev *14*, 3191-3203.

Adini, I., Rabinovitz, I., Sun, J.F., Prendergast, G.C., and Benjamin, L.E. (2003). RhoB controls Akt trafficking and stage-specific survival of endothelial cells during vascular development. Gene Dev *17*, 2721-2732.

Allen, E., Ding, J.Q., Wang, W., Pramanik, S., Chou, J., Yau, V., and Yang, Y.M. (2005). Gigaxonin-controlled degradation of MAP1B light chain is critical to neuronal survival. Nature *438*, 224-228.

Amano, M., Fukata, Y., and Kaibuchi, K. (2000). Regulation and functions of Rho-associated kinase. Experimental Cell Research *261*, 44-51.

Anastasiadis, P.Z., Moon, S.Y., Thoreson, M.A., Mariner, D.J., Crawford, H.C., Zheng, Y., and Reynolds, A.B. (2000). Inhibition of RhoA by p120 catenin. Nat Cell Biol *2*, 637-644.

Bader, B.L., Rayburn, H., Crowley, D., and Hynes, R.O. (1998). Extensive vasculogenesis, angiogenesis, and organogenesis precede lethality in mice lacking all alpha v integrins. Cell *95*, 507-519.

Bamburg, J.R., and Wiggan, O.P. (2002). ADF/cofilin and actin dynamics in disease. Trends in Cell Biology *12*, 598-605.

Bao, W., Thullberg, M., Zhang, H., Onischenko, A., and Stromblad, S. (2002). Cell attachment to the extracellular matrix induces proteasomal degradation of p21(CIP1) via Cdc42/Rac1 signaling. Mol Cell Biol *22*, 4587-4597.

Beckers, C.M.L., van Hinsbergh, V.W.M., and Amerongen, G.P.V. (2010). Driving Rho GTPase activity in endothelial cells regulates barrier integrity. Thromb Haemostasis *103*, 40-55.

Bernard, O. (2007). Lim kinases, regulators of actin dynamics. Int J Biochem Cell B *39*, 1071-1076.

Bhatt, A.J., Amin, S.B., Chess, P.R., Watkins, R.H., and Maniscalco, W.M. (2000). Expression of vascular endothelial growth factor and Flk-1 in developing and glucocorticoid-treated mouse lung. Pediatr Res *47*, 606-613.

Birukova, A.A., Birilikov, K.G., Adyshev, D., Usatyuk, P., Natarajan, V., Garcia, J.G.N., and Verin, A.D. (2005). Involvement of microtubules and rho pathway in TGF-beta 1-induced lung vascular barrier dysfunction. J Cell Physiol *204*, 934-947.

Birukova, A.A., Zagranichnaya, T., Alekseeva, E., Bokoch, G.M., and Birukov, K.G. (2008). Epac/Rap and PKA are novel mechanisms of ANP-induced Rac-mediated pulmonary endothelial barrier protection. J Cell Physiol *215*, 715-724.

Birukova, A.A., Zagranichnaya, T., Fu, P., Alekseeva, E., Chen, W., Jacobson, J.R., and Birukov, K.G. (2007). Prostaglandins PGE(2) and PGI(2) promote endothelial barrier enhancement via PKA- and Epac1/Rap1-dependent Rac activation. Experimental Cell Research *313*, 2504-2520.

Bouvard, D., Brakebusch, C., Gustafsson, E., Aszodi, A., Bengtsson, T., Berna, A., and Fassler, R. (2001). Functional consequences of integrin gene mutations in mice. Circ Res *89*, 211-223.

Bryan, B.A., and D'Amore, P.A. (2007). What tangled webs they weave: Rho-GTPase control of angiogenesis. Cell Mol Life Sci *64*, 2053-2065.

Burri, P.H., Hlushchuk, R., and Djonov, V. (2004). Intussusceptive angiogenesis: its emergence, its characteristics, and its significance. Dev Dyn *231*, 474-488.

Bustelo, X.R., Sauzeau, V., and Berenjeno, I.M. (2007). GTP-binding proteins of the Rho/Rac family: regulation, effectors and functions in vivo. Bioessays *29*, 356-370.

Carmeliet, P. (2003). Angiogenesis in health and disease. Nat Med *9*, 653-660.

Carmeliet, P., Ferreira, V., Breier, G., Pollefeyt, S., Kieckens, L., Gertsenstein, M., Fahrig, M., Vandenhoeck, A., Harpal, K., Eberhardt, C*., et al.* (1996). Abnormal blood vessel development and lethality in embryos lacking a single VEGF allele. Nature *380*, 435-439.

Carmeliet, P., Lampugnani, M.G., Moons, L., Breviario, F., Compernolle, V., Bono, F., Balconi, G., Spagnuolo, R., Oosthuyse, B., Dewerchin, M*., et al.* (1999). Targeted deficiency or cytosolic truncation of the VE-cadherin gene in mice impairs VEGF-mediated endothelial survival and angiogenesis. Cell *98*, 147-157.

Centanin, L., Dekanty, A., Romero, N., Irisarri, M., Gorr, T.A., and Wappner, P. (2008). Cell autonomy of HIF effects in Drosophila: Tracheal cells sense hypoxia and induce terminal branch sprouting. Developmental Cell *14*, 547-558.

Chun, C.Z., Kaur, S., Samant, G.V., Wang, L., Pramanik, K., Garnaas, M.K., Li, K., Field, L., Mukhopadhyay, D., and Ramchandran, R. (2009). Snrk-1 is involved in multiple steps of angioblast development and acts via notch signaling pathway in artery-vein specification in vertebrates. Blood *113*, 1192-1199.

Cleaver, O., and Melton, D.A. (2003). Endothelial signaling during development. Nature Medicine *9*, 661-668.

Cleveland, D.W., Yamanaka, K., and Bomont, P. (2009). Gigaxonin controls vimentin organization through a tubulin chaperone-independent pathway. Hum Mol Genet *18*, 1384-1394.

Coggins, K.G., Latour, A., Nguyen, M.S., Audoly, L., Coffman, T.M., and Koller, B.H. (2002). Metabolism of PGE2 by prostaglandin dehydrogenase is essential for remodeling the ductus arteriosus. Nat Med *8*, 91-92.

Cole, T.J., Blendy, J.A., Monaghan, A.P., Krieglstein, K., Schmid, W., Aguzzi, A., Fantuzzi, G., Hummler, E., Unsicker, K., and Schutz, G. (1995). Targeted disruption of the glucocorticoid receptor gene blocks adrenergic chromaffin cell development and severely retards lung maturation. Genes Dev *9*, 1608-1621.

Conway, S.J., Kruzynska-Frejtag, A., Kneer, P.L., Machnicki, M., and Koushik, S.V. (2003). What cardiovascular defect does my prenatal mouse mutant have, and why? Genesis *35*, 1-21.

Croft, D.R., and Olson, M.F. (2006). The Rho GTPase effector ROCK regulates cyclin A, cyclin D1, and p27Kip1 levels by distinct mechanisms. Mol Cell Biol *26*, 4612-4627.

D'Amico, G., Robinson, S.D., Germain, M., Reynolds, L.E., Thomas, G.J., Elia, G., Saunders, G., Fruttiger, M., Tybulewicz, V., Mavria, G*., et al.* (2010). Endothelial-Rac1 is not required for tumor angiogenesis unless alphavbeta3-integrin is absent. Plos One *5*, e9766.

Dave, V., Childs, T., Xu, Y., Ikegami, M., Besnard, V., Maeda, Y., Wert, S.E., Neilson, J.R., Crabtree, G.R., and Whitsett, J.A. (2006). Calcineurin/Nfat signaling is required for perinatal lung maturation and function. J Clin Invest *116*, 2597-2609.

Davies, S.P., Reddy, H., Caivano, M., and Cohen, P. (2000). Specificity and mechanism of action of some commonly used protein kinase inhibitors. Biochem J *351*, 95-105.

de Bruijn, M.F., Ma, X., Robin, C., Ottersbach, K., Sanchez, M.J., and Dzierzak, E. (2002). Hematopoietic stem cells localize to the endothelial cell layer in the midgestation mouse aorta. Immunity *16*, 673-683.

De Smet, F., Segura, I., De Bock, K., Hohensinner, P.J., and Carmeliet, P. (2009). Mechanisms of Vessel Branching. Filopodia on Endothelial Tip Cells Lead the Way. Arterioscler Thromb Vasc Biol.

Dejana, E. (2004). Endothelial cell-cell junctions: happy together. Nat Rev Mol Cell Biol *5*, 261-270.

Dejana, E., Orsenigo, F., and Lampugnani, M.G. (2008). The role of adherens junctions and VE-cadherin in the control of vascular permeability. Journal of Cell Science *121*, 2115-2122.

Dejana, E., Tournier-Lasserve, E., and Weinstein, B.M. (2009). The control of vascular integrity by endothelial cell junctions: molecular basis and pathological implications. Dev Cell *16*, 209-221.

DerMardirossian, C., and Bokoch, G.M. (2005). GDIs: central regulatory molecules in Rho GTPase activation. Trends Cell Biol *15*, 356-363.

Dieterlen-Lievre, F., Pardanaud, L., Bollerot, K., and Jaffredo, T. (2002). Hemangioblasts and hemopoietic stem cells during ontogeny. C R Biol *325*, 1013-1020.

Diez, H., Fischer, A., Winkler, A., Hu, C.J., Hatzopoulos, A.K., Breier, G., and Gessler, M. (2007). Hypoxia-mediated activation of Dll4-Notch-Hey2 signaling in endothelial progenitor cells and adoption of arterial cell fate. Experimental Cell Research *313*, 1-9.

Ding, J.Q., Allen, E., Wang, W., Valle, A., Wu, C.B., Nardine, T., Cui, B.X., Yi, J., Taylor, A., Jeon, N.L*., et al.* (2006). Gene targeting of GAN in mouse causes a toxic accumulation of microtubule-associated protein 8 and impaired retrograde axonal transport. Hum Mol Genet *15*, 1451-1463.

Djonov, V., and Makanya, A.N. (2005). New insights into intussusceptive angiogenesis. EXS, 17-33.

Dormond, O., Foletti, A., Paroz, C., and Ruegg, C. (2001). NSAIDs inhibit alpha V beta 3 integrin-mediated and Cdc42/Rac-dependent endothelial-cell spreading, migration and angiogenesis. Nature Medicine *7*, 1041-1047.

Downs, K.M. (2003). Florence Sabin and the mechanism of blood vessel lumenization during vasculogenesis. Microcirculation *10*, 5-25.

Dumont, D.J., Gradwohl, G., Fong, G.H., Puri, M.C., Gertsenstein, M., Auerbach, A., and Breitman, M.L. (1994). Dominant-negative and targeted null mutations in the endothelial receptor tyrosine kinase, tek, reveal a critical role in vasculogenesis of the embryo. Genes Dev *8*, 1897-1909.

Dumont, D.J., Jussila, L., Taipale, J., Lymboussaki, A., Mustonen, T., Pajusola, K., Breitman, M., and Alitalo, K. (1998). Cardiovascular failure in mouse embryos deficient in VEGF receptor-3. Science *282*, 946-949.

Dupe, V., Matt, N., Garnier, J.M., Chambon, P., Mark, M., and Ghyselinck, N.B. (2003). A newborn lethal defect due to inactivation of retinaldehyde dehydrogenase type 3 is prevented by maternal retinoic acid treatment. Proc Natl Acad Sci U S A *100*, 14036-14041.

Dvorak, A.M., Kohn, S., Morgan, E.S., Fox, P., Nagy, J.A., and Dvorak, H.F. (1996). The vesiculo-vacuolar organelle (VVO): A distinct endothelial cell structure that provides a transcellular pathway for macromolecular extravasation. J Leukocyte Biol *59*, 100-115.

Dvorak, H.F., Nagy, J.A., Feng, D., Brown, L.F., and Dvorak, A.M. (1999). Vascular permeability factor/vascular endothelial growth factor and the significance of microvascular hyperpermeability in angiogenesis. Curr Top Microbiol Immunol *237*, 97-132.

Engerman, R.L., Pfaffenbach, D., and Davis, M.D. (1967). Cell turnover of capillaries. Lab Invest *17*, 738-743.

Engers, R., Springer, E., Michiels, F., Collard, J.G., and Gabbert, H.E. (2001). Rac affects invasion of human renal cell carcinomas by up-regulating tissue inhibitor of metalloproteinases (TIMP)-1 and TIMP-2 expression. Journal of Biological Chemistry *276*, 41889-41897.

Epting, D., Wendik, B., Bennewitz, K., Dietz, C.T., Driever, W., and Kroll, J. (2010). The Rac1 regulator ELMO1 controls vascular morphogenesis in zebrafish. Circ Res *107*, 45-55.

Ferguson, M.W. (1988). Palate development. Development *103 Suppl*, 41-60.

Ferrara, N., Carver-Moore, K., Chen, H., Dowd, M., Lu, L., O'Shea, K.S., Powell-Braxton, L., Hillan, K.J., and Moore, M.W. (1996). Heterozygous embryonic lethality induced by targeted inactivation of the VEGF gene. Nature *380*, 439-442.

Ferrara, N., Gerber, H.P., and LeCouter, J. (2003). The biology of VEGF and its receptors. Nat Med *9*, 669-676.

Fischer, A., Schumacher, N., Maier, M., Sendtner, M., and Gessler, M. (2004). The Notch target genes Hey1 and Hey2 are required for embryonic vascular development. Gene Dev *18*, 901-911.

Folkman, J., and DAmore, P.A. (1996). Blood vessel formation: What is its molecular basis? Cell *87*, 1153-1155.

Fong, G.H., Rossant, J., Gertsenstein, M., and Breitman, M.L. (1995). Role of the Flt-1 Receptor Tyrosine Kinase in Regulating the Assembly of Vascular Endothelium. Nature *376*, 66-70.

Fryer, B.H., and Field, J. (2005). Rho, Rac, Pak and angiogenesis: old roles and newly identified responsibilities in endothelial cells. Cancer Lett *229*, 13-23.

Fujimura, L., Matsudo, Y., Kang, M., Takamori, Y., Tokuhisa, T., and Hatano, M. (2004). Protective role of Nd1 in doxorubicin-induced cardiotoxicity. Cardiovascular Research *64*, 315-321.

Fujisawa, K., Fujita, A., Ishizaki, T., Saito, Y., and Narumiya, S. (1996). Identification of the Rho-binding domain of p160ROCK, a Rho-associated coiled-coil containing protein kinase. J Biol Chem *271*, 23022-23028.

Funaki, H., Yamamoto, T., Koyama, Y., Kondo, D., Yaoita, E., Kawasaki, K., Kobayashi, H., Sawaguchi, S., Abe, H., and Kihara, I. (1998). Localization and expression of AQP5 in cornea, serous salivary glands, and pulmonary epithelial cells. Am J Physiol *275*, C1151-1157.

Furuse, M., and Tsukita, S. (2006). Claudins in occluding junctions of humans and flies. Trends in Cell Biology *16*, 181-188.

Gale, N.W., Dominguez, M.G., Noguera, I., Pan, L., Hughes, V., Valenzuela, D.M., Murphy, A.J., Adams, N.C., Lin, H.C., Holash, J.*, et al.* (2004). Haploinsufficiency of delta-like 4 ligand results in embryonic lethality due to major defects in arterial and vascular development. P Natl Acad Sci USA *101*, 15949-15954.

Garcia-Otin, A.L., and Guillou, F. (2006). Mammalian genome targeting using site-specific recombinases. Front Biosci *11*, 1108-1136.

Garnaas, M.K., Moodie, K.L., Liu, M.L., Samant, G.V., Li, K., Marx, R., Baraban, J.M., Horowitz, A., and Ramchandran, R. (2008). Syx, a RhoA guanine exchange factor, is essential for angiogenesis in Vivo. Circ Res *103*, 710-716.

Gavard, J., and Gutkind, J.S. (2006). VEGF controls endothelial-cell permeability by promoting the beta-arrestin-dependent endocytosis of VE-cadherin. Nature Cell Biology *8*, 1223-U1217.

Gerety, S.S., Wang, H.U., Chen, Z.F., and Anderson, D.J. (1999). Symmetrical mutant phenotypes of the receptor EphB4 and its specific transmembrane ligand ephrin-B2 in cardiovascular development. Mol Cell *4*, 403-414.

Gerhardt, H. (2008). VEGF and endothelial guidance in angiogenic sprouting. Organogenesis *4*, 241-246.

Gerhardt, H., Golding, M., Fruttiger, M., Ruhrberg, C., Lundkvist, A., Abramsson, A., Jeltsch, M., Mitchell, C., Alitalo, K., Shima, D.*, et al.* (2003). VEGF guides angiogenic sprouting utilizing endothelial tip cell filopodia. J Cell Biol *161*, 1163-1177.

Gerhardt, H., Wolburg, H., and Redies, C. (2000). N-cadherin mediates pericytic-endothelial interaction during brain angiogenesis in the chicken. Dev Dynam *218*, 472-479.

Geyer, R., Wee, S., Anderson, S., Yates, J., and Wolf, D.A. (2003). BTB/POZ domain proteins are putative substrate adaptors for cullin 3 ubiquitin ligases. Molecular Cell *12*, 783-790.

Goeckeler, Z.M., and Wysolmerski, R.B. (1995). Myosin Light-Chain Kinase-Regulated Endothelial-Cell Contraction - the Relationship between Isometric Tension, Actin Polymerization, and Myosin Phosphorylation. Journal of Cell Biology *130*, 613-627.

Gorovoy, M., Niu, J.X., Bernard, O., Profirovic, J., Minshall, R., Neamu, R., and Voyno-Yasenetskaya, T. (2005). LIM kinase 1 coordinates microtubule stability and actin polymerization in human endothelial cells. Journal of Biological Chemistry *280*, 26533-26542.

Gory-Faure, S., Prandini, M.H., Pointu, H., Roullot, V., Pignot-Paintrand, I., Vernet, M., and Huber, P. (1999). Role of vascular endothelial-cadherin in vascular morphogenesis. Development *126*, 2093-2102.

Goumans, M.J., Liu, Z., and ten Dijke, P. (2009). TGF-beta signaling in vascular biology and dysfunction. Cell Res *19*, 116-127.

Gu, C.H., Rodriguez, E.R., Reimert, D.V., Shu, T.Z., Fritzsch, B., Richards, L.J., Kolodkin, A.L., and Ginty, D.D. (2003). Neuropilin-1 conveys semaphorin and VEGF signaling during neural and cardiovascular development. Developmental Cell *5*, 45-57.

Gumbiner, B.M. (1996). Cell adhesion: The molecular basis of tissue architecture and morphogenesis. Cell *84*, 345-357.

Hainaud, P., Contreres, J.O., Villemain, A., Liu, L.X., Plouet, J., Tobelem, G., and Dupuy, E. (2006). The role of the vascular endothelial growth factor-Delta-like 4 ligand/Notch4-ephrin B2 cascade in tumor vessel remodeling and endothelial cell functions. Cancer Research *66*, 8501-8510.

Han, R.N., Babaei, S., Robb, M., Lee, T., Ridsdale, R., Ackerley, C., Post, M., and Stewart, D.J. (2004). Defective lung vascular development and fatal respiratory distress in endothelial NO synthase-deficient mice: a model of alveolar capillary dysplasia? Circ Res *94*, 1115-1123.

Hansen, J., Floss, T., Van Sloun, P., Fuchtbauer, E.M., Vauti, F., Arnold, H.H., Schnutgen, F., Wurst, W., von Melchner, H., and Ruiz, P. (2003). A large-scale, gene-driven mutagenesis approach for the functional analysis of the mouse genome. P Natl Acad Sci USA *100*, 9918-9922.

Hara, T., Ishida, H., Raziuddin, R., Dorkhom, S., Kamijo, K., and Miki, T. (2004). Novel kelch-like protein, KLEIP, is involved in actin assembly at cell-cell contact sites of Madin-Darby canine kidney cells. Molecular Biology of the Cell *15*, 1172-1184.

Hata, Y., Miura, M., Nakao, S., Kawahara, S., Kita, T., and Ishibashi, T. (2008). Antiangiogenic properties of fasudil, a potent Rho-Kinase inhibitor. Jpn J Ophthalmol *52*, 16-23.

He, Y., Luo, Y., Tang, S., Rajantie, I., Salven, P., Heil, M., Zhang, R., Luo, D., Li, X., Chi, H., *et al.* (2006a). Critical function of Bmx/Etk in ischemia-mediated arteriogenesis and angiogenesis. J Clin Invest *116*, 2344-2355.

He, Y., Zu, T., Benzow, K.A., Orr, H.T., Clark, H.B., and Koob, M.D. (2006b). Targeted deletion of a single Sca8 ataxia locus allele in mice causes abnormal gait, progressive loss of motor coordination, and Purkinje cell dendritic deficits. Journal of Neuroscience *26*, 9975-9982.

Heasman, S.J., and Ridley, A.J. (2008). Mammalian Rho GTPases: new insights into their functions from in vivo studies. Nat Rev Mol Cell Bio *9*, 690-701.

Hellstrom, M., Gerhardt, H., Kalen, M., Li, X., Eriksson, U., Wolburg, H., and Betsholtz, C. (2001). Lack of pericytes leads to endothelial hyperplasia and abnormal vascular morphogenesis. J Cell Biol *153*, 543-553.

Hellstrom, M., Kalen, M., Lindahl, P., Abramsson, A., and Betsholtz, C. (1999). Role of PDGF-B and PDGFR-beta in recruitment of vascular smooth muscle cells and pericytes during embryonic blood vessel formation in the mouse. Development *126*, 3047-3055.

Herbert, S.P., Huisken, J., Kim, T.N., Feldman, M.E., Houseman, B.T., Wang, R.A., Shokat, K.M., and Stainier, D.Y. (2009). Arterial-venous segregation by selective cell sprouting: an alternative mode of blood vessel formation. Science *326*, 294-298.

Heroult, M., Schaffner, F., and Augustin, H.G. (2006). Eph receptor and ephrin ligand-mediated interactions during angiogenesis and tumor progression. Experimental Cell Research *312*, 642-650.

Hobson, B., and Denekamp, J. (1984). Endothelial proliferation in tumours and normal tissues: continuous labelling studies. Br J Cancer *49*, 405-413.

Horowitz, A., and Simons, M. (2008). Branching morphogenesis. Circulation Research *103*, 784-795.

Huang, S., and Ingber, D.E. (2002). A discrete cell cycle checkpoint in late G(1) that is cytoskeleton-dependent and MAP kinase (Erk)-independent. Exp Cell Res *275*, 255-264.

Hudry-Clergeon, H., Stengel, D., Ninio, E., and Vilgrain, I. (2005). Platelet-activating factor increases VE-cadherin tyrosine phosphorylation in mouse endothelial cells and its association with the PtdIns3'-kinase. FASEB J *19*, 512-520.

Hummler, E., Barker, P., Gatzy, J., Beermann, F., Verdumo, C., Schmidt, A., Boucher, R., and Rossier, B.C. (1996). Early death due to defective neonatal lung liquid clearance in alpha-ENaC-deficient mice. Nat Genet *12*, 325-328.

Humphries, M.J. (2000). Integrin structure. Biochem Soc T *28*, 311-340.

Ikenoya, M., Hidaka, H., Hosoya, T., Suzuki, M., Yamamoto, N., and Sasaki, Y. (2002). Inhibition of rho-kinase-induced myristoylated alanine-rich C kinase substrate (MARCKS) phosphorylation in human neuronal cells by H-1152, a novel and specific Rho-kinase inhibitor. J Neurochem *81*, 9-16.

Isogai, S., Lawson, N.D., Torrealday, S., Horiguchi, M., and Weinstein, B.M. (2003). Angiogenic network formation in the developing vertebrate trunk. Development *130*, 5281-5290.

Ivan, M., Kondo, K., Yang, H.F., Kim, W., Valiando, J., Ohh, M., Salic, A., Asara, J.M., Lane, W.S., and Kaelin, W.G. (2001). HIF alpha targeted for VHL-mediated destruction by proline hydroxylation: Implications for O-2 sensing. Science *292*, 464-468.

Jacobson, J.R., Dudek, S.M., Singleton, P.A., Kolosova, I.A., Verin, A.D., and Garcia, J.G.N. (2006). Endothelial cell barrier enhancement by ATP is mediated by the small GTPase Rac and cortactin. Am J Physiol-Lung C *291*, L289-L295.

Jarecki, J., Johnson, E., and Krasnow, M.A. (1999). Oxygen regulation of airway branching in Drosophila is mediated by branchless FGF. Cell *99*, 211-220.

Jarzynka, M.J., Hu, B., Hui, K.M., Bar-Joseph, I., Gu, W., Hirose, T., Haney, L.B., Ravichandran, K.S., Nishikawa, R., and Cheng, S.Y. (2007). ELMO1 and Dock180, a bipartite Rac1 guanine nucleotide exchange factor, promote human glioma cell invasion. Cancer Res *67*, 7203-7211.

Jiang, R., Lan, Y., Chapman, H.D., Shawber, C., Norton, C.R., Serreze, D.V., Weinmaster, G., and Gridley, T. (1998). Defects in limb, craniofacial, and thymic development in Jagged2 mutant mice. Genes Dev *12*, 1046-1057.

Jobe, A.H. (2010). Lung maturation: the survival miracle of very low birth weight infants. Pediatr Neonatol *51*, 7-13.

Jou, T.S., and Nelson, W.J. (1998). Effects of regulated expression of mutant RhoA and Rac1 small GTPases on the development of epithelial (MDCK) cell polarity. Journal of Cell Biology *142*, 85-100.

Kaartinen, V., Voncken, J.W., Shuler, C., Warburton, D., Bu, D., Heisterkamp, N., and Groffen, J. (1995). Abnormal lung development and cleft palate in mice lacking TGF-beta 3 indicates defects of epithelial-mesenchymal interaction. Nat Genet *11*, 415-421.

Kessler, O., Shraga-Heled, N., Lange, T., Gutmann-Raviv, N., Sabo, E., Baruch, L., Machluf, M., and Neufeld, G. (2004). Semaphorin-3F is an inhibitor of tumor angiogenesis. Cancer Res *64*, 1008-1015.

Kimmel, C.B., Ballard, W.W., Kimmel, S.R., Ullmann, B., and Schilling, T.F. (1995). Stages of embryonic development of the zebrafish. Dev Dyn *203*, 253-310.

Kleyman, T.R., Zuckerman, J.B., Middleton, P., McNulty, K.A., Hu, B.F., Su, X.F., An, B., Eaton, D.C., and Smith, P.R. (2001). Cell surface expression and turnover of the alpha-subunit of the epithelial sodium channel. Am J Physiol-Renal *281*, F213-F221.

Kluk, M.J., and Hla, T. (2002). Signaling of sphingosine-1-phosphate via the S1P/EDG-family of G-protein-coupled receptors. Biochim Biophys Acta *1582*, 72-80.

Kobayashi, A., Kang, M.I., Okawa, H., Ohtsuji, M., Zenke, Y., Chiba, T., Igarashi, K., and Yamamoto, M. (2004). Oxidative stress sensor Keap1 functions as an adaptor for Cul3-based E3 ligase to regulate for proteasomal degradation of Nrf2. Molecular and Cellular Biology *24*, 7130-7139.

Kondapalli, J., Flozak, A.S., and Albuquerque, M.L.C. (2004). Laminar shear stress differentially modulates gene expression of p120 catenin, Kaiso transcription factor, and vascular endothelial cadherin in human coronary artery endothelial cells. Journal of Biological Chemistry *279*, 11417-11424.

Kranenburg, O., Gebbink, M.F.B.G., and Voest, E.E. (2004). Stimulation of angiogenesis by Ras proteins. Bba-Rev Cancer *1654*, 23-37.

Krebs, L.T., Shutter, J.R., Tanigaki, K., Honjo, T., Stark, K.L., and Gridley, T. (2004). Haploinsufficient lethality and formation of arteriovenous malformations in Notch pathway mutants. Gene Dev *18*, 2469-2473.

Kroll, J., Epting, D., Kern, K., Dietz, C.T., Feng, Y., Hammes, H.P., Wieland, T., and Augustin, H.G. (2009). Inhibition of Rho-dependent kinases ROCK I/II activates VEGF-driven retinal neovascularization and sprouting angiogenesis. Am J Physiol Heart Circ Physiol *296*, H893-899.

Kroll, J., Shi, X.Z., Caprioli, A., Liu, H.H., Waskow, C., Lin, K.M., Miyazaki, T., Rodewald, H.R., and Sato, T.N. (2005). The BTB-kelch protein KLHL6 is involved in B-lymphocyte antigen receptor signaling and germinal center formation. Molecular and Cellular Biology *25*, 8531-8540.

Ku, D.D., Zaleski, J.K., Liu, S., and Brock, T.A. (1993). Vascular endothelial growth factor induces EDRF-dependent relaxation in coronary arteries. Am J Physiol *265*, H586-592.

Kuhnert, F., Mancuso, M.R., Shamloo, A., Wang, H.T., Choksi, V., Florek, M., Su, H., Fruttiger, M., Young, W.L., Heilshorn, S.C.*, et al.* (2010). Essential regulation of CNS angiogenesis by the orphan G protein-coupled receptor GPR124. Science *330*, 985-989.

Kumar, P., Shen, Q., Pivetti, C.D., Lee, E.S., Wu, M.H., and Yuan, S.Y. (2009). Molecular mechanisms of endothelial hyperpermeability: implications in inflammation. Expert Rev Mol Med *11*, -.

Lampugnani, M.G., Corada, M., Andriopoulou, P., Esser, S., Risau, W., and Dejana, E. (1997). Cell confluence regulates tyrosine phosphorylation of adherens junction components in endothelial cells. J Cell Sci *110 (Pt 17)*, 2065-2077.

Lampugnani, M.G., Zanetti, A., Corada, M., Takahashi, T., Balconi, G., Breviario, F., Orsenigo, F., Cattelino, A., Kemler, R., Daniel, T.O.*, et al.* (2003). Contact inhibition of VEGF-induced proliferation requires vascular endothelial cadherin, beta-catenin, and the phosphatase DEP-1/CD148. Journal of Cell Biology *161*, 793-804.

Larrivee, B., Freitas, C., Suchting, S., Brunet, I., and Eichmann, A. (2009). Guidance of vascular development: lessons from the nervous system. Circ Res *104*, 428-441.

Lawson, N.D., Vogel, A.M., and Weinstein, B.M. (2002). sonic hedgehog and vascular endothelial growth factor act upstream of the notch pathway during arterial endothelial differentiation. Developmental Cell *3*, 127-136.

Lawson, N.D., and Weinstein, B.M. (2002). In vivo imaging of embryonic vascular development using transgenic zebrafish. Dev Biol *248*, 307-318.

le Noble, F., Klein, C., Tintu, A., Pries, A., and Buschmann, I. (2008). Neural guidance molecules, tip cells, and mechanical factors in vascular development. Cardiovasc Res *78*, 232-241.

Lee, S., Jilani, S.M., Nikolova, G.V., Carpizo, D., and Iruela-Arispe, M.L. (2005). Processing of VEGF-A by matrix metalloproteinases regulates bioavailability and vascular patterning in tumors. Journal of Cell Biology *169*, 681-691.

Lee, T., Shah, C., and Xu, E.Y. (2007). Gene trap mutagenesis: a functional genomics approach towards reproductive research. Mol Hum Reprod *13*, 771-779.

Lee, Y.R., Yuan, W.C., Ho, H.C., Chen, C.H., Shih, H.M., and Chen, R.H. (2010). The Cullin 3 substrate adaptor KLHL20 mediates DAPK ubiquitination to control interferon responses. Embo Journal *29*, 1748-1761.

Leveen, P., Pekny, M., Gebremedhin, S., Swolin, B., Larsson, E., and Betsholtz, C. (1994). Mice Deficient for Pdgf-B Show Renal, Cardiovascular, and Hematological Abnormalities. Gene Dev *8*, 1875-1887.

Lindahl, P., Johansson, B.R., Leveen, P., and Betsholtz, C. (1997). Pericyte loss and microaneurysm formation in PDGF-B-deficient mice. Science *277*, 242-245.

Liu, A.X., Rane, N., Liu, J.P., and Prendergast, G.C. (2001). RhoB is dispensable for mouse development, but it modifies susceptibility to tumor formation as well as cell adhesion and growth factor signaling in transformed cells. Molecular and Cellular Biology *21*, 6906-6912.

Liu, Y.J., Wada, R., Yamashita, T., Mi, Y.D., Deng, C.X., Hobson, J.P., Rosenfeldt, H.M., Nava, V.E., Chae, S.S., Lee, M.J*., et al.* (2000). Edg-1, the G protein-coupled receptor for sphingosine-1-phosphate, is essential for vascular maturation. Journal of Clinical Investigation *106*, 951-961.

Lobov, I.B., Renard, R.A., Papadopoulos, N., Gale, N.W., Thurston, G., Yancopoulos, G.D., and Wiegand, S.J. (2007). Delta-like ligand 4 (DII4) is induced by VEGF as a negative regulator of angiogenic sprouting. P Natl Acad Sci USA *104*, 3219-3224.

Loftin, C.D., Trivedi, D.B., Tiano, H.F., Clark, J.A., Lee, C.A., Epstein, J.A., Morham, S.G., Breyer, M.D., Nguyen, M., Hawkins, B.M*., et al.* (2001). Failure of ductus arteriosus closure and remodeling in neonatal mice deficient in cyclooxygenase-1 and cyclooxygenase-2. Proc Natl Acad Sci U S A *98*, 1059-1064.

Lu, M., and Ravichandran, K.S. (2006). Dock180-ELMO cooperation in Rac activation. Methods Enzymol *406*, 388-402.

Luo, Y., and Radice, G.L. (2005). N-cadherin acts upstream of VE-cadherin in controlling vascular morphogenesis. Journal of Cell Biology *169*, 29-34.

Maeda, Y., Dave, V., and Whitsett, J.A. (2007). Transcriptional control of lung morphogenesis. Physiol Rev *87*, 219-244.

Maerki, S., Olma, M.H., Staubli, T., Steigemann, P., Gerlich, D.W., Quadroni, M., Sumara, I., and Peter, M. (2009). The Cul3-KLHL21 E3 ubiquitin ligase targets Aurora B to midzone microtubules in anaphase and is required for cytokinesis. Journal of Cell Biology *187*, 791-800.

Mahon, P.C., Hirota, K., and Semenza, G.L. (2001). FIH-1: a novel protein that interacts with HIF-1 alpha and VHL to mediate repression of HIF-1 transcriptional activity. Gene Dev *15*, 2675-2686.

Maisonpierre, P.C., Suri, C., Jones, P.F., Bartunkova, S., Wiegand, S., Radziejewski, C., Compton, D., McClain, J., Aldrich, T.H., Papadopoulos, N*., et al.* (1997). Angiopoietin-2, a natural antagonist for Tie2 that disrupts in vivo angiogenesis. Science *277*, 55-60.

Makanya, A.N., Hlushchuk, R., and Djonov, V.G. (2009). Intussusceptive angiogenesis and its role in vascular morphogenesis, patterning, and remodeling. Angiogenesis.

Masson, N., Willam, C., Maxwell, P.H., Pugh, C.W., and Ratcliffe, P.J. (2001). Independent function of two destruction domains in hypoxia-inducible factor-alpha chains activated by prolyl hydroxylation. Embo Journal *20*, 5197-5206.

Matter, K., and Balda, M.S. (2003). Signalling to and from tight junctions. Nat Rev Mol Cell Bio *4*, 225-236.

Mavria, G., Vercoulen, Y., Yeo, M., Paterson, H., Karasarides, M., Marais, R., Bird, D., and Marshall, C.J. (2006). ERK-MAPK signaling opposes Rho-kinase to promote endothelial cell survival and sprouting during angiogenesis. Cancer Cell *9*, 33-44.

McCarty, J.H., Monahan-Earley, R.A., Brown, L.F., Keller, M., Gerhardt, H., Rubin, K., Shani, M., Dvorak, H.F., Wolburg, H., Bader, B.L.*, et al.* (2002). Defective associations between blood vessels and brain parenchyma lead to cerebral hemorrhage in mice lacking alpha v integrins. Molecular and Cellular Biology *22*, 7667-7677.

Mehta, D., and Malik, A.B. (2006). Signaling mechanisms regulating endothelial permeability. Physiological Reviews *86*, 279-367.

Miki, T., Smith, C.L., Long, J.E., Eva, A., and Fleming, T.P. (1993). Oncogene Ect2 Is Related to Regulators of Small Gtp-Binding Proteins (Vol 362, Pg 462, 1993). Nature *364*, 737-737.

Millan, J., Cain, R.J., Reglero-Real, N., Bigarella, C., Marcos-Ramiro, B., Fernandez-Martin, L., Correas, I., and Ridley, A.J. (2010). Adherens junctions connect stress fibres between adjacent endothelial cells. Bmc Biol *8*, -.

Moore, C.A., Parkin, C.A., Bidet, Y., and Ingham, P.W. (2007). A role for the Myoblast city homologues Dock1 and Dock5 and the adaptor proteins Crk and Crk-like in zebrafish myoblast fusion. Development *134*, 3145-3153.

Morgan, S.M., Samulowitz, U., Darley, L., Simmons, D.L., and Vestweber, D. (1999). Biochemical characterization and molecular cloning of a novel endothelial-specific sialomucin. Blood *93*, 165-175.

Moy, A.B., VanEngelenhoven, J., Bodmer, J., Kamath, J., Keese, C., Giaever, I., Shasby, S., and Shasby, D.M. (1996). Histamine and thrombin modulate endothelial focal adhesion through centripetal and centrifugal forces. Journal of Clinical Investigation *97*, 1020-1027.

Muller, Y.A., Li, B., Christinger, H.W., Wells, J.A., Cunningham, B.C., and DeVos, A.M. (1997). Vascular endothelial growth factor: Crystal structure and functional mapping of the kinase domain receptor binding site. P Natl Acad Sci USA *94*, 7192-7197.

Nacak, T.G., Alajati, A., Leptien, K., Fulda, C., Weber, H., Miki, T., Czepluch, F.S., Waltenberger, J., Wieland, T., Augustin, H.G.*, et al.* (2007). The BTB-Kelch protein KLEIP controls endothelial migration and sprouting angiogenesis. Circ Res *100*, 1155-1163.

Nacak, T.G., Leptien, K., Fellner, D., Augustin, H.G., and Kroll, J. (2006). The BTB-kelch protein LZTR-1 is a novel Golgi protein that is degraded upon induction of apoptosis. Journal of Biological Chemistry *281*, 5065-5071.

Nagae, A., Abe, M., Becker, R.P., Deddish, P.A., Skidgel, R.A., and Erdos, E.G. (1993). High concentration of carboxypeptidase M in lungs: presence of the enzyme in alveolar type I cells. Am J Respir Cell Mol Biol *9*, 221-229.

Nagy, A. (2000). Cre recombinase: the universal reagent for genome tailoring. Genesis *26*, 99-109.

Navarro, P., Ruco, L., and Dejana, E. (1998). Differential localization of VE- and N-cadherins in human endothelial cells: VE-cadherin competes with N-cadherin for junctional localization. Journal of Cell Biology *140*, 1475-1484.

Neufeld, G., Cohen, T., Gengrinovitch, S., and Poltorak, Z. (1999). Vascular endothelial growth factor (VEGF) and its receptors. FASEB J *13*, 9-22.

Nitta, T., Hata, M., Gotoh, S., Seo, Y., Sasaki, H., Hashimoto, N., Furuse, M., and Tsukita, S. (2003). Size-selective loosening of the blood-brain barrier in claudin-5-deficient mice. Journal of Cell Biology *161*, 653-660.

Nohria, A., Grunert, M.E., Rikitake, Y., Noma, K., Prsic, A., Ganz, P., Liao, J.K., and Creager, M.A. (2006). Rho kinase inhibition improves endothelial function in human subjects with coronary artery disease. Circ Res *99*, 1426-1432.

North, T.E., de Bruijn, M.F., Stacy, T., Talebian, L., Lind, E., Robin, C., Binder, M., Dzierzak, E., and Speck, N.A. (2002). Runx1 expression marks long-term repopulating hematopoietic stem cells in the midgestation mouse embryo. Immunity *16*, 661-672.

Nyqvist, D., Giampietro, C., and Dejana, E. (2008). Deciphering the functional role of endothelial junctions by using in vivo models. Embo Rep *9*, 742-747.

Oas, R.G., Xiao, K., Summers, S., Wittich, K.B., Chiasson, C.M., Martin, W.D., Grossniklaus, H.E., Vincent, P.A., Reynolds, A.B., and Kowalczyk, A.P. (2010). p120-Catenin is required for mouse vascular development. Circ Res *106*, 941-951.

Ogawa, S., Oku, A., Sawano, A., Yamaguchi, S., Yazaki, Y., and Shibuya, M. (1998). A novel type of vascular endothelial growth factor, VEGF-E (NZ-7 VEGF), preferentially utilizes KDR/FlK-1 receptor and carries a potent mitotic activity without heparin-binding domain. Journal of Biological Chemistry *273*, 31273-31282.

Oh, J., Diaz, T., Wei, B., Chang, H., Noda, M., and Stetler-Stevenson, W.G. (2006). TIMP-2 upregulates RECK expression via dephosphorylation of paxillin tyrosine residues 31 and 118. Oncogene *25*, 4230-4234.

Olsson, A.K., Dimberg, A., Kreuger, J., and Claesson-Welsh, L. (2006). VEGF receptor signalling - in control of vascular function. Nat Rev Mol Cell Biol *7*, 359-371.

Olver, R.E., Walters, D.V., and S, M.W. (2004). Developmental regulation of lung liquid transport. Annu Rev Physiol *66*, 77-101.

Ozerdem, U., Grako, K.A., Dahlin-Huppe, K., Monosov, E., and Stallcup, W.B. (2001). NG2 proteoglycan is expressed exclusively by mural cells during vascular morphogenesis. Dev Dynam *222*, 218-227.

Page, K., Li, J., and Hershenson, M.B. (1999). Platelet-derived growth factor stimulation of mitogen-activated protein kinases and cyclin D1 promoter activity in cultured airway smooth-muscle cells. Role of Ras. Am J Respir Cell Mol Biol *20*, 1294-1302.

Park, C., Ma, Y.L.D., and Choi, K.H. (2005). Evidence for the hemangioblast. Experimental Hematology *33*, 965-970.

Pepper, M.S. (1997). Transforming growth factor-beta: vasculogenesis, angiogenesis, and vessel wall integrity. Cytokine Growth Factor Rev *8*, 21-43.

Petrache, I., Birukova, A., Ramirez, S.I., Garcia, J.G.N., and Verin, A.D. (2003). The role of the microtubules in tumor necrosis factor-alpha-induced endothelial cell permeability. Am J Resp Cell Mol *28*, 574-581.

Philips, A., Roux, P., Coulon, V., Bellanger, J.M., Vie, A., Vignais, M.L., and Blanchard, J.M. (2000). Differential effect of Rac and Cdc42 on p38 kinase activity and cell cycle progression of nonadherent primary mouse fibroblasts. J Biol Chem *275*, 5911-5917.

Prag, S., and Adams, J.C. (2003). Molecular phylogeny of the kelch-repeat superfamily reveals an expansion of BTB/kelch proteins in animals. Bmc Bioinformatics *4*, -.

Pugh, C.W., and Ratcliffe, P.J. (2003). Regulation of angiogenesis by hypoxia: role of the HIF system. Nature Medicine *9*, 677-684.

Qian, X.L., Esteban, L., Vass, W.C., Upadhyaya, C., Papageorge, A.G., Yienger, K., Ward, J.M., Lowy, D.R., and Santos, E. (2000). The Sos1 and Sos2 Ras-specific exchange factors: differences in placental expression and signaling properties. Embo Journal *19*, 642-654.

Rafii, S., Lyden, D., Benezra, R., Hattori, K., and Heissig, B. (2002). Vascular and haematopoietic stem cells: Novel targets for anti-angiogenesis therapy? Nat Rev Cancer *2*, 826-835.

Raftopoulou, M., and Hall, A. (2004). Cell migration: Rho GTPases lead the way. Dev Biol *265*, 23-32.

Reynolds, A.B., and Roczniak-Ferguson, A. (2004). Emerging roles for p120-catenin in cell adhesion and cancer. Oncogene *23*, 7947-7956.

Risau, W. (1997). Mechanisms of angiogenesis. Nature *386*, 671-674.

Robinson, D.N., Cant, K., and Cooley, L. (1994). Morphogenesis of Drosophila Ovarian Ring Canals. Development *120*, 2015-2025.

Rondou, P., Haegeman, G., Vanhoenacker, P., and Van Craenenbroeck, K. (2008). BTB protein KLHL12 targets the dopamine D4 receptor for ubiquitination by a Cul3-based E3 ligase. Journal of Biological Chemistry *283*, 11083-11096.

Rossman, K.L., Der, C.J., and Sondek, J. (2005). GEF means go: turning on RHO GTPases with guanine nucleotide-exchange factors. Nat Rev Mol Cell Biol *6*, 167-180.

Ruhrberg, C. (2003). Growing and shaping the vascular tree: multiple roles for VEGF. Bioessays *25*, 1052-1060.

Sahai, E., and Marshall, C.J. (2002). ROCK and Dia have opposing effects on adherens junctions downstream of Rho. Nature Cell Biology *4*, 408-415.

Samakovlis, C., Hacohen, N., Manning, G., Sutherland, D.C., Guillemin, K., and Krasnow, M.A. (1996). Development of the Drosophila tracheal system occurs by a series of morphologically distinct but genetically coupled branching events. Development *122*, 1395-1407.

Sambrook, J., and Russell, D.W. (2001). Molecular cloning : a laboratory manual, 3rd ed. edn (Cold Spring Harbor, N.Y. : Cold Spring Harbor Laboratory Press).

Sato, T.N., and Bartunkova, S. (2000). Analysis of embryonic vascular morphogenesis. Methods Mol Biol *137*, 223-233.

Scharpfenecker, M., Fiedler, U., Reiss, Y., and Augustin, H.G. (2005). The Tie-2 ligand Angiopoietin-2 destabilizes quiescent endothelium through an internal autocrine loop mechanism. Journal of Cell Science *118*, 771-780.

Schupbach, T., and Wieschaus, E. (1991). Female Sterile Mutations on the 2nd Chromosome of Drosophila-Melanogaster .2. Mutations Blocking Oogenesis or Altering Egg Morphology. Genetics *129*, 1119-1136.

Sekine, K., Ohuchi, H., Fujiwara, M., Yamasaki, M., Yoshizawa, T., Sato, T., Yagishita, N., Matsui, D., Koga, Y., Itoh, N.*, et al.* (1999). Fgf10 is essential for limb and lung formation. Nature Genetics *21*, 138-141.

Semenza, G.L. (2007). Vasculogenesis, angiogenesis, and arteriogenesis: mechanisms of blood vessel formation and remodeling. J Cell Biochem *102*, 840-847.

Senger, D.R. (1983). Tumor cells secrete a vascular permeability factor that promotes accumulation of ascites fluid. Science *219*, 983-985.

Seo, S., Fujita, H., Nakano, A., Kang, M., Duarte, A., and Kume, T. (2006). The forkhead transcription factors, Foxc1 and Foxc2, are required for arterial specification and lymphatic sprouting during vascular development. Developmental Biology *294*, 458-470.

Shalaby, F., Rossant, J., Yamaguchi, T.P., Gertsenstein, M., Wu, X.F., Breitman, M.L., and Schuh, A.C. (1995). Failure of blood-island formation and vasculogenesis in Flk-1-deficient mice. Nature *376*, 62-66.

Shestopalov, I.A., Sinha, S., and Chen, J.K. (2007). Light-controlled gene silencing in zebrafish embryos. Nature Chemical Biology *3*, 650-651.

Skarnes, W.C. (2005). Two ways to trap a gene in mice. Proc Natl Acad Sci U S A *102*, 13001-13002.

Soltysik-Espanola, M., Rogers, R.A., Jiang, S.X., Kim, T.A., Gaedigk, R., White, R.A., Avraham, H., and Avraham, S. (1999). Characterization of Mayven, a novel actin-binding protein predominantly expressed in brain. Molecular Biology of the Cell *10*, 2361-2375.

Soriano, P. (1994). Abnormal Kidney Development and Hematological Disorders in Pdgf Beta-Receptor Mutant Mice. Gene Dev *8*, 1888-1896.

Spindler, V., Schlegel, N., and Waschke, J. (2010). Role of GTPases in control of microvascular permeability. Cardiovascular Research *87*, 243-253.

Steingrimsson, E., Tessarollo, L., Reid, S.W., Jenkins, N.A., and Copeland, N.G. (1998). The bHLH-Zip transcription factor Tfeb is essential for placental vascularization. Development *125*, 4607-4616.

Stogios, P.J., and Prive, G.G. (2004). The BACK domain in BTB-kelch proteins. Trends Biochem Sci *29*, 634-637.

Su, Z.J., Hahn, C.N., Goodall, G.J., Reck, N.M., Leske, A.F., Davy, A., Kremmidiotis, G., Vadas, M.A., and Gamble, J.R. (2004). A vascular cell-restricted RhoGAP, p73RhoGAP, is a key regulator of angiogenesis. P Natl Acad Sci USA *101*, 12212-12217.

Sugihara, K., Nakatsuji, N., Nakamura, K., Nakao, K., Hashimoto, R., Otani, H., Sakagami, H., Kondo, H., Nozawa, S., Aiba, A.*, et al.* (1998). Rac1 is required for the formation of three germ layers during gastrulation. Oncogene *17*, 3427-3433.

Sumara, I., Quadroni, M., Frei, C., Olma, M.H., Sumara, G., Ricci, R., and Peter, M. (2007). A Cul3-based E3 ligase removes aurora B from mitotic chromosomes, regulating mitotic progression and completion of cytokinesis in human cells. Developmental Cell *12*, 887-900.

Suri, C., Jones, P.F., Patan, S., Bartunkova, S., Maisonpierre, P.C., Davis, S., Sato, T.N., and Yancopoulos, G.D. (1996). Requisite role of angiopoietin-1, a ligand for the TIE2 receptor, during embryonic angiogenesis. Cell *87*, 1171-1180.

Suto, K., Yamazaki, Y., Morita, T., and Mizuno, H. (2005). Crystal structures of novel vascular endothelial growth factors (VEGF) from snake venoms - Insight into selective VEGF binding to kinase insert domain-containing receptor but not to fms-like tyrosine kinase-1. Journal of Biological Chemistry *280*, 2126-2131.

Swift, M.R., and Weinstein, B.M. (2009). Arterial-Venous Specification During Development. Circulation Research *104*, 576-588.

Szatmari, I., Vamosi, G., Brazda, P., Balint, B.L., Benko, S., Szeles, L., Jeney, V., Ozvegy-Laczka, C., Szanto, A., Barta, E.*, et al.* (2006). Peroxisome proliferator-activated receptor gamma-regulated ABCG2 expression confers cytoprotection to human dendritic cells. Journal of Biological Chemistry *281*, 23812-23823.

Tada, T., and Kishimoto, H. (1990). Ultrastructural and histological studies on closure of the mouse ductus arteriosus. Acta Anat (Basel) *139*, 326-334.

Takaishi, K., Sasaki, T., Kotani, H., Nishioka, H., and Takai, Y. (1997). Regulation of cell-cell adhesion by Rac and Rho small G proteins in MDCK cells. Journal of Cell Biology *139*, 1047-1059.

Takakura, N., Huang, X.L., Naruse, T., Hamaguchi, I., Dumont, D.J., Yancopoulos, G.D., and Suda, T. (1998). Critical role of the TIE2 endothelial cell receptor in the development of definitive hematopoiesis. Immunity *9*, 677-686.

Tan, W., Palmby, T.R., Gavard, J., Amornphimoltham, P., Zheng, Y., and Gutkind, J.S. (2008). An essential role for Rac1 in endothelial cell function and vascular development. FASEB J *22*, 1829-1838.

Tanaka, Y., Naruse, I., Hongo, T., Xu, M., Nakahata, T., Maekawa, T., and Ishii, S. (2000). Extensive brain hemorrhage and embryonic lethality in a mouse null mutant of CREB-binding protein. Mech Dev *95*, 133-145.

Tatsumoto, T., Xie, X.Z., Blumenthal, R., Okamoto, I., and Miki, T. (1999). Human ECT2 is an exchange factor for Rho GTPases, phosphorylated in G2/M phases, and involved in cytokinesis. Journal of Cell Biology *147*, 921-927.

Tcherkezian, J., and Lamarche-Vane, N. (2007). Current knowledge of the large RhoGAP family of proteins. Biol Cell *99*, 67-86.

Thompson, J.D., Gibson, T.J., and Higgins, D.G. (2002). Multiple sequence alignment using ClustalW and ClustalX. Curr Protoc Bioinformatics *Chapter 2*, Unit 2 3.

Tillet, E., Vittet, D., Feraud, O., Moore, R., Kemler, R., and Huber, P. (2005). N-cadherin deficiency impairs pericyte recruitment, and not endothelial differentiation or sprouting, in embryonic stem cell-derived angiogenesis. Experimental Cell Research *310*, 392-400.

Tomasini, A.J., Schuler, A.D., Zebala, J.A., and Mayer, A.N. (2009). PhotoMorphs (TM): A Novel Light-Activated Reagent for Controlling Gene Expression in Zebrafish. Genesis *47*, 736-743.

Torres-Vaazquez, J., Kamei, M., and Weinstein, B.M. (2003). Molecular distinction between arteries and veins. Cell and Tissue Research *314*, 43-59.

Turchi, L., Chassot, A.A., Bourget, I., Baldescchi, C., Ortonne, J.P., Meneguzzi, G., Lemichez, E., and Ponzio, G. (2003). Cross-talk between RhoGTPases and stress activated kinases for matrix metalloproteinase-9 induction in response to keratinocytes injury. J Invest Dermatol *121*, 1291-1300.

Turgeon, B., and Meloche, S. (2009). Interpreting neonatal lethal phenotypes in mouse mutants: insights into gene function and human diseases. Physiol Rev *89*, 1-26.

Turner, N.A., O'Regan, D.J., Ball, S.G., and Porter, K.E. (2005). Simvastatin inhibits MMP-9 secretion from human saphenous vein smooth muscle cells by inhibiting the RhoA/ROCK pathway and reducing MMP-9 mRNA levels. FASEB J *19*, 804-806.

Van Itallie, C.M., and Anderson, J.M. (2006). Claudins and epithelial paracellular transport. Annual Review of Physiology *68*, 403-429.

van Nieuw Amerongen, G.P., Koolwijk, P., Versteilen, A., and van Hinsbergh, V.W. (2003). Involvement of RhoA/Rho kinase signaling in VEGF-induced endothelial cell migration and angiogenesis in vitro. Arterioscler Thromb Vasc Biol *23*, 211-217.

van Nieuw Amerongen, G.P., and van Hinsbergh, V.W. (2009). Role of ROCK I/II in vascular branching. Am J Physiol Heart Circ Physiol *296*, H903-905.

Vandenbroucke, E., Mehta, D., Minshall, R., and Malik, A.B. (2008). Regulation of endothelial junctional permeability. Control and Regulation of Transport Phenomena in the Cardiac System *1123*, 134-145.

Vaughan, C.J., and Basson, C.T. (2000). Molecular determinants of atrial and ventricular septal defects and patent ductus arteriosus. Am J Med Genet *97*, 304-309.

Villa, N., Walker, L., Lindsell, C.E., Gasson, J., Iruela-Arispe, M.L., and Weinmaster, G. (2001). Vascular expression of Notch pathway receptors and ligands is restricted to arterial vessels. Mech Develop *108*, 161-164.

Vinals, F., and Pouyssegur, J. (1999). Confluence of vascular endothelial cells induces cell cycle exit by inhibiting p42/p44 mitogen-activated protein kinase activity. Molecular and Cellular Biology *19*, 2763-2772.

Visconti, R.P., Richardson, C.D., and Sato, T.N. (2002). Orchestration of angiogenesis and arteriovenous contribution by angiopoietins and vascular endothelial growth factor (VEGF). P Natl Acad Sci USA *99*, 8219-8224.

Vogeli, K.M., Jin, S.W., Martin, G.R., and Stainier, D.Y. (2006). A common progenitor for haematopoietic and endothelial lineages in the zebrafish gastrula. Nature *443*, 337-339.

von Tell, D., Armulik, A., and Betsholtz, C. (2006). Pericytes and vascular stability. Exp Cell Res *312*, 623-629.

Wakabayashi, N., Itoh, K., Wakabayashi, J., Motohashi, H., Noda, S., Takahashi, S., Imakado, S., Kotsuji, T., Otsuka, F., Roop, D.R.*, et al.* (2003). Keap1-null mutation leads to postnatal lethality due to constitutive Nrf2 activation. Nature Genetics *35*, 238-245.

Wan, H., Xu, Y., Ikegami, M., Stahlman, M.T., Kaestner, K.H., Ang, S.L., and Whitsett, J.A. (2004). Foxa2 is required for transition to air breathing at birth. Proc Natl Acad Sci U S A *101*, 14449-14454.

Wang, H., and Dey, S.K. (2006). Roadmap to embryo implantation: clues from mouse models. Nat Rev Genet *7*, 185-199.

Wang, H.U., Chen, Z.F., and Anderson, D.J. (1998). Molecular distinction and angiogenic interaction between embryonic arteries and veins revealed by ephrin-B2 and its receptor Eph-B4. Cell *93*, 741-753.

Ward, C., Hannah, S., Chilvers, E.R., Farrow, S., Haslett, C., and Rossi, A.G. (1997). Transforming growth factor-beta increases the inhibitory effects of GM-CSF and dexamethasone on neutrophil apoptosis. Biochem Soc T *25*, S244-S244.

Watanabe, N., Madaule, P., Reid, T., Ishizaki, T., Watanabe, G., Kakizuka, A., Saito, Y., Nakao, K., Jockusch, B.M., and Narumiya, S. (1997). p140mDia, a mammalian homolog of Drosophila diaphanous, is a target protein for Rho small GTPase and is a ligand for profilin. Embo Journal *16*, 3044-3056.

Weed, S.A., Du, Y.R., and Parsons, J.T. (1998). Translocation of cortactin to the cell periphery is mediated by the small GTPase Rac1. Journal of Cell Science *111*, 2433-2443.

Weis, W.I., and Nelson, W.J. (2006). Re-solving the cadherin-catenin-actin conundrum. J Biol Chem *281*, 35593-35597.

Wennerberg, K., Rossman, K.L., and Der, C.J. (2005). The Ras superfamily at a glance. Journal of Cell Science *118*, 843-846.

Williams, C.K., Li, J.L., Murga, M., Harris, A.L., and Tosato, G. (2006). Up-regulation of the Notch ligand Delta-like 4 inhibits VEGF-induced endothelial cell function. Blood *107*, 931-939.

Williams, S.K., Spence, H.J., Rodgers, R.R., Ozanne, B.W., Fitzgerald, U., and Barnett, S.C. (2005). Role of Mayven, a Kelch-related protein in oligodendrocyte process formation. J Neurosci Res *81*, 622-631.

Wu, M.H., Ustinova, E., and Granger, H.J. (2001). Integrin binding to fibronectin and vitronectin maintains the barrier function of isolated porcine coronary venules. J Physiol-London *532*, 785-791.

Xia, L.J., Ju, T.Z., Westmuckett, A., An, G.Y., Ivanciu, L., McDaniel, J.M., Lupu, F., Cummings, R.D., and McEver, R.P. (2004). Defective angiogenesis and fatal embryonic hemorrhage in mice lacking core 1-derived O-glycans. Journal of Cell Biology *164*, 451-459.

Xia, X.B., Mariner, D.J., and Reynolds, A.B. (2003). Adhesion-associated and PKC-modulated changes in serine/threonine phosphorylation of p120-catenin. Biochemistry *42*, 9195-9204.

Xue, F.Y., and Cooley, L. (1993). Kelch Encodes a Component of Intercellular Bridges in Drosophila Egg Chambers. Cell *72*, 681-693.

Yan, W., Ma, L., Burns, K.H., and Matzuk, M.M. (2004). Haploinsufficiency of kelch-like protein homolog 10 causes infertility in male mice. P Natl Acad Sci USA *101*, 7793-7798.

Yanagisawa, M., Kaverina, I.N., Wang, A.X., Fujita, Y., Reynolds, A.B., and Anastasiadis, P.Z. (2004). A novel interaction between kinesin and p120 modulates p120 localization and function. Journal of Biological Chemistry *279*, 9512-9521.

Yang, J.T., Rayburn, H., and Hynes, R.O. (1993). Embryonic mesodermal defects in alpha 5 integrin-deficient mice. Development *119*, 1093-1105.

Yaniv, K., Isogai, S., Castranova, D., Dye, L., Hitomi, J., and Weinstein, B.M. (2006). Live imaging of lymphatic development in the zebrafish. Nat Med *12*, 711-716.

Yin, L.M., Morishige, K., Takahashi, T., Hashimoto, K., Ogata, S., Tsutsumi, S., Takata, K., Ohta, T., Kawagoe, J., Takahashi, K.*, et al.* (2007). Fasudil inhibits vascular endothelial growth factor - induced angiogenesis in vitro and in vivo. Molecular Cancer Therapeutics *6*, 1517-1525.

You, L.R., Lin, F.J., Lee, C.T., DeMayo, F.J., Tsai, M.J., and Tsai, S.Y. (2005). Suppression of Notch signalling by the COUP-TFII transcription factor regulates vein identity. Nature *435*, 98-104.

Yuan, L., Moyon, D., Pardanaud, L., Breant, C., Karkkainen, M.J., Alitalo, K., and Eichmann, A. (2002). Abnormal lymphatic vessel development in neuropilin 2 mutant mice. Development *129*, 4797-4806.

Zhao, J., Singleton, P.A., Brown, M.E., Dudek, S.M., and Garcia, J.G.N. (2009). Phosphotyrosine protein dynamics in cell membrane rafts of sphingosine-1-phosphate-stimulated human endothelium: Role in barrier enhancement. Cell Signal *21*, 1945-1960.

Zhao, Z.S., and Manser, E. (2005). PAK and other Rho-associated kinases - effectors with surprisingly diverse mechanisms of regulation. Biochem J *386*, 201-214.

Zhu, J.W., Motejlek, K., Wang, D.N., Zang, K.L., Schmidt, A., and Reichardt, L.F. (2002). beta 8 integrins are required for vascular morphogenesis in mouse embryos. Development *129*, 2891-2903.

Ziche, M., Morbidelli, L., Choudhuri, R., Zhang, H.T., Donnini, S., Granger, H.J., and Bicknell, R. (1997). Nitric oxide synthase lies downstream from vascular endothelial growth factor-induced but not basic fibroblast growth factor-induced angiogenesis. J Clin Invest *99*, 2625-2634.

Ziche, M., Morbidelli, L., Masini, E., Amerini, S., Granger, H.J., Maggi, C.A., Geppetti, P., and Ledda, F. (1994). Nitric oxide mediates angiogenesis in vivo and endothelial cell growth and migration in vitro promoted by substance P. J Clin Invest *94*, 2036-2044.